Winter 2014

Flavin-dependent thymidylate synthase : putting together the mechanistic puzzle from reaction intermediate pieces

Tatiana Vladimirovna Mishanina
University of Iowa

FLAVIN-DEPENDENT THYMIDYLATE SYNTHASE: PUTTING TOGETHER THE MECHANISTIC PUZZLE FROM REACTION INTERMEDIATE PIECES

by

Tatiana Vladimirovna Mishanina

A thesis submitted in partial fulfillment
of the requirements for the Doctor of
Philosophy degree in Chemistry
in the Graduate College of
The University of Iowa

December 2014

Thesis Supervisor: Professor Amnon Kohen

Graduate College
The University of Iowa
Iowa City, Iowa

CERTIFICATE OF APPROVAL

_____

PH.D. THESIS

_____

This is to certify that the Ph.D. thesis of

Tatiana Vladimirovna Mishanina

has been approved by the Examining Committee
for the thesis requirement for the Doctor of Philosophy
degree in Chemistry at the December 2014 graduation.

Thesis Committee: _____
Amnon Kohen, Thesis Supervisor

_____
Daniel M. Quinn

_____
James B. Gloer

_____
Johna Leddy

_____
M. Todd Washington

To Elena Mishanina, my patient mother and best friend

Stupid is as stupid does.

Forrest Gump
"Forrest Gump" (1994)

ACKNOWLEDGMENTS

I have been in school all my life… well, at least from the age of seven. Therefore, it is quite a liberating and empowering feeling to be at the end of my PhD studies – the most significant milestone a student could achieve! This landmark in my life, however, would not have been possible without the support of many great people.

First and foremost, I am deeply grateful to my PhD advisor, Prof. Amnon Kohen, for his patience with and faith in a shy, soft-spoken me 5 years ago. He saw the potential in me as a scientist back then and gently guided me towards its realization. He encouraged me to express my opinions and defend my point of view while keeping an open mind in the ever-changing field of science. I could not have wished for a better mentor.

Time flies when you are in good company. And Kohen group has always been an amazing bunch to work with. In particular, I want to thank Dr. Eric Koehn, my FDTS buddy, for starting me out on the project in the lab, teaching me how to scavenge and improvise with pieces of glassware to put together a usable anaerobic setup, and all of the scientific discussions over the years. I am grateful to my giant sister Dr. Zhen Wang, for being a wonderful and supporting friend when research and life got tough; to Dr. Daniel Roston, my long-term desk neighbor, for patiently teaching me how to use Mathematica, our refreshing chats and having such a great sense of humor; to Drs. Vanja Stojković and Arundhuti Sen for useful advice in the lab; to Thelma Abeysinghe and Priyanka Singh for being great co-workers and good mates in the thesis-writing process; to Qi Guo (Gail) for being a fun and helpful co-worker and a friend; to Kalani Karunaratne for being an attentive and hard-working teammate on the FDTS project. From the bottom of my heart, I would like to thank my friend Dr. Marie Pierre, with whom I struggled through the hardest years of grad school and who was always there for me in times of need. I thank

my friend Dr. Yulia Tataurova for her support and encouragement, our many chats over coffee and keeping me from forgetting Russian.

I also want to express my gratitude to faculty and staff at the University of Iowa. My experiments would not have happened without the glassware masterfully built and many-a-time repaired by Peter Hatch (Pete) and Benjamin Revis (Benj) in the glass shop. Dr. Lynn Teesch and Vic Parcell (Mass Spectrometry Facility) have been an enormous help to me with mass spec use/analysis over the years, and I am sincerely grateful to them. Frank Turner in the machine shop saved my day on multiple occasions by fixing HPLC loops and columns. I am thankful to Mike Estenson (electronics shop), Andy Lynch and Tim Koon (chemistry stores) for their help; to charming Janet Kugley, the first face of Chemistry Department I saw and one of the reasons I joined the Department; to Sharon Robertson and Lindsay Elliott for their patience with me bugging them about scheduling, graduation requirements, etc.; to Earlene Erbe for helping me become a better teacher. I would like to thank Prof. Dan Quinn for his help and letters of recommendation, Prof. Jim Gloer for his assistance with mass spec data analysis, Prof. Johna Leddy for teaching me electrochemistry, and Prof. M. Todd Washington for lending his quench-flow instrument and making me feel welcome in his lab space. The Department of Chemistry has been my home for the past six years, and I will miss everyone in it very much.

Last but certainly not least, my thanks go out to everyone in Kansas (my American family) and my amazing mother, Elena Mishanina (my Tajikistan family). Without Pat Radford, Lanora Turner and Dr. Bill Gardner I would not be where I am today. In 2004, my mother watched her 16-year-old daughter leave for a foreign country literally half-way around the world away. We have been apart ever since. It is difficult for me, but I cannot even imagine how hard it is for her. I want to thank her for her sacrifices, support and faith in my abilities and judgment.

ABSTRACT

Antibiotic resistance represents a real threat in the modern world. The problem of resistance is brought about by the fast evolution of bacteria, accelerated by misuse and over-prescription of antibiotics and compounded by the decline in the discovery and development of new classes of antibiotics. Consequently, new targets for antibiotics are in high demand. Flavin-dependent thymidylate synthase (FDTS), which is not present in humans and is responsible for the biosynthesis of a DNA building block in several human pathogens (e.g., *M. tuberculosis*, *B. anthracis*, *H. pylori*), is one such novel target. FDTS catalyzes the reductive methylation of 2′-deoxyuridine-5′-monophosphate (dUMP) to produce 2′-deoxythymidine-5′-monophosphate (dTMP), with N^5,N^{10}-methylene-5,6,7,8-tetrahydrofolate (CH_2H_4fol) serving as the carbon source and a nicotinamide cofactor as the electron source. No efficient inhibitors of FDTS are known, despite high-throughput screening attempts to find them. Intermediate and transition-state mimics are likely to bind the enzyme with greater affinity and hence have a better chance at inhibiting FDTS. Therefore, the understanding of the chemical mechanism of FDTS is critical to the informed design of compounds capable of disrupting its function in bacteria. We utilized various techniques, including chemical trapping of reaction intermediates, substrate isotope exchange and stopped-flow, to investigate the FDTS mechanism and determine what sets it apart from other pyrimidine methylases. We found that at least two different intermediates kinetically accumulate in the FDTS-catalyzed reaction. Both of these intermediates are trapped in acid in the form of 5-hydroxymethyl-dUMP, which has never been isolated in other uracil-methylating enzymes. Under basic conditions, however, the earlier intermediate is converted to a species with an unusual flavin-derived adduct, while the later intermediate is converted to dTMP product. Our experiments also suggest that dUMP is activated for the reaction by the reduced flavin – a substrate

activation mechanism distinct from the one employed by the classical pyrimidine-methylating enzymes.

TABLE OF CONTENTS

LIST OF FIGURES

Figure

CHAPTER I

INTRODUCTION: MECHANISMS AND INHIBITION OF URACIL METHYLATING ENZYMES[i]

Abstract

Uracil methylation is essential for survival of organisms and passage of information from generation to generation with high fidelity. Two alternative uridyl methylation enzymes, flavin-dependent thymidylate synthase and folate/FAD-dependent RNA methyltransferase, have joined the long-known classical enzymes, thymidylate synthase and SAM-dependent RNA methyltransferase. These alternative enzymes differ significantly from their classical counterparts in structure, cofactor requirements and chemical mechanism. This chapter covers the available structural and mechanistic knowledge of the classical and alternative enzymes in biological uracil methylation, and offers a possibility of using inhibitors specifically aiming at microbial thymidylate production as antimicrobial drugs.

Introduction

Methylation of uracil at C5 to form thymine moieties is an important transformation in both DNA biosynthesis and posttranslational modification of RNA (Fig. 1.1). The DNA building block 2'-deoxythymidine-5'-monophosphate (dTMP, or thymidylate) is formed by methylation of 2'-deoxyuridine-5'-monophosphate (dUMP). Thymidylate is essential for survival of all organisms, since without a pool of thymidylate for DNA biosynthesis cellular reproduction ceases.[1] In RNA, methylated uracils are found at a single site in tRNAs and two sites in the ribosome.[2] The 5-methyluridyl at

[i] This chapter is reprinted from Mishanina, T.V.; Koehn, E.M.; Kohen, A. 2012. *Bioorg. Chem.*, 43, 37-43, with permission from Elsevier Inc.

position 54 in the T-loop of tRNAs in almost all living cells (designated as T54) plays a role in maintaining the tertiary structure of tRNA.[3] One of the methylated uracils in rRNA, U1939 located at the interface of ribosomal subunits, has been proposed to be involved in interaction between the subunits and in sensing uncharged tRNAs.[4, 5] The second methylated uracil in rRNA (U747) is situated in the ribosomal tunnel through which the emerging peptide chain passes during protein synthesis, and hence might be involved in regulatory interactions with the synthesized peptide.[6]

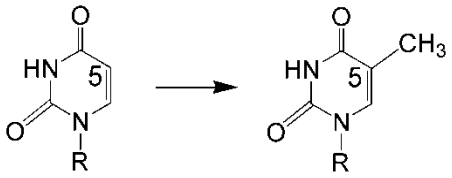

Figure 1.1 Uracil methylation reaction catalyzed by the enzymes reviewed here. R = 2'-deoxyribose or RNA.

Different enzymes are responsible for uracil methylation in DNA biosynthesis and RNA modification. Conversion of dUMP to dTMP is catalyzed by thymidylate synthase (TSase) enzymes. Two different classes of TSases are known which are dissimilar in their sequence, structure, cofactor requirements and chemical mechanism. The extensively studied ThyA TSase is a homodimeric enzyme (Fig. 1.2A) that utilizes (*R*)-N^5,N^{10}-methylene-5,6,7,8-tetrahydrofolate (CH_2H_4folate) as both a methylene and a hydride source for the C7 methyl of dTMP (Fig. 1.3A). On the other hand, a recently discovered ThyX TSase is a homotetrameric catalyst (Fig. 1.2B) that uses CH_2H_4folate only for its methylene, and acquires the reducing hydride from nicotinamide adenine dinucleotide phosphate (NADPH) or other reducing agents (e.g. dithionite, ferredoxin, etc.). The redox chemistry in ThyX TSase is mediated by flavin adenine dinucleotide (FAD) cofactor (Fig. 1.3B). Many human pathogens, including biological warfare agents, lack the genes

for ThyA TSase and rely on this alternative flavin-dependent TSase instead.[7-10] Since ThyX differs from ThyA TSase in structure and chemistry and is absent in humans, it can potentially serve as a target of antibiotics with low toxicities.

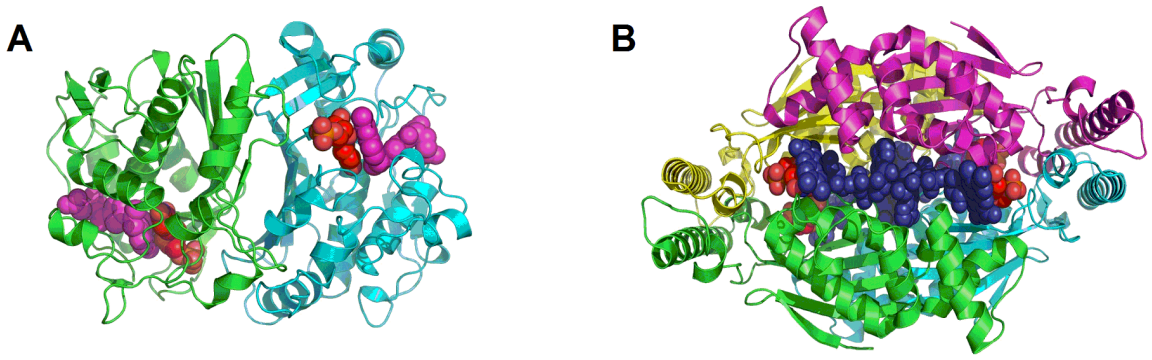

Figure 1.2 Structures of thymidylate synthases. A) Classical thymidylate synthase dimer from *E. coli* (PDB ID 2KCE). The dUMP substrate is red and the CH_2H_4folate analog (Zd 1694, Raltitrexed) is magenta, shown as space filling shapes. B) Flavin-dependent thymidylate synthase tetramer from *T. maritima* (PDB ID 1O26). FAD prosthetic group is blue and dUMP is red.

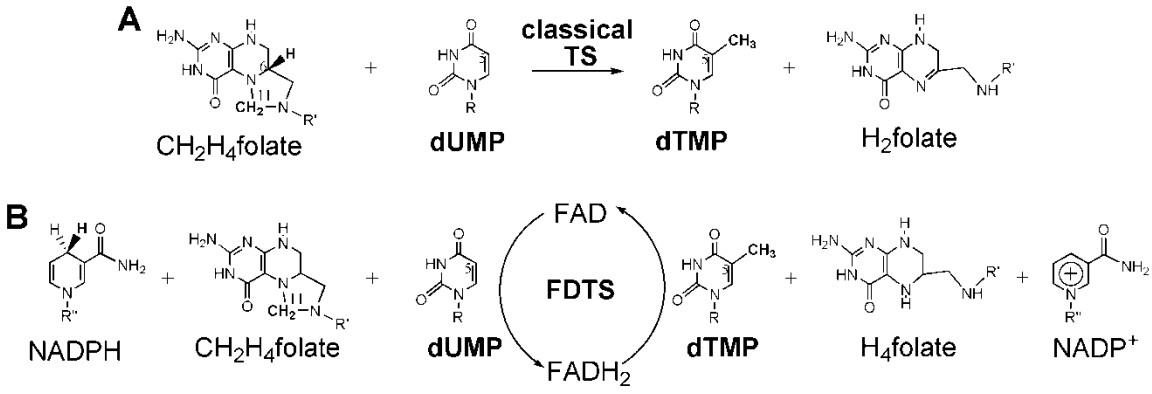

Figure 1.3 Reactions catalyzed by thymidylate synthases. A) The overall reaction catalyzed by classical TSase. The atoms of importance are numbered. B) The overall reaction catalyzed by FDTS. R=2'-deoxyribose-5'-phosphate; R'=(*p*-aminobenzoyl)-glutamate; R"=adenosine-5'-pyrophosphate-ribityl. Reproduced with permission from ref. 11.

The methylation of U1939 and U747 in rRNA of the ribosome is carried out by RumA and RumB methyltransferases, respectively. In tRNA, the enzyme TrmA catalyzes the production of T54. Although RumA, RumB and TrmA share little sequence and structure homology, all three enzymes use *S*-adenosylmethionine (SAM) as a methyl donor and follow the same chemical mechanism, described in detail later.

In the late 1970s, an alternative class of enzymes was discovered for T54 production in tRNA. Unlike TrmA, the enzyme responsible for catalysis in this alternative pathway does not depend on SAM, but rather uses reduced FAD and CH_2H_4folate, and is therefore designated as TrmFO methyltransferase. Even though TrmA and TrmFO phylogenic distribution is mutually exclusive, with TrmFO present in several pathogens, early studies[12] showed little effect of TrmFO on bacterial growth. If further investigation demonstrates some essential activity of TrmFO in the cell, this enzyme could become of interest as an antibiotic target.

This chapter highlights the available structural and mechanistic knowledge of the classical and alternative enzymes in biological uracil methylation, and offers a possibility of using inhibitors specifically aiming at microbial thymidylate production as antimicrobial drugs.

Uracil-methylating enzymes

Classical thymidylate synthase (TSase, EC 2.1.1.45) and flavin-dependent thymidylate synthase (FDTS, EC 2.1.1.148)

ThyA thymidylate synthase has been intensively studied for decades, with over a hundred crystal structures available to date, and consequently is referred to as classical TSase. ThyA is a homodimer with one active site per subunit, as shown in Fig. 1.2A. The enzyme uses CH_2H_4folate as both the source of a one-carbon unit and the reducing hydride to form the C7 methyl of dTMP, and produces 7,8-dihydrofolate (H_2folate,

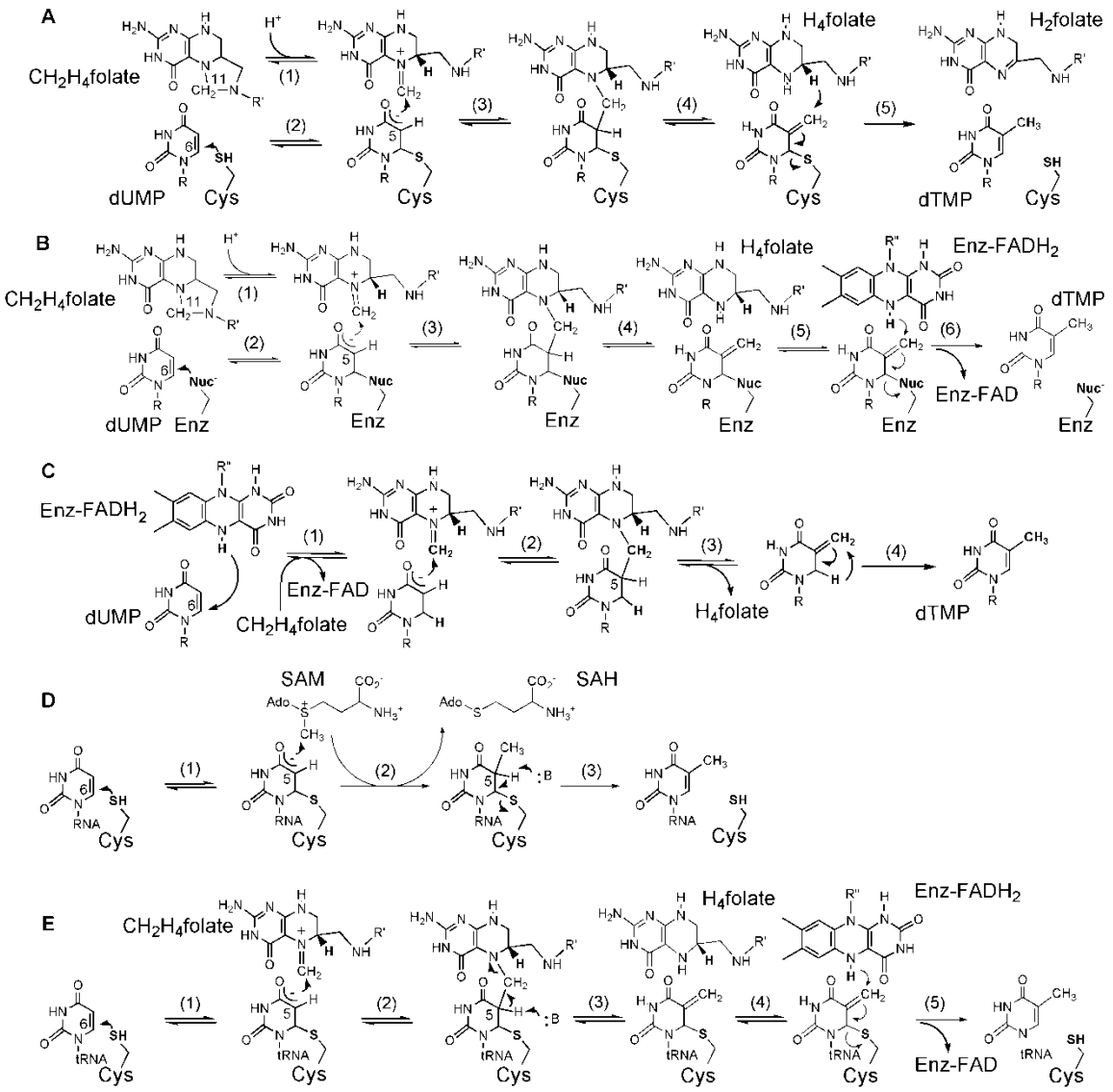

Figure 1.4 Proposed chemical mechanisms of various uracil methylation enzymes. A) The mechanism of classical TSase-catalyzed reaction. B) The mechanism of FDTS-catalyzed reaction involving an enzymatic nucleophile. C) The mechanism of FDTS-catalyzed reaction where reduced flavin acts as the nucleophile. R=2′-deoxyribose-5′-phosphate; R′=(*p*-aminobenzoyl)-glutamate; R″=adenosine-5′-pyrophosphate-ribityl. D) The mechanism of S-adenosylmethionine-dependent RNA methyltransferases (Rum A and TrmA). SAM = S-adenosylmethionine; SAH = S-adenosylhomocysteine. E) The mechanism of folate/FAD-dependent tRNA methyltransferase (TrmFO).

Fig. 1.3A). CH_2H_4folate is regenerated for subsequent TSase turnovers by reduction of H_2folate by dihydrofolate reductase (DHFR, encoded by *folA* gene) to form H_4folate and

then conversion to CH_2H_4folate catalyzed by serine hydroxymethyl transferase (SHMT). The TSase/DHFR cycle is central to thymidylate biosynthesis in the organisms relying on ThyA.

The currently proposed chemical mechanism of classical TSase is presented in Fig. 1.4A.[1, 13] Upon binding, N10 protonation of CH_2H_4folate results in a reactive iminium cation (step 1). A conserved active site cysteine covalently activates dUMP via Michael addition (step 2), and the C5 of the resulting enolate reacts in a Mannich-type condensation with the N5 imine of CH_2H_4folate (step 3). The enzyme-bound bridged intermediate undergoes Hofmann elimination of H_4folate (step 4) to form an exocyclic methylene intermediate. Finally, the C7 of this intermediate is reduced by the *6S* hydride from H_4folate (step 5) producing H_2folate and dTMP.

Establishment of the chemical mechanism for classical TSase relied on key kinetic, chemical and structural studies. Michael-addition (Fig. 1.4A, step 2) and subsequent enolate condensation (Fig. 1.4A, step 3) of the mechanism are supported by the crystal structure of the wild-type *E. coli* enzyme in a covalent complex with 5-fluorouridylate and CH_2H_4folate (Protein Data Bank ID 1TLS).[14] The mechanism for the formation of this complex is outlined in Fig. 1.5A. This covalent ternary intermediate (Fig. 1.4A, between steps 3 and 4) has also been detected in quenching experiments with wild-type TSase[15] and by isolation on SDS-PAGE in reactions of E60A and E60L mutants of *L. casei* TSase with radiolabeled substrates.[16] The formation of the exocyclic methylene intermediate (Fig. 1.4A, between steps 4 and 5) was confirmed in experiments with a W82Y mutant of *L. casei* TSase,[17] which allowed premature release of H_4folate from the active-site and subsequent chemical trapping of the intermediate with β-mercaptoethanol under steady-state conditions.

The kinetic mechanism of classical TSase is generally sequential with dUMP binding first. This is supported by structural studies and monitoring the release of 5F-dUMP as a function of CH_2H_4folate concentration. The ordered mechanism is also

supported by the complete suppression of dUMP kinetic isotope effects (KIEs) at high CH_2H_4folate concentrations.[18] Under certain conditions, however, such as when using polyglutamyl CH_2H_4folates and with some mutants, the order of binding can become random. For this reason, it is accepted that the binding order of substrates to TSase is mostly preferential but subject to change based on reaction conditions.[13]

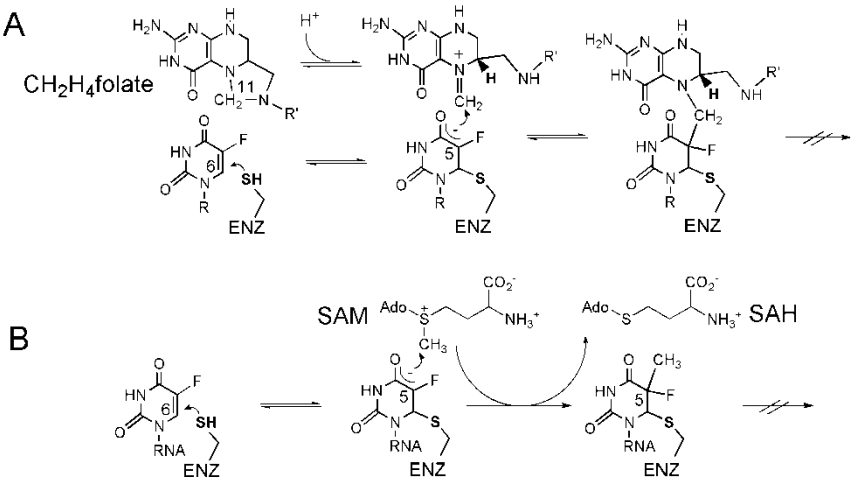

Figure 1.5 Mechanism of inhibition of SAM- and folate-dependent uracil methyltransferases by 5-fluorouridylate. A) Mechanism of formation of an inhibitory covalent complex in CH_2H_4folate-dependent enzymes (classical TSase and TrmFO). B) Mechanism of formation of an inhibitory covalent complex in SAM-dependent enzymes (RumA and TrmA). SAM = *S*-adenosylmethionine; SAH = *S*-adenosylhomocysteine.

Several clinical drugs (e.g. 5-fluorouracil, 5-trifluoromethyl 2'-deoxyuridine, etc.), used for chemotherapy and treatment of other conditions, have been shown to act through inhibition of classical TSase.[19] Competitive inhibitors of TSase have been developed based both on the pyrimidine (5-substituted uridylates) and folate (raltitrexed, 10-methylfolate, 10-propargyl-5,8-dideazafolate and others) moieties. Many of the 5-substituted substrate, intermediate, and product nucleotide analogs function by reaction with the enzyme, thus causing mechanism-based inactivation. Covalent anchoring of

these inhibitors by the active-site cysteine of classical TSase is a key feature of their mechanism of inactivation. A well-studied example, 5F-dUMP ($K_d \approx 10^{-12}$ M), reacts with the active site cysteine and undergoes condensation with CH_2H_4folate but prevents proton abstraction and elimination of the H_4folate, as a consequence stalling the reaction at the covalent ternary complex (Fig. 1.5A). Other dUMP analogs carry C5 substituents that upon cysteine attack at C6 become reactive and covalently bind to other proximal residues of the enzyme, or react with solvent water. The enzyme inactivation by this type of inhibitors is independent of CH_2H_4folate. The same is true for substrate analogs with electrophilic C5 substituents that serve as a sink for the negative charge generated in cysteine attack at C6 (e.g. 5-NO_2-dUMP, dAzMP and others).[13, 20]

The extensive study of classical TSase resulted in its well-characterized structure and mechanism, and identification of key compounds that inhibit its activity. This knowledge has been useful not only clinically in light of the drugs that target TSase, but also in establishing a model of catalysis for many other enzymes. For instance, such enzymes as dUMP and dCMP hydroxymethyltransferases, DNA and RNA cytosine methyltransferases, and RNA uridyl methyltransferases (considered later) share similar catalytic features.[13, 21] The use of classical TSase as a model system has recently extended even further with detailed mechanistic study using KIEs and other methods to probe the enzyme's role in activating and catalyzing C-H bond cleavage.[18, 22]This underscores the importance of classical TSase and continued studies of this enzyme to understand general features of biological catalysts.

In 2002, several organisms were identified that lacked the genes coding for classical TSase, DHFR, or thymidine kinase (a thymidine-scavenging enzyme), yet produced thymidine as indicated by their growth in thymidine-depleted media.[7, 23, 24] This finding led to the discovery of an alternative thymidylate synthase enzyme, ThyX. ThyX thymidylate synthase catalyzes the same net conversion of dUMP to dTMP, as classical TSase (Fig. 1.3B). However, unlike classical TSase, ThyX uses CH_2H_4folate only as a

methylene donor and employs a flavin adenine dinucleotide (FAD) prosthetic group to catalyze the redox chemistry, and is therefore referred to as flavin-dependent thymidylate synthase (FDTS).

FDTS accomplishes the combined activities of classical TSase and DHFR, converting dUMP to dTMP and producing H_4folate instead of H_2folate (Fig. 1.3B). Since some organisms that depend on FDTS lack the gene for DHFR, it was suggested that FDTS might be a bifunctional enzyme, with classical TSase and flavin-dependent DHFR activities. Such bifunctional classical TSase-DHFR enzymes are common in protozoa[25] and plants.[26] However, several observations have ruled out the possibility of FDTS being a bifunctional catalyst: (i) in studies with *(R)*-[6-^{3}H]-CH_2H_4folate, the tritium was retained by H_4folate and not transferred to dTMP,[27] as with the classical TSase;[1, 28] (ii) in contrast to classical TSase, reactions carried out in D_2O produced deuterated dTMP, which points to proton exchange between the reduced flavin and the solvent prior to a hydride transfer from the flavin directly to the nucleotide; and (iii) when using tritiated NADPH to reduce the flavin, the tritium was found in water and not H_4folate,[27] ruling out a flavin-dependent DHFR functionality of FDTS. Overall these findings support a mechanism in which NADPH reduces FAD to $FADH_2$ and the uracil moiety accepts a hydride from the $FADH_2$ to form dTMP.[11]

Very few crystal structures of FDTS enzymes are available today. The first crystal structure of FDTS, obtained from the organism *Thermotoga maritima*, showed no structural similarity with classical TSase.[29] Unlike dimeric classical TSase, FDTS is a homotetramer with four active sites, each at the interface of three of the subunits (Fig. 1.2B). Since then, crystal structures for FDTSs from *Mycobacterium tuberculosis*,[30] *Paramecium bursaria chlorella* virus-1,[31] and, more recently, *Helicobacter pylori*[32] have been solved, with FAD only and FAD in combination with dUMP, 5F-dUMP or 5Br-dUMP. Additionally, a structure with $NADP^+$ has been solved for *M. tuberculosis* FDTS where nicotinamide replaced the flavin cofactor in the enzyme during crystallization.

However, the mechanistic importance of this finding has yet to be realized.[33] Structures with CH_2H_4folate or any other folate moieties, on the other hand, have not been obtained. Although FDTSs from different organisms differ in sequence and size, tetrameric structure and key residues involved in substrate binding and catalysis are conserved.

Structural comparison of classical TSase and FDTS provides insight into the differences in catalysis of these two enzymes. The binding sites for dUMP and FAD within the FDTS active-site have been characterized. In the structures, the N5 of isoalloxazine ring of FAD is located sufficiently close to the uracil moiety to donate its hydride to the nucleotide (<4 Å). The conserved cysteine crucial to classical TSase activity is absent from the FDTS active site, and some FDTSs lack cysteines altogether. The only likely candidate for cysteine's role as an enzymatic nucleophile in FDTS is a conserved serine residue located 4 Å away from the electrophilic C6 of dUMP. The hypothesis of serine acting as a nucleophile was supported by studies of FDTS from *M. tuberculosis* and *H. pylori* (*Mtb*FDTS[34] and *Hp*FDTS[35], respectively). A chemical mechanism where serine acts as the catalytic nucleophile similar to the cysteine of classical TSase is presented in Fig. 1.4B.[27] In this mechanism, serine activates dUMP (step 2) for subsequent reaction with CH_2H_4folate (steps 3-5). In the final step, the enzyme-bound exocyclic methylene intermediate is reduced by a hydride from $FADH_2$ (step 6), releasing the product dTMP.

The mechanism with serine as an active-site nucleophile was further investigated by conducting mutation studies with *T. maritima* FDTS (*Tm*FDTS)[36], similar to those with *Mtb*FDTS[34] and *Hp*FDTS[35]. Surprisingly, mutation of the only conserved serine in the *Tm*FDTS active site (S88) to alanine resulted in an active enzyme. Moreover, an S88C mutant was 400 times less active than the wild-type enzyme and did not display any classical TSase activity (i.e. catalysis without the reducing equivalents from NADPH or dithionite). The search for other potential nucleophiles in active site of *Tm*FDTS revealed the conserved residues S83 and Y91 as possible candidates. Tyrosine mutation

to phenylalanine in *Hp*FDTS, however, yields an enzyme with 50% more, not less activity than the wild type.[35] The S83, on the other hand, is too far away (17 Å) from the electrophilic C6 of dUMP to activate it and is hydrogen-bonded to the adenosine moiety of FAD at the core of the FDTS tetramer, and is thus not a capable nucleophile. These observations suggested that FDTS catalysis does not rely on an enzymatic nucleophile.[36]

Experiments with halogenated dUMP analogs further strengthen the lack of an enzymatic anchor in FDTS-catalyzed reaction. With classical TSase, isolation of a covalent complex of the enzyme with 5F-dUMP and CH_2H_4folate (PDB ID 1TLS) served as an evidence for Michael addition. No such complex has been identified for FDTS either in MALDI-TOF mass spectrometry[36] or X-ray crystallography[37] analyses. Furthermore, 5F-dUMP was shown to inhibit FDTS only at micromolar concentrations − orders of magnitude higher than observed for classical TSase − and inhibition was completely reversible. Another test for a Michael nucleophile in enzyme's active site is the dehalogenation of 5Br-dUMP. While classical TSase catalyzes this dehalogenation,[38] FDTS fails to do so.

Other possible non-enzymatic nucleophiles include a hydroxide from the water and the N5 of the flavin, proposed to be the nucleophile in UDP-galactopyranose mutase catalysis.[39] However, the basic environment in the FDTS active site necessary for deprotonation of water to form hydroxide is lacking. Studies with 5-carba-5-deaza-FAD, i.e. FAD with a carbon in place of the N5, resulted in an active enzyme, thus eliminating the N5 nucleophilic involvement.[36]

With the data supporting the absence of an enzymatic nucleophile, a revised version of mechanism in Fig. 1.4B is necessary for FDTS-catalyzed reaction. To follow the flow of hydrogens from the reduced flavin, isotopic labeling experiments were conducted with *Tm*FDTS.[36] In reactions in D_2O at 65^oC (close to the physiological temperature of *T. maritima*), 7-D-dTMP was identified as the sole product. However,

similar reactions done at 37^{o}C produced up to 60% of 6-D-dTMP, which suggested that the hydrogen could be directly transferred from the reduced flavin to C6 of the uracil.[36]

In light of the studies described above, a mechanism consistent with all current mechanistic and structural data was proposed where a hydride from $FADH_2$ nucleophilically attacks the C6 of dUMP (Fig. 1.4C, step 1). The subsequent steps lead to the formation of a putative exocyclic methylene intermediate (Fig. 1.4C, between steps 3 and 4), analogous to the classical TSase intermediate (Fig. 1.4A, between steps 4 and 5) except for the lack of the covalent bond to the enzyme. This intermediate is an isomer of dTMP and needs to undergo rearrangement to form that product (Fig. 1.4C, step 4). Interestingly, the chemistry proposed in Fig. 1.4C is quite different from that of classical TSase and uridyl methyltransferases in general.

In addition to efforts to establish the chemical cascade for FDTS-catalyzed reaction, its kinetic mechanism has been explored over the past several years. Altogether, FDTS seems to follow a sequential order of substrate binding, with little data available on the order of product release. The multisubstrate nature of the FDTS reaction makes its comprehensive kinetic analysis challenging. Furthermore, the activation kinetics observed for dUMP, substrate inhibition and negative cooperativity observed for CH_2H_4folate, and the ability for FDTS to function as an oxidase (reducing molecular oxygen to hydrogen peroxide) have also added to the complications involved in deconvolution of the entire kinetic mechanism.[11] While the oxidase activity of FDTS can compete with the synthase activity and potentially interfere with dTMP production, it has proved instrumental in probing the nature of substrate binding. In studies of FDTS oxidase activity, it was demonstrated that the rate of H_2O_2 formation increases as a function of dUMP concentration when CH_2H_4folate is not present suggesting that dUMP may activate the redox chemistry of the flavin. The observation that CH_2H_4folate and O_2 compete for the same activated enzyme complex allowed an approximation of binding affinities for these species. Importantly, this has led to better approximations for

functional binding constants for both dUMP and CH_2H_4folate, giving a more realistic picture of binding than offered by standard Michaelis analysis.[40]

Potent classical TSase inhibitors (as mentioned above) have been tested in the past against FDTS activity but showed no or little effect.[41] This enhances the promise for the development of inhibitors specific to FDTS with low effects on the classical enzyme, and thus lower toxicity to the host. One avenue for such selective inhibition is the development of analogs that mimic the non-covalent intermediates in FDTS mechanism (Fig. 1.4C) or the transition states for their formation. These molecules might bind tightly to FDTS, but not to classical TSase. Another possibility is to exploit the structural differences in the active sites of classical TSase and FDTS. Namely, classical TSase has a deep and well organized active site that closely interacts with the functional groups of the bound folate and dUMP moieties.[27, 42] FDTS, on the other hand, seems to have much larger, flexible and solvent-exposed active site. As a result, bulkier analogs of the substrates may selectively bind to the accessible FDTS active site, but not to the sheltered classical TSase pocket. To date there are very few compounds that are known to inhibit FDTS and none have proven to be highly specific or mechanism-based. Recently, a series of derivatives based on a thiazolidine core were synthesized and shown to inhibit FDTS activity.[43] This resulted in the identification of two classes of submicromolar inhibitors, which either competed with dUMP or inactivated FDTS independently of dUMP concentration. To date, none of these compounds have been demonstrated to be selective for FDTS lowering their potential to serve as drug leads. The only report of a selective FDTS inhibitor is that of a 5-propynyl-dUMP derivative, with additional eight-carbon amide attached to the side chain (N-(3-(5-(2'-deoxyuridine-5'-monophosphate))prop-2-ynyl)-octanamide),[44] which inhibited *Mtb*FDTS almost 100 times more than classical *Mtb*TSase enzyme. The mechanism for the selective inhibition for this compound is not known but could be due to the ability of the accessible FDTS active site, but not the sheltered TSase pocket, to accommodate the bulky inhibitor.

SAM-dependent RNA methyltransferases (EC 2.1.1.35) and folate/FAD-dependent tRNA methyltransferase (EC 2.1.1.74)

Methylation of uracil moeties also occurs in posttranscriptional modification of RNA. These important biological modifications are carried out by either the *S*-adenosylmethionine (SAM)-dependent enzymes RumA, RumB and TrmA, or folate-dependent TrmFO enzymes.

RumA and RumB methyltransferases methylate U1939 and U747, respectively, of 23S rRNA. The first reported RNA uridine methyltransferase crystal structure was that of *E. coli* RumA, in complex with *S*-adenosylhomocysteine (i.e. SAM without its *S*-methyl) and a 37-nucleotide fragment of 23S rRNA (PDB ID 1UWV and 2BH2).[45] Interestingly, the structure showed RumA to be a monomeric metalloprotein containing a [4Fe4S] cluster, which was proposed to play a role in correct protein folding and/or rRNA binding. In the structure, the C5 of U1939 to be methylated within the nucleotide fragment was replaced with fluorine. This substitution stalled the methylation and led to formation of a stable covalent enzyme-RNA complex (Fig. 1.5B), which indicated involvement of an enzymatic nucleophile analogous to cysteine in classical thymidylate synthase mechanism (Fig. 1.4A). The proposed chemical mechanism for RumA with Michael addition of a catalytic cysteine (C389 in *E. coli*) to C6 of the uridine is shown in Fig. 1.4D.[46] Based on the structure, the conserved glutamate (E424) was suggested to be the general base in step 3 of the mechanism, and this hypothesis was confirmed by mutagenesis.[45]

In most Gram negative bacteria, some archae and all eukaryotes, TrmA enzyme is responsible for catalyzing SAM-dependent U54 methylation within tRNA. Although TrmA shares little sequence homology with RumA, a recently obtained crystal structure of *E. coli* TrmA E358Q mutant complexed with a 19-nucleotide tRNA fragment (PDB ID 3BT7) showed RNA binding in a manner similar to RumA,[47] and suggested TrmA

chemical mechanism to be analogous to that of RumA (Fig. 1.4D). Mutation of the glutamate 358 to glutamine arrested catalysis and allowed crystallization of the covalent complex (Fig. 1.4D, between steps 2 and 3). Isolation of this complex supported the role of E358 as a general base in TrmA, similarly to E424 in RumA.

Over three decades ago, it was reported that tRNA U54 methylation in the Gram-positive bacteria *Bacillus subtilis* and pathogenic *Enterococcus faecalis* does not depend on SAM. Instead the purified methytransferases from these organisms use CH_2H_4folate as a methylene donor and $FADH_2$ as a reductant, as supported by incorporation of tritium from [5-^{3}H]-5-deaza-$FMNH_2$ into the methyl of thymidine product.[48] More recently, a gene coding for the folate/FAD-dependent tRNA methyltransferase, named TrmFO, has been identified in most Gram-positive and some Gram-negative bacteria, including *T. maritima* and *Thermus thermophilus*.[49, 50] Notably, the phylogenic distribution of TrmFO and TrmA enzymes is mutually exclusive.

The chemical mechanism of TrmFO-catalyzed reaction has remained elusive due to lack of structural information. The recent crystal structure of *T. thermophilus* TrmFO-H_4folate complex (PDB ID 3G5R) provided some insight into the methylene transfer step in this enzyme's catalysis.[51] In the complex, the pterin ring of the folate is sandwiched between the isoalloxazine moiety of FAD and the imidazole of a histidine residue. Modeling of CH_2H_4folate and manual docking of a tRNA into TrmFO-H_4folate structure places the target U54 in close enough proximity for a direct methylene transfer from CH_2H_4folate to the uracil. Additionally, a conserved cysteine (C51 in *T. thermophilus* TrmFO) located in the vicinity of flavin ring was speculated to nucleophilically activate U54, analogously to the catalytic mechanisms of ThyA and TrmA uridyl methylases (Figs. 1.4A and 1.4D, respectively). Indeed, mutation of C51 to alanine abolished TrmFO activity.

The possibility of covalent catalysis in TrmFO reaction, and the role of the active-site cysteine in particular, were further explored in studies with *B. subtilis* enzyme,[52]

whose structure has not yet been solved. Using a gel mobility-shift assay, it was shown that the wild-type enzyme and several of its mutants formed a covalent adduct with a substrate analog (5F-U54-miniRNA). Contrary to expectations, the alanine mutant of cysteine-53 (equivalent to C51 in *T. thermophilus* TrmFO) was still capable of forming the covalent complex, despite the inability of alanine to act as a nucleophile. Instead, a conserved cysteine-226 far away from the active site (>20 Å in *T. thermophilus* enzyme) appears to fulfill the nucleophilic function, since C226A mutant failed to produce the covalent adduct and to methylate tRNA. On the basis of these observations, a catalytic cascade for TrmFO shown in Fig. 1.4E was proposed. Because C53A mutation abolishes the methylation activity of TrmFO, this residue was suggested to be the general base in step 3 of the mechanism. The C226A/C51A double mutant, just like C226A, formed neither the protein-RNA adduct nor the methylated tRNA product.

Although C226 proposed to activate the uracil is a large distance away from the active site, one possible scenario considered[52] was that a conformational change in protein occurs upon tRNA binding to bring this cysteine closer to the site of chemistry. Partial proteolysis experiments with *B. subtilis* TrmFO showed that enzyme becomes more susceptible to proteolysis in the presence of tRNA, indeed pointing to the changes in protein conformation. In another scenario, TrmFO could dimerize upon binding of tRNA, and C226 of one monomer could activate the C6 of U54-tRNA bound in the active site of the other monomer. Modeling of *T. thermophilus* TrmFO dimer with the target uridine of tRNA in one of the active sites put the uridine C6 atom ~ 6 Å away from the C223 nucleophile, suggesting that a structural change would still be needed to allow C223 to participate in the catalysis. Certainly, a crystal structure of TrmFO enzyme in complex with tRNA substrate could clarify the aspects of its catalysis in the future.

Conclusions

Over the years, structural and mechanistic studies of uracil methylating enzymes provided an insight into how these enzymes work. Majority of these methyltransferases appear to share a catalytic theme (e.g., RumA, TrmA, TrmFO and classical TSase), while others (e.g., FDTS) seem to perform their function via unique chemistry. Such studies are of broad potential utility, ranging from using uracil methyltransferases as potential antibiotic targets to conducting basic research on how various enzymes catalyze the same transformation using different chemical mechanisms. Studies of FDTS enzymes in particular are still in their infancy, and many aspects of their catalysis need further elucidation, which is a major reason for the current scarcity of potent and selective FDTS inhibitors.[43, 44] Considering that FDTS represents an important but under-characterized antibiotic target, future investigation of its chemical mechanism and interactions with the substrates will likely provide the basis for rational design of mechanism-based inhibitors. To this date, the relevance of the folate/FAD-dependent tRNA methyltransferase (TrmFO) to the survival of pathogens has not been elucidated. If future studies reveal its specific activity in the cell, TrmFO might join FDTS on the list of potential enzymatic targets for future antibiotics.

CHAPTER II

TRAPPING OF AN INTERMEDIATE IN THE REACTION CATALYZED BY FLAVIN-DEPENDENT THYMIDYLATE SYNTHASE (FDTS)[ii]

Abstract

Thymidylate is a DNA nucleotide that is essential to all organisms and is synthesized by the enzyme thymidylate synthase (TSase). Several human pathogens rely on an alternative flavin-dependent thymidylate synthase (FDTS), which differs from the human TSase both in structure and molecular mechanism. Recently it has been shown that FDTS catalysis does not rely on an enzymatic nucleophile and the proposed reaction intermediates are not covalently bound to the enzyme during catalysis, an important distinction from the human TSase. This chapter describes the chemical trapping, isolation, and identification of a derivative of such an intermediate in the FDTS-catalyzed reaction. The chemically modified reaction intermediate is consistent with currently proposed FDTS mechanisms that do not involve an enzymatic nucleophile, and has never been observed during any other TSase reaction. These findings establish the timing of the methylene transfer during FDTS catalysis. The presented methodology provides an important experimental tool for further studies of FDTS, which may assist the efforts to rationally design inhibitors as leads for future antibiotics.

Introduction

Thymidylate synthases (TSases) catalyze the last step in the de novo biosynthesis of the DNA nucleotide 2′-deoxythymidine-5′-monophosphate (dTMP) by reductively

---

[ii] This chapter is reprinted from Mishanina, T.V.; Koehn, E.M.; Conrad, J.A.; Palfey, B.A.; Lesley, S.A.; Kohen, A. 2012. *J. Am. Chem. Soc.*, 134, 4442-4448, with permission from ACS.

methylating the uracil moiety of 2′-deoxyuridine-5′-monophosphate (dUMP).[53, 54] There are two currently known classes of TSases that differ in structure, sequence, and cofactor requirements.[55] The homodimeric enzymes encoded by the *thy*A gene (the *TYMS* gene in humans) are referred to here as classical TSases. These have been extensively studied, leading to the established kinetic and chemical mechanisms. Classical TSase enzymes use N^5,N^{10}-methylenetetrahydrofolate (CH_2H_4folate) for both the one-carbon methylene and the reducing hydride to form the C7 methyl of the dTMP product (Figure 2.1a).[54] The more recently discovered *thy*X-encoded proteins utilize a non-covalently-bound flavin adenine dinucleotide (FAD) prosthetic group to catalyze the redox chemistry and use

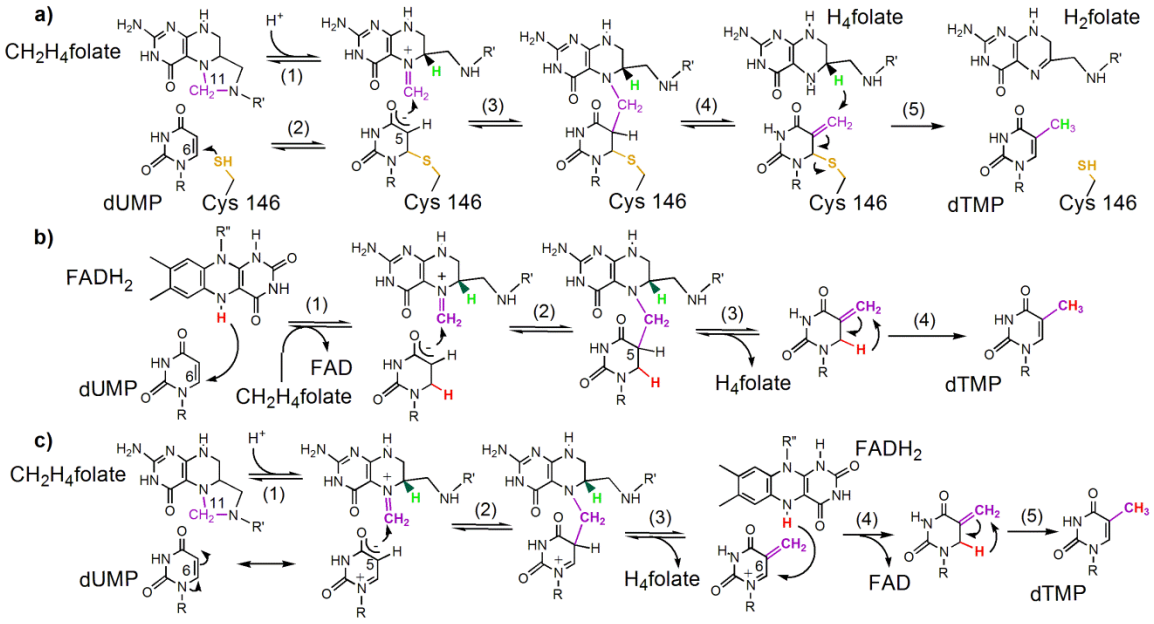

Figure 2.1 Thymidylate synthase chemical mechanisms. a) The mechanism for classical TSase.[53, 54] b) A mechanism proposed for FDTS where dUMP reduction occurs prior to methylene transfer.[56] c) An alternative mechanism proposed for FDTS where reduction happens after methylene transfer.[57] The enzymatic nucleophile is orange, the methylene is purple, the reducing hydride from H_4folate is green, and the hydride from $FADH_2$ is red. R=2′-deoxyribose-5′-phosphate; R′=(*p*-aminobenzoyl)-glutamate; R″=adenosine-5′-pyrophosphate-ribityl.

CH_2H_4folate only as a methylene donor. These flavin-dependent thymidylate synthases (FDTSs) are found primarily in prokaryotes, including several pathogens and biological warfare agents.[29, 55] The structural and mechanistic differences between FDTS and classical TSase present an enticing new avenue for the development of antibiotics with a potential for minimal toxicity to humans.

Several mechanism-based drugs targeting classical TSase are available today (e.g. 5-fluorouracil, 5-trifluoromethyl 2′-deoxyuridine, raltitrexed, etc.).[19, 58, 59] Development and identification of these compounds relied greatly on the knowledge of the molecular mechanism of catalysis and identification of reaction intermediates for the classical TSase reaction. To emphasize the differences in catalysis from the FDTS enzymes under study here, we present the established chemical mechanism of the classical TSase (Figure 2.1a). In short, the classical TSase reaction begins with an active site cysteine covalently activating dUMP via Michael addition (step 2), which then undergoes a Mannich-type condensation with the methylene of CH_2H_4folate (step 3). The resulting bridged intermediate eliminates H_4folate (step 4) to form an enzyme-bound exocyclic methylene intermediate, which accepts a hydride from H_4folate (step 5) producing H_2folate and the product dTMP.[53, 54] Step 3 of this mechanism is supported by the quenching experiments with wild-type *Lactobacillus casei* TSase[15], the crystal structure of the covalent complex of wild-type *Escherichia coli* enzyme with 5F-dUMP and CH_2H_4folate, and the isolation on SDS-PAGE of the enzyme-bound bridged intermediate (between steps 3 and 4) in reactions of E60A and E60L mutants of *Lc*TSase with radiolabeled substrates.[16] The existence of the exocyclic methylene intermediate (between steps 4 and 5) was supported by experiments with a W82Y mutant of *Lc*TSase, which allowed chemical trapping with β-mercaptoethanol under steady state conditions.[60]

A few moderate inhibitors of FDTS enzymes have been developed, none of which are mechanism-based nor have shown highly specific inhibition of FDTS over classical TSase.[43, 61] Potent inhibitors of classical TSase, such as 5F-dUMP, produce moderate

reversible inhibition of FDTS, and crystal structures of FDTS with 5F-dUMP (e.g. P.D.B accession 1tls) present non-covalently bound complexes that do not provide significant information about the catalytic mechanism or intermediate structures.[56, 62]

One of the most convincing evidence for any chemical mechanism is the identification and characterization of reaction intermediates. Although several chemical mechanisms have been proposed for FDTS, direct evidence of the identity of any of the proposed reaction intermediates has been previously unavailable.[56, 57, 62-66] In this chapter we show that a reaction intermediate can be chemically trapped and isolated during a single-turnover oxidative half-reaction of FDTS (conversion of dUMP to dTMP only occurs during the oxidative half-reaction where $FADH_2$ reacts to form FAD). The identification of the trapped intermediate described below indicates that it is not covalently bound to the enzyme and already includes the methylene originally carried by the CH_2H_4folate. This finding together with the time course of accumulation and decay of this intermediate limits the options for potential mechanisms and provides a timeframe for key chemical events of FDTS catalysis.

Results and Discussion

Identification of reaction intermediates is key to elucidation of any chemical reaction's mechanism. Our spectroscopic findings (ref 57) suggested possible accumulation of intermediate(s) in the oxidative half-reaction of FDTS. Below, we present the chemical trapping of such a reaction intermediate(s) and the identification of the trapped species.

Acid-quenching of the oxidative half-reaction of FDTS

In order to determine whether any intermediate(s) accumulate during the FDTS-catalyzed reaction, a series of quench-flow experiments were performed. To increase the chance for intermediate trapping, we used a hyperthermophilic FDTS from *T. maritima* and carried out the reactions at room temperature – significantly below *T. maritima*'s

physiological 80 ^{o}C − enhancing the duration and magnitude of intermediate accumulation. Briefly, the FAD bound to *T. maritima* FDTS enzyme was stoichiometrically reduced with dithionite under anaerobic conditions, allowing $FADH_2$ to serve as the limiting reactant in the oxidative half-reaction under study (i.e., conversion of dUMP to dTMP). The dUMP was bound to the pre-reduced enzyme prior to the reaction since in the catalytic turnover this substrate binds before CH_2H_4folate and probably even prior to the flavin reduction.[57, 67, 68] Oxidative FDTS half-reactions were then initiated by rapid mixing with CH_2H_4folate and quenched with 1 M HCl at various reaction times (for details see Methods section below).

By quantitatively tracking the substrate dUMP and product dTMP by LC-MS, we were able to construct a time course for the oxidative FDTS half-reaction. Figure 2.2 shows the total ion counts measured at various reaction times for dUMP, dTMP, and their sum (which represents the total amount of material accounted for by these species). It was noticed that for time points between ~ 0.5-10 seconds the sum of the ion counts for dUMP and dTMP was substantially less than at the beginning and the end of the reaction. This observation suggests that a reaction intermediate has accumulated during this time period. This finding is in accordance with the observed lag in product formation,[57] but does not reveal the identity of the intermediate, leading to the next set of experiments.

Following intermediate formation using radiolabeled substrates

To characterize the acid-trapped intermediate, it was first necessary to identify this material in the chromatographic analysis. To do so, ^{14}C-radiolabled substrates were used where the labeled carbon was either on the dUMP or the methylene of the CH_2H_4folate. The oxidative turnover of FDTS with the radiolabeled nucleotide, [2-^{14}C]-

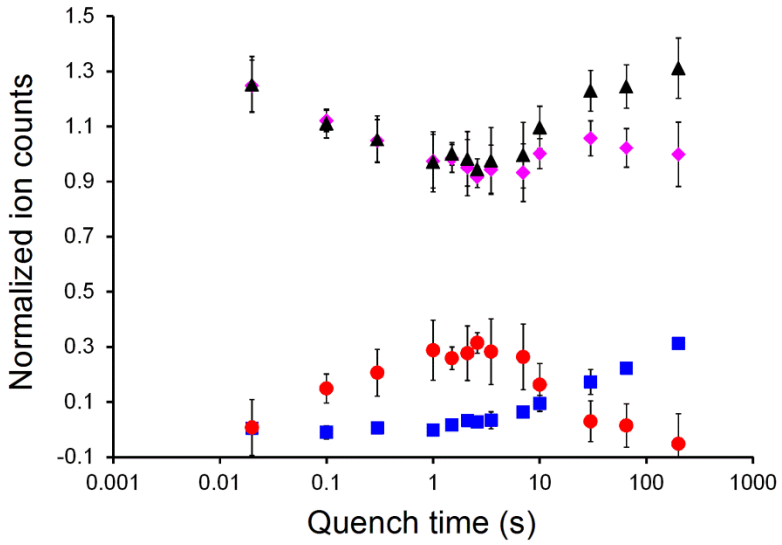

Figure 2.2 Single-turnover FDTS reaction. Total ion counts for dUMP and dTMP determined by LC-MS analysis are given for dUMP (purple diamonds) and dTMP (blue squares). Notably, the sum of the counts for dUMP and dTMP (black triangles) is not conserved during the reaction, suggesting the accumulation of an intermediate (red circles).

dUMP, was quenched with acid at various times, as described above and under the Methods. Figure 2.3a shows an HPLC-radiogram of a reaction quenched at 2 seconds, where under the reaction conditions about 80% of the total radioactivity was in the form of the trapped intermediate. All the initial radioactivity was accounted for in the radiograms and the total radioactive counts (dUMP, dTMP, and the newly identified peak) remained constant at all quenched reaction times (Figure 2.3c, in which each time point originates from a radiogram like the one presented in Figure 2.3a), suggesting that all the missing nucleotide observed in the LC-MS analysis above was being accounted for by this single newly developing radioactive peak. It is also noteworthy that the fraction of total radioactivity associated with the new radioactive material accumulates and decays during the course of the singe-turnover half-reaction, a behavior typical of enzymatic intermediates (Figure 2.3c).

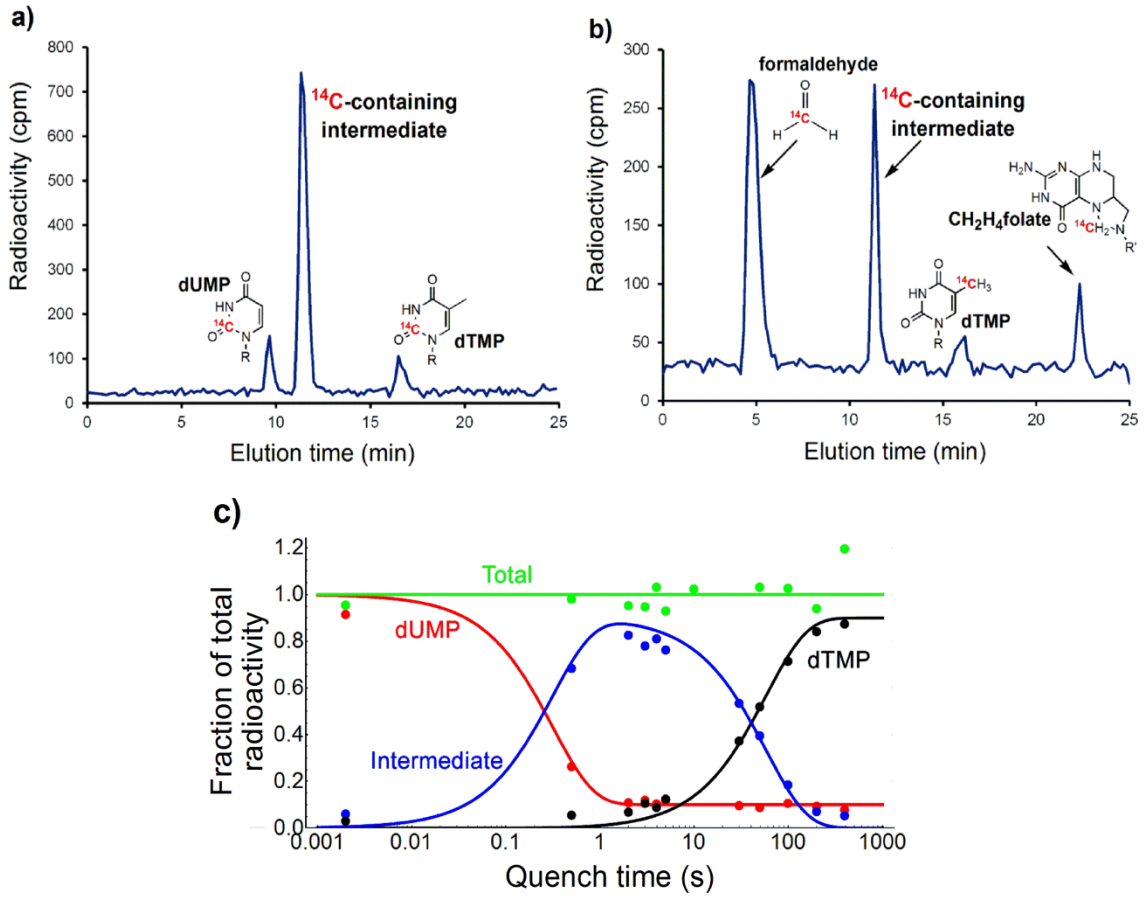

Figure 2.3 Intermediate trapping using ^{14}C-labeled substrates. HPLC radiograms for FDTS reactions quenched at 2 seconds with 1M HCl starting with either (a) ^{14}C-labeled dUMP, or (b) ^{14}C-labeled CH_2H_4folate. The labeled carbon is shown in red. In both cases, ^{14}C-containing trapped intermediate elutes at ~11 minutes, representing the same trapped species. Panel (c) presents single-turnover FDTS reaction with [2-^{14}C]-dUMP as a radiotracer as a function of oxidative half-reaction time. Each time point results from a radiogram like 2.3a (2 sec reaction point). The curves represent dUMP (red), intermediate (blue), and dTMP (black) kinetics globally fitted to a mechanism with one intermediate, i.e., minimal model, as described under Methods. The total radioactive counts (dUMP, dTMP and the intermediate combined) are shown in green.

To test whether the trapped species already contains the methylene from the cofactor CH_2H_4folate, we performed another crucial experiment wherein the enzyme mixed with non-labeled dUMP was reacted with [11-^{14}C]-CH_2H_4folate under the same conditions as above. By following the radiolabeled methylene we found that when

quenching at 2 seconds a new radioactive peak developed that had the same retention time as the peak observed when starting with [2-^{14}C]-dUMP (Figure 2.3b). This clearly shows that the intermediate nucleotide that is being chemically trapped during the acid-quenching has already undergone the condensation with CH_2H_4folate, and the carbon-carbon bond between the C5 of dUMP and the methylene has been formed prior to the formation of that intermediate.

Since reactions of classical TSase with the radioactive starting materials above would have led to an enzyme bound intermediate, we carefully checked for radioactivity bound to enzyme in our experiments (see Methods below). In accordance with the fact that all radioactivity was accounted for in the radiograms (Figure 2.3), no radioactivity was identified on the enzyme from the same quenched samples, providing no support for enzyme bound intermediate(s).

Characterization and identification of the acid-trapped intermediate

Once the chromatographic elution time of the trapped intermediate was known, non-radioactive FDTS reactions were quenched at ~2 seconds, which produced the largest amount of trapped intermediate, and were purified by HPLC. The purified trapped intermediate was analyzed by high-resolution ESI-MS and was found to have an $[M-H]^-$ ion at *m/z* 337.0432, which is consistent with the exact mass and atomic composition of the product dTMP plus a hydroxyl group (i.e. 17 a.m.u.). The possibility of the trapped intermediate being 5-hydroxymethyl-dUMP was tested by comparison of HPLC retention time, HRMS, and MS-MS data for the purified trapped intermediate with those of the synthetic 5-hydroxymethyl-dUMP (see Methods), as shown in Figure 2.4. LC-MS analyses of reactions quenched at short (2 msec) or long (400 sec) times did not contain 5-hydroxymethyl-dUMP, indicating that it is not a pre-existing contaminant. Furthermore, the accumulation and decay pattern observed when using radioactive

substrates (Figure 2.3c) was consistent with the accumulation and decay of the intermediate as analyzed by LC-MS (Figure 2.2).

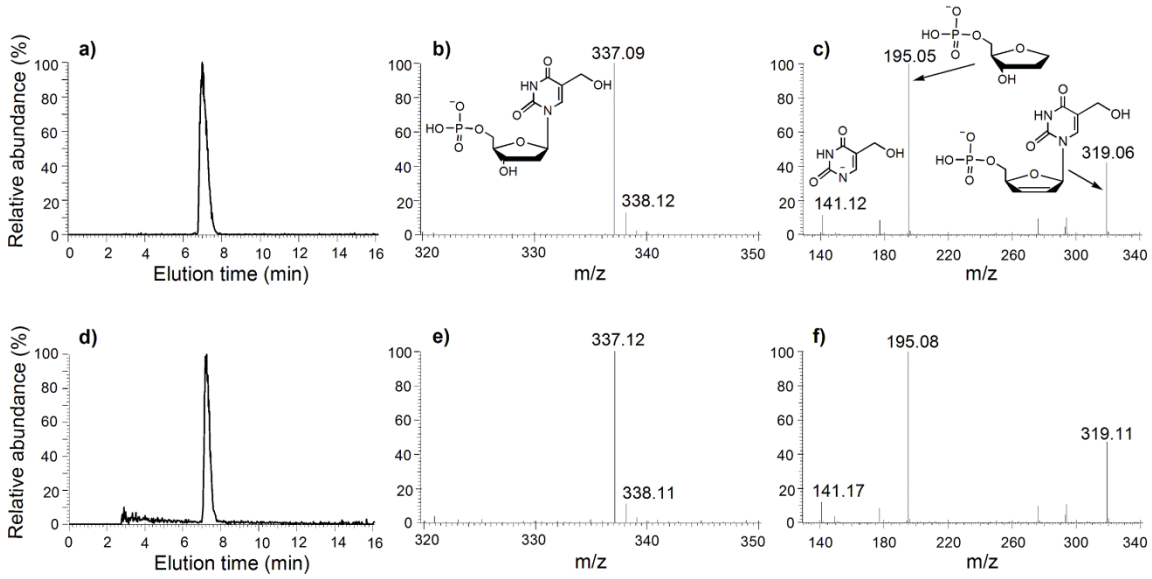

Figure 2.4 LC-ESI data for the synthesized 5-hydroxymethyl-dUMP standard (top panel) and the trapped intermediate (bottom panel). Shown are the chromatograms (a and d), MS (b and e) and MS-MS data (c and f) for the standard and the trapped intermediate, respectively. All spectra were collected in the negative-ion mode. The structures of the ions with the observed masses are shown. By these analyses, the synthesized standard was indistinguishable from the trapped intermediate.

Mechanistic implications

Reactions of classical TSase enzymes with the same radiolabeled substrates, as described above, led to accumulation and isolation of the covalent bridged intermediate (Figure 2.1a, between steps 3 and 4).[16] No such enzyme-bound species was found with FDTS (see Methods), and all the radiolabeled trapped material was accounted for in the reactant, product, and a single, soluble intermediate. Thiol addition to the enzyme-bound exocyclic methylene intermediate in classical TSase mutants (Figure 2.1a, between steps 4 and 5) resulted in chemical modification at C7 to form the thioether.[60] Our efforts to

use thiols as trapping reagents (see Methods) resulted in no trapped species during the FDTS-catalyzed reaction. These observations further emphasize the mechanistic differences between classical TSase and FDTS.

Substantial evidence has been published indicating that the FDTS-catalyzed reaction occurs without participation of an enzymatic nucleophile, a notable deviation from not only classical TSase but also other uridyl-methylating enzymes.[56, 62] The mechanism for FDTS catalysis presented in Figure 2.1b was proposed following mutagenesis and isotope labeling studies with *Tm*FDTS that did not support a nucleophilic attack on dUMP by any enzymatic residue.[56] In this mechanism, dUMP accepts a hydride from the N5 of $FADH_2$ (step 1) generating an enolate that attacks the iminium form of CH_2H_4folate (step 2). Elimination of tetrahydrofolate (H_4folate, step 3) results in a putative exocyclic methylene intermediate, which would need to isomerize to form dTMP (step 4). In Figure 2.5a, we suggest a mechanism for water addition under acidic conditions to the isomer of dTMP proposed in Figure 2.1b. Notably, if 5-hydroxymethyl-dUMP does originate from treating this isomer of dTMP with acid, it requires oxidation (i.e. loss of a proton and two electrons) to form the acid-trapped

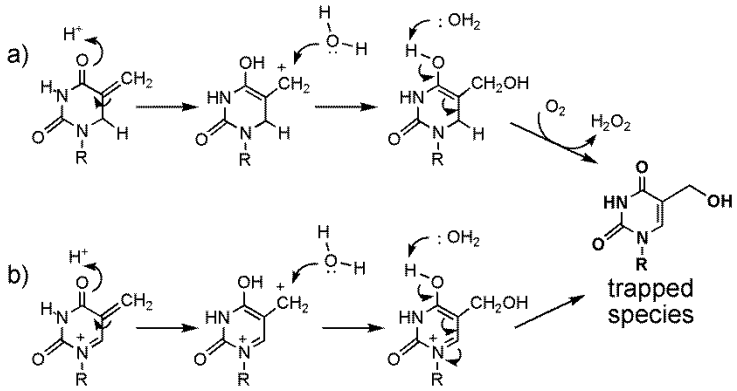

Figure 2.5 Possible mechanisms for acid trapping of the intermediates proposed in Figures 2.1b (a) and 2.1c (b).

species. Molecular oxygen is proposed as a likely hydride acceptor in the last step of mechanism 2.5a because quenched reactions are exposed to oxygen immediately after quenching.

More recent studies, following flavin absorbance in an oxidative half-reaction by stopped-flow technique, showed that flavin oxidation is not likely to be the initial step in FDTS catalysis and led to an alternative mechanistic option for FDTS catalysis, presented in Figure 2.1c.[57] In this mechanism, dUMP is electronically polarized upon binding the enzyme, leading to nucleophilic attack from C5 of dUMP with no covalent activation at C6. Methylene transfer can then occur (step 2), followed by elimination of H_4folate (step 3). The resulting exocyclic-methylene cation is then reduced by a hydride from $FADH_2$ (step 4) to form the exocyclic isomer of dTMP (if reduced at the C6 as suggested in ref 14 based on deuteration of C6), which can isomerize to form dTMP (step 5). The exocyclic-methylene cation proposed to form after step 3 could readily undergo hydroxyl addition in acidic media to yield 5-hydroxymethyl-dUMP, as depicted in Figure 2.5b. In this last case, water addition to the methylene of the cationic intermediate could also occur without prior protonation of the carbonyl oxygen, still resulting in 5-hydroxymethyl-dUMP.

The mechanism proposed in Figure 2.1b requires a hydride transfer from the reduced flavin prior to the formation of a methylene-bridged intermediate, while the mechanism in Figure 2.1c offers an option that does not require flavin redox chemistry until after the methylene transfer. In attempt to further distinguish between these two mechanisms, we repeated quenching experiments without pre-reducing the flavin, i.e., the enzyme had bound FAD rather than $FADH_2$, and [2-^{14}C]-dUMP prior to mixing with CH_2H_4folate. We found no intermediates that accumulate, suggesting that the reduced flavin is required to form the intermediate that we have shown to contain the transferred methylene. While this observation is in accordance with the mechanism proposed in Figure 2.1b, it does not eliminate the mechanism in Figure 2.1c, because it is possible

that even though the reduced flavin might not participate in redox chemistry until after the elimination of H_4folate (as suggested in Figure 2.1c), it does play a role in a conformational change in the enzyme, which is needed to bring both substrates in a reactive configuration.

Spectral evidence has also suggested that more than one reaction intermediate may accumulate during the FDTS reaction.[57] Yet, at all reaction times analyzed here, only one acid-trapped species was identified. Furthermore, in reactions using radiolabeled substrates, the total radioactive counts are always conserved amongst dUMP, 5-hydroxymethyl-dUMP, and dTMP, and the reaction time-course fits reasonably well to a simple mechanism with one intermediate (Figure 2.3c). The two spectral species and the single acid-trapped intermediate could be consolidated if the acid modification of more than one intermediate leads to the formation of 5-hydroxymethyl-dUMP, e.g., bridged dUMP-CH_2H_4folate species transiently accumulating prior to the formation of the exocyclic methylene intermediate.

Methods

Materials

All chemicals were reagent grade and used as purchased without further purification, unless specified. 2′-deoxyuridine 5′-monophosphate (dUMP), 5-hydroxymethyl-2′-deoxyuridine (5-hydroxymethyl-dU), glucose oxidase powder, D-glucose, D_2O, and formaldehyde solution (36.5% by weight) were obtained from Sigma. N^5,N^{10}-methylene-5,6,7,8-tetrahydrofolate (CH_2H_4folate) was provided by Eprova Inc. (Schaffhausen, Switzerland). Radiolabeled [2-^{14}C]-dUMP was purchased from Moravek Biochemicals. Radiolabeled [11-^{14}C]-CH_2H_4folate was prepared according to the previously developed chemoenzymatic synthesis procedure.[69] Sodium dithionite powder was purchased from J.T. Baker, and tris(hydroxymethyl)aminomethane was obtained from Research Products International Corp. The FDTS from *Thermatoga maritima*

(TM0449, GenBank accession number NP228259) was expressed and purified as previously described.[29] Human deoxycytidine kinase mutant dCK-DM was a generous gift from Dr. Arnon Lavie at the University of Illinois-Chicago.

Synthesis of 5-hydroxymethyl-2′-deoxyuridine-5′-monophosphate (5-hydroxymethyl-dUMP)

The synthesis procedure has been previously reported and was adapted from ref 70. More specifically, the 5-hydroxymethyl-dUMP was synthesized by phosphorylation of commercial 5-hydroxymethyl-dU at 37 ºC in a 100 mM Tris, 10 mM $MgCl_2$, 100 mM KCl buffer at pH 7.5. The final reaction mixture contained 2 mM 5-hydroxymethyl-dU, 4 mM ATP, and 10 units/mL of deoxycytidine kinase (dCK-DM). The 5-hydroxymethyl-dUMP product was purified by HPLC-UV/Vis and analyzed by LC-ESI-MS and MS-MS (Figure 2.4).

Analytical Methods

Separations were carried out on an Agilent series HPLC, with UV/vis diode array detector and 500TR series Packard flow scintillation analyzer. An analytical reverse phase Supelco column (C18, Discovery series 250 mm X 4.6 mm) was used with 50 mM KH_2PO_4 at pH 6 followed by a gradient of methanol. The concentration of enzyme for rapid-quenching experiments was determined by the 454 nm absorbance of bound FAD (ε = 11,300 $cm^{-1}M^{-1}$). Liquid chromatography-mass spectrometry (LC-MS) analysis was performed on UltiMate 3000 Dionex LC system, using an eluent gradient of water and acetonitrile containing 0.1% formic acid, followed by a Finnigan LCQ deca mass spectrometer. High-resolution mass analysis was done on a Waters Q-TOF mass spectrometer.

Purification Methods

The trapped intermediate and 5-hydroxymethyl-dUMP were purified by HPLC using an analytical (Discovery series 250 mm X 4.6 mm) or a semipreparative (Discovery series 250 mm X 10 mm) reverse phase Supelco columns, respectively. Mobile phase used for separation was a gradient of 50 mM KH_2PO_4 at pH 6 (for purification of the intermediate) or 100 mM KH_2PO_4 at pH 2 (for purification of synthesized 5-hydroxymethyl-dUMP) and methanol. Elution of the species of interest was monitored by UV absorbance (at 267 nm). Eluent containing the purified species was collected, lyophilized to dryness, and dissolved in H_2O for LC-MS, MS-MS, and high-resolution-MS analyses.

Acid quenching of FDTS during the oxidative half-reaction

A solution of oxidized FDTS (100 μM) was made anaerobic in a sealed tonometer by cycles of applied vacuum and equilibration with purified argon. The anaerobic enzyme was reduced stoichiometrically with a dithionite solution as followed spectrophotometrically (at 454 nm). The reduced FDTS was then mixed with dUMP (92 μM) from a side-arm of the tonometer and loaded on a KinTek Chemical Quench-Flow instrument (model RQF-3), which had been previously scrubbed of oxygen with a glucose/glucose oxidase solution (50 units/mL). An anaerobic 400 μM CH_2H_4folate solution was prepared containing 50 units/mL glucose oxidase, 10 mM glucose (to assure anaerobic conditions) and 30 mM formaldehyde (to stabilize CH_2H_4folate). FDTS reactions were initiated by rapid mixing of the enzyme/dUMP and CH_2H_4folate solutions in the instrument and quenched at various time points with 1 M HCl. The quenched reactions were analyzed by HPLC with UV-vis diode array, radioactivity flow detection and by LC-MS.

Searching for an enzyme-bound intermediate(s)

The acid-quenched oxidative half-reactions of FDTS with [2-^{14}C]-dUMP were spun in a microcentrifuge, and the radioactivity in supernatant was quantified by liquid-scintillation counting (LSC). The FDTS protein pellets (denatured enzyme) were analyzed on 10% SDS-PAGE. To test for protein-bound radioactive nucleotide, coomassie-stained FDTS bands were excised, solubilized with 30% hydrogen peroxide, and counted by LSC. In a separate analysis, the enzyme pellets were re-suspended in water and filtered to remove the residual soluble radioactivity. Both the filtrate and the washed pellets were then analyzed by LSC.

Searching for intermediates by thiol trapping during the FDTS reaction

Steady-state reactions containing 1 μM FDTS, 100 μM dUMP, 500 μM NADPH, 500 μM CH_2H_4folate and a trace of [2-^{14}C]-dUMP were incubated at 37^{o}C. β-mercaptoethanol (3 M) was added at 1 minute and aliquots were withdrawn at 1.5, 3 and 5 min for analysis. Single turnover FDTS (20 μM) reactions with 10 mM dithionite (excess to ensure a high quantity of reactive thiol), 500 μM CH_2H_4folate and limiting [2-^{14}C]-dUMP (10 μM) were manually quenched with 1 M HCl at 1-2 seconds. The aliquots from both experiments were dried by speed-vacuum and re-suspended in water or neutralized (for HCl samples) and analyzed by HPLC with a radioactivity flow detector.

Data fitting for FDTS reaction kinetics

Mathematica was used to fit the data to a mechanism with one reaction intermediate (Figure 2.3c):

$$\text{dUMP} \xrightarrow{k_1} \text{Intermediate} \xrightarrow{k_2} \text{dTMP}$$

The following set of rate equations was used in the fitting:

$$\frac{d}{dt}[dUMP] = -k_1 \cdot [dUMP]$$

$$\frac{d}{dt}[Intermediate] = k_1 \cdot [dUMP] - k_2 \cdot [Intermediate]$$

$$\frac{d}{dt}[dTMP] = k_2 \cdot [Intermediate]$$

Conclusions

Rapid acid-quenching experiments with *Tm*FDTS at room temperature resulted in chemical trapping of a reaction intermediate, which was not covalently bound to the enzyme and was identified as 5-hydroxymethyl-dUMP. This provides evidence for the existence of non-covalently bound intermediates (Figures 2.1b and 2.1c) and indicates the timing of carbon bond formation between dUMP and CH_2H_4folate. Importantly, this trapped species has not been isolated from any classical TSase, supporting the notion that the FDTS-catalyzed reaction proceeds via a unique chemical mechanism, providing a new and unique target for mechanism based antibiotic drug design. The identification of this acid-trapped intermediate adds new restrictions to possible mechanism and eliminates several mechanisms proposed in the past.[63-66, 71] The identified timing of intermediate(s) accumulation will be crucial for future efforts to characterize the intermediate following different chemical trapping agents, or the unmodified intermediate(s). While the trapping of 5-hydroxymethyl-dUMP in the FDTS reaction emphasizes the mechanistic distinctions from classical TSase and eliminates some proposed mechanisms, further examination is needed before the mechanisms proposed in Figures 2.1b and 2.1c are distinguished and/or revised. Additionally, now that the acid quenched intermediate has been identified, the synthesized 5-hydroxymethyl-dUMP can serve as a standard in acid-quenching experiments with FDTSs from mesophilic organisms and pathogens. This will test whether these enzymes follow the same catalytic mechanism as *Tm*FDTS, where for these FDTSs at room temperature an intermediate is expected to accumulate to a lesser extent and at much earlier time points.

CHAPTER III

SUBSTRATE ACTIVATION IN FLAVIN-DEPENDENT THYMIDYLATE SYNTHASE[iii]

Abstract

Thymidylate is a critical DNA nucleotide that has to be synthesized in cells *de novo* by all organisms. Flavin-dependent thymidylate synthase (FDTS) catalyzes the final step in this *de novo* production of thymidylate in many human pathogens, but is absent from humans. FDTS reaction proceeds via chemical route that is different from its human enzyme analogue, making FDTS a potential antimicrobial target. The chemical mechanism of FDTS is still not understood, and the two most recently proposed mechanisms involve reaction intermediates unusual to pyrimidine biosynthesis and biology in general. These mechanisms differ in the relative timing of the reaction of the flavin with the substrate. The consequence of this difference is significant: the intermediates are cationic in one case and neutral in the other, an important consideration in the construction of mechanism-based enzyme inhibitors. Here we test these mechanisms via chemical trapping of reaction intermediates, stopped-flow and hydrogen isotope exchange techniques. The findings described in this chapter suggest that an initial activation of the pyrimidine substrate by reduced flavin is required for catalysis, and a revised mechanism is proposed based on previous and new data. These findings and the newly proposed mechanism add an important piece to the mechanistic puzzle of FDTS, and suggest a new class of intermediates that in the future may serve as targets for mechanism-based design of FDTS-specific inhibitors.

[iii] This chapter (by Tatiana V. Mishanina, John M. Corcoran and Amnon Kohen) has been accepted for publication as a Communication in *Journal of American Chemical Society* on July 15, 2014.

Research Report

Thymidylate (2′-deoxythymidine-5′-monophosphate, or dTMP), an important DNA precursor, can either be scavenged by the cells from thymidine in the environment, via thymidine kinase-catalyzed phosphorylation, or generated in cells *de novo*. The last committed step in the intracellular *de novo* biosynthesis of dTMP is catalyzed by the enzyme thymidylate synthase (TSase). TSase is encoded by *thyA* gene in eukaryotes and *TYMS* gene in mammals, while in many pathogenic bacteria and viruses this protein is the product of a completely different gene, *thyX*.[7, 35, 42] TSase enzymes realize two chemical transformations: the substitution of the C5 hydrogen of substrate 2′-deoxyuridine-5′-monophosphate (dUMP) with the methylene from the N^5,N^{10}-methylene-5,6,7,8-tetrahydrofolate (CH_2H_4fol) cofactor, and the reduction of the transferred methylene by a hydride to form the C5 methyl of the product dTMP (Figure 3.1). The *thyA*-encoded TSase uses CH_2H_4fol as a source of both the methylene and the reducing hydride.[1, 13] In *thyX*-encoded TSase, on the other hand, the hydride is supplied by the reduced flavin adenine dinucleotide prosthetic group ($FADH_2$).[27, 72] Furthermore, the *thyA*- and *thyX*-encoded TSases share no sequence or structural resemblance and have been shown to catalyze dUMP→dTMP conversion by completely different chemical mechanisms.[73] This structural and mechanistic divergence of the two enzymes provides an attractive direction for the design of drugs tailored to microbial thymidylate biosynthesis.

The catalytic mechanism of *thyA*-encoded classical TSase enzymes has been studied for many years. In the chemical mechanism of classical TSase,[1, 13] the enzyme activates dUMP for subsequent reaction via a nucleophilic attack at C6 of the uracil by an active-site cysteine. This mechanistic feature is conserved in all *thyA*-encoded TSases, as well as in other uracil-methylating enzymes (e.g. rRNA- and tRNA-methyltrasferases),[73] and has been exploited by chemotherapeutic drugs targeting TSase (e.g. 5-fluorouracil).[19] In contrast to *thyA*-encoded TSase, flavin-dependent TSase (FDTS) bypasses the need for an active-site nucleophile.[36] Instead, FDTS has been proposed to accomplish substrate

activation by either direct $FADH_2$ reduction of dUMP to form reactive enolate (step 1 in Figure 3.1a), or polarization of the uracil moiety in the active site to make the C5 nucleophilic (resonance form of dUMP in Figure 3.1b).[74] The possibility that the N5 of $FADH_2$ nucleophilically activates dUMP has been eliminated by the observation that 5-carbe-5-deaza-FAD-FDTS is still active.[36] As described below, the hydrogen isotope exchange on dUMP supports substrate activation by the reduced flavin (Figure 3.1a). However, the deuteration of the substrate and product but not the trapped intermediate in FDTS reactions in D_2O cannot be explained by either one of the mechanisms in Figure 3.1, and call for an alternative proposal.

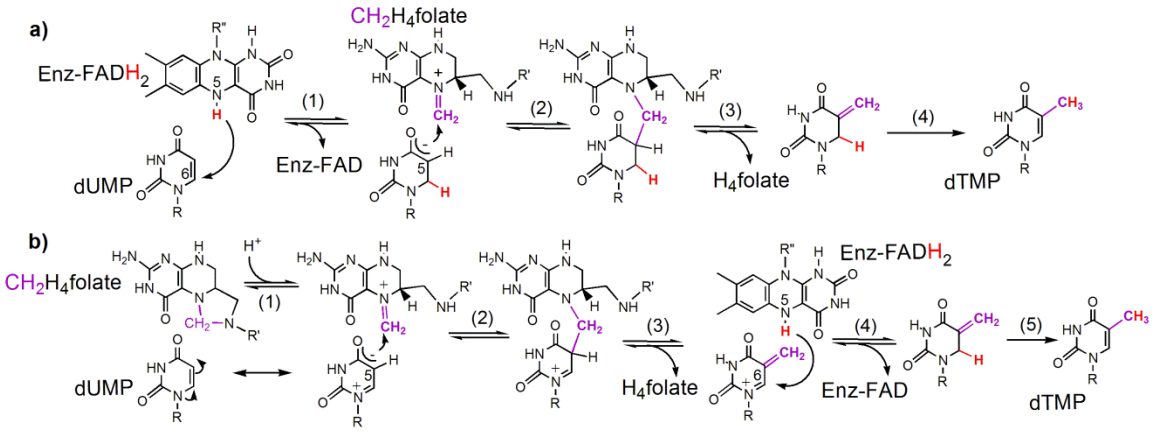

Figure 3.1 Proposed chemical mechanisms for FDTS (adapted from ref 74 with copyright permission from ACS). R=2′-deoxyribose-5′-phosphate; R′=(*p*-aminobenzoyl)-glutamate; R″=adenosine-5′-pyrophosphate-ribityl.

The direct hydride transfer from the N5 of reduced flavin to dUMP (Figure 3.1a) was proposed to initiate the reaction based on the deuterium incorporation at C6 of dTMP, in the reactions of *Thermatoga maritima* FDTS in D_2O conducted at sub-physiological temperatures.[36] In all FDTS crystal structures in complex with both FAD and dUMP, the N5 of the FAD is indeed in close proximity of the C6 of dUMP (ca. 3.4

Å), consistent with the postulated direct hydride transfer from the flavin. This chemistry is unusual to thymidylate biosynthesis and uridine methylation in general, but not without precedent in enzymology. For example, direct hydride addition from reduced flavin to an equivalent position of α,β-unsaturated substrates similar to dUMP occurs in the reactions catalyzed by the old-yellow enzyme[75] and dihydroorotate dehydrogenase.[76] By the proposal in Figure 3.1a, substrate reduction by $FADH_2$ (i.e. flavin oxidation) takes place *prior* to the methylene transfer; consequently, the reaction intermediates along this path are reduced and non-aromatic in nature.

In an alternative mechanism (Figure 3.1b), dUMP is activated for the reaction with CH_2H_4fol via electronic polarization of the uracil moiety in the enzyme's active site upon binding. This dUMP polarization was proposed as the initial step based on disappearance of dUMP in a single turnover experiment occurring before flavin oxidation (ref 74 and green trace in Figure 3.2). To the best of our knowledge, no such addition of

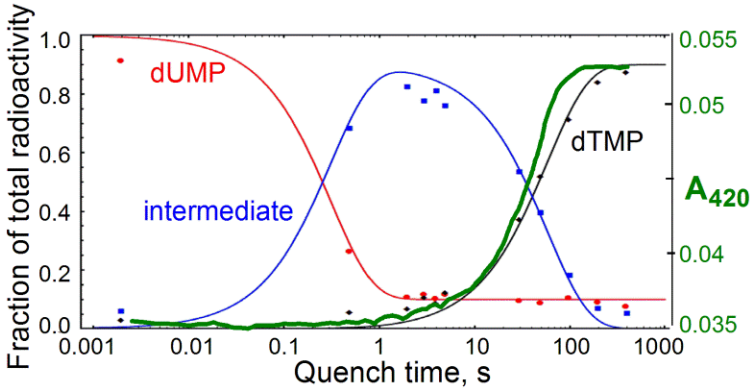

Figure 3.2 Single-turnover FDTS reaction kinetics overlaid with stopped-flow flavin absorbance trace (green, this work). Reduced flavin ($FADH_2$) has no 420 nm absorbance, while oxidized flavin (FAD) does. Adapted from ref 74 with permission from ACS.

formaldehyde and/or Mannich amines (analogous to iminium CH_2H_4fol) to the C5 of uracil has ever been observed without the aid of a nucleophile, either in enzymes or solution; nevertheless, such chemistry does not violate any obvious chemical rules. Following elimination of H_4fol from the dUMP-folate adduct (step 3 in Figure 3.1b), a positively charged exocyclic-methylene intermediate would be obtained. This intermediate can then be reduced by $FADH_2$ at C6 to yield the same isomer proposed in Figure 3.1a, accounting for the observed D6 in the product dTMP.[36] In such a mechanism, flavin oxidation happens *after* the methylene transfer, and as a consequence, the reaction intermediates are not reduced, in sharp contrast to the mechanism in Figure 3.1a.

Recently, a derivative of an intermediate(s) in FDTS-catalyzed thymidylate synthesis has been isolated and characterized, in rapid acid-quenching experiments conducted at room temperature (see chapter II of this thesis and ref 74). This trapped species (5-hydroxymethyl-dUMP, or 5-HM-dUMP, in Figure 3.3) already contains the methylene of CH_2H_4fol. 5-HM-dUMP is consistent with either of the two proposed mechanisms for FDTS (Figure 3.1) and does not distinguish between them. In the current chapter, in an attempt to differentiate between the mechanisms, we repeated acid-quenching experiments with FDTS reactions taking place in deuterated water (D_2O). The reaction conditions were kept the same as in the quenching studies in H_2O,[74] except all reactants and buffers were exchanged into D_2O by cycles of lyophilization and re-suspension in heavy water (99.9% D). In D_2O all exchangeable hydrogens, including the N5 hydrogen of the reduced flavin to be transferred to the uracil moiety, are exchanged with their heavier isotopes. Thus we anticipated that if the hydride from the flavin is transferred to the dUMP before the methylene (Figure 3.1a), then a portion of acid-trapped 5-HM-dUMP would be deuterated, i.e. one mass unit heavier than in the reactions conducted in H_2O (Figure 3.3a). On the other hand, by the mechanism proposed in Figure 3.1b, no effect on the mass of the trapped intermediate was expected (Figure

3.3b). As seen in Figure 3.4, no deuterium enrichment is observed in 5-HM-dUMP isolated in the D_2O experiment. Importantly, all dTMP product present in D_2O reactions was singly deuterated, eliminating the possibility of protium contamination in the experiment and in accordance with previously reported deuterium incorporation into dTMP.[36]

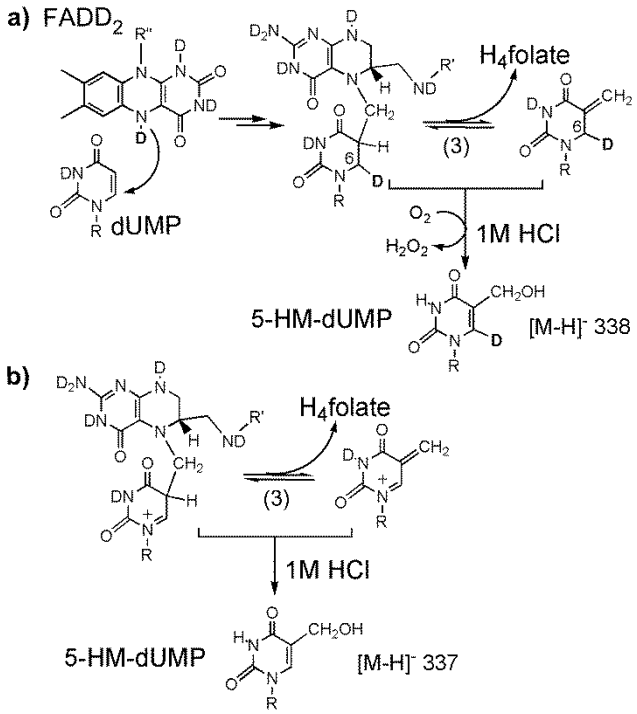

Figure 3.3 Acid trapping of the proposed intermediates in the reaction with deuterium-labeled flavin ($FADD_2$). Formation of 5-HM-dUMP in (a) requires oxidation of the reduced intermediates at C6, i.e. loss of a hydron (H^+ or D^+) and two electrons. Due to an isotope effect on this non-enzymatic oxidation, majority of 5-HM-dUMP is expected to be deuterated. Molecular oxygen has been proposed as the oxidant[74] since quenched reactions are exposed to oxygen during quenching.

The above observation appears to support the mechanism suggested in Figure 3.1b; however, while analyzing acid-quenched FDTS reactions conducted in D_2O by MS, we noticed that a significant portion (>60%) of unreacted substrate, dUMP, was singly

deuterated (Figure 3.5b). Much longer incubations of the same reaction mixture with the oxidized FDTS yielded no trace of deuterated dUMP (Figure 3.5c). This observation is inconsistent with the polarization mechanism in Figure 3.1b, which does not require

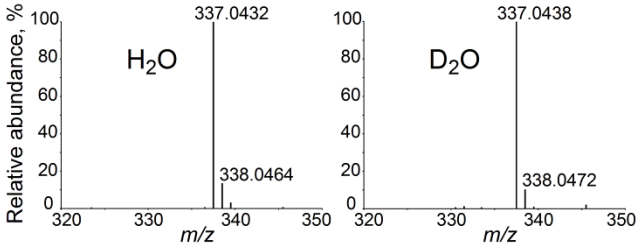

Figure 3.4 HRMS of 5-hydroxymethyl-dUMP isolated from the acid-quenched FDTS reactions in H_2O and D_2O.

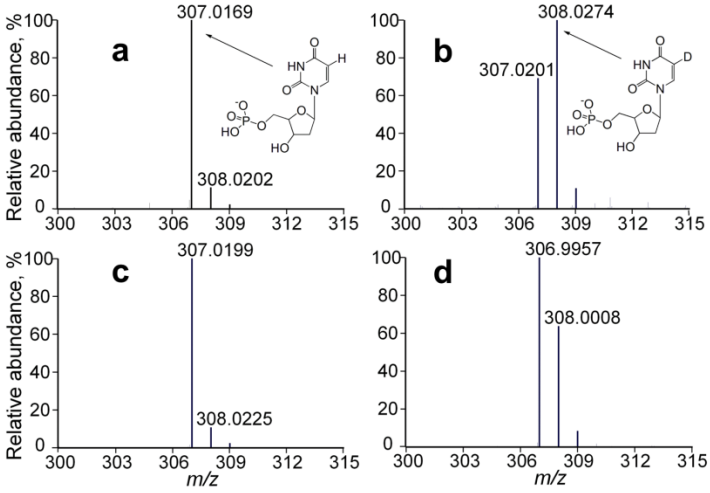

Figure 3.5 ESI-MS of dUMP incubated in D_2O with dithionite (a), dithionite-reduced FDTS (b), oxidized FDTS (c), and NADPH-reduced FDTS (d). All spectra were collected in the negative-ion mode.

reduced flavin. In stark contrast to classical TSase-catalyzed H/D exchange at C5 of dUMP, which is strongly dependent on CH_2H_4folate,[77] the dUMP in FDTS reactions is

deuterated to the same extent whether CH_2H_4folate is present or absent, and only depends on the flavin being reduced (Figure 3.5c). The location of the incorporated deuterium was confirmed to be the C5 of uracil by the following series of observations: (i) incubation of reduced enzyme with 5D-dUMP in H_2O resulted in loss of the deuterium label (Figure 3.8b); (ii) tritium of [5-^{3}H]-dUMP was released into water upon incubation with reduced FDTS (Figure 3.9e) but not with oxidized FDTS or without the enzyme, and (iii) in the same experiment with [6-^{3}H]-dUMP, all of tritium remained on dUMP (Figure 3.9b), indicating that the reduced enzyme catalyzes the exchange of the C5 hydrogen and not that of C6. The choice of the reducing agent (sodium dithionite vs. NADPH) had no effect on the observed dUMP deuteration (Figures 3.5b and 3.5d), ruling against dithionite decomposition products (e.g. thiosulfate)[78] as uracil activators. The exchange on C5 of uracil generally requires Michael addition at C6 (Figure 3.7), as demonstrated with a variety of nucleophiles in solution (see Supporting Information for references). Altogether, the above observations and controls are in line with the H/D exchange at C5 of dUMP being catalyzed by the attack of hydride from the enzyme-bound $FADH_2$ on the C6 of dUMP, as proposed in step 1 of Figure 3.1a. The possibility that substrate H/D exchange is enabled by a significant conformational change in FDTS upon reduction is not supported by any of the current crystal structures of FDTSs from several organisms and with various ligands and mutations, but cannot be positively excluded.

Neither of the mechanisms in Figure 3.1 can explain all of the findings described in this work. Specifically: when incubating the mixture in D_2O, deuteration of the substrate dUMP at C5 only occurs with reduced enzyme-bound flavin; in D_2O the product dTMP is mono-deuterated at either C6 or C7, yet the acid-trapped intermediate is not deuterated and the flavin is still reduced as this intermediate is trapped (Figure 3.2). A new proposed mechanism is illustrated in Figure 3.6 that reconciles these seemingly contradictory observations. By this mechanism the H/D exchange at C5 of dUMP in D_2O (after step 1) requires the flavin to be reduced, as observed experimentally (Figure 3.5). A

reversible stereospecific hydride transfer from the N5 of the reduced flavin to the C6 of uracil moiety, similar to the one proposed in Figure 3.6 (steps 1 and 3), has been observed before in dihydrouridine synthase[79, 80] and dihydropyrimidine dehydrogenase.[81] If steps 1-3 are fast and occur within the dead-time of the flow experiments (2 ms), this would also be in accordance with the presence of the methylene in the earliest intermediate trapped.[74] We attempted to detect the presumed initial intermediate that follows the first hydride transfer from the flavin (step 1 in Figure 3.6) using the substrate

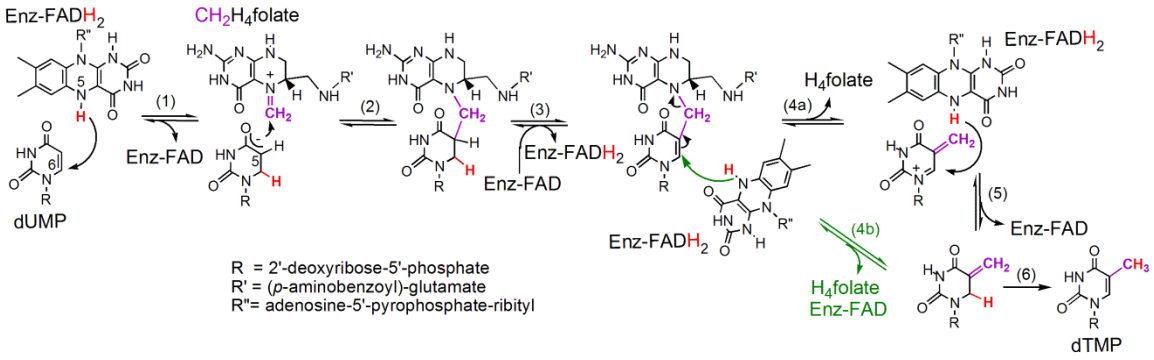

Figure 3.6 A proposed alternative mechanism for FDTS which agrees with both current and past findings. The hypothesis is that steps 1-3 occur within the dead-time of the flow experiments (2 ms), and that intermediates between steps 3 and 5 accumulate and are trapped by the acid in the quench-flow experiment.[74] At this time it is not clear if the elimination of H_4fol precedes the hydride transfer from the flavin (step 4a) or is concerted with it (the green arrows in step 4b). Note that FAD prosthetic group remains bound to the enzyme throughout the catalytic cycle, although its isoalloxazine ring fluctuates towards and away from the substrate as described in ref 82.

dUMP with and without the unreactive CH_2H_4folate analogue, folinic acid (see Supporting Information below for experimental details and results). That step is reversible, and if at equilibrium a significant amount of oxidized flavin were to accumulate, its detection would have supported the mechanism in Figure 3.6. As no oxidation of $FADH_2$ was detected, this attempt cannot support or rule out the proposed

mechanism. The unusual intermediates between steps 3 and 5 accumulate and are trapped by the acid in the quench-flow experiment.[74] Step 5 (or 4b) seems to occur ~20 s before step 6, in accordance with the delay observed between the stopped-flow kinetics and the formation of dTMP product (Figure 3.2). Because the oxidized FAD is formed only transiently and does not accumulate kinetically, the flavin is expected to appear spectrally reduced, in agreement with the stopped-flow kinetics in Figure 3.2. Finally, the intermediates forming between steps 3 and 5 would contain no deuterium in D_2O, and could readily undergo hydroxyl addition at the methylene carbon to yield non-deuterated 5-hydroxymethyl-dUMP observed in acid-quenched FDTS reactions (Figure 3.4). It is noteworthy that the bridged intermediate between steps 3 and 4 has recently been suggested by QM/MM calculations in classical thymidylate synthase.[83]

FDTS is a promising antibiotic drug target because while absent from humans, it is present in ~30% of all microorganisms, several of which are severe human pathogens. For example, all *Rickettsia* rely solely on FDTS for thymidylate, and the essentiality of FDTS has been recently illustrated in *M. tuberculosis*.[84] FDTS is the only known uracil-methylating enzyme that does not employ an enzymatic nucleophile for uridylate activation,[73] thus presenting a unique target for small molecule inhibition. The current study sheds new light on the complex reaction mechanism catalyzed by this enzyme. Further investigation of the proposed mechanistic features is underway to build the platform for mechanism-based design of FDTS inhibitors. The mechanism proposed here is unique to FDTS, which lends confidence in high specificity of such inhibitors.

Supporting Information

Materials

All chemicals were reagent grade and used as purchased without further purification. 2'-deoxyuridine 5'-monophosphate (dUMP), glucose oxidase from *Aspergillus niger*, D-glucose, D_2O (99.9% D), flavin adenine dinucleotide (FAD),

reduced β-nicotinamide adenine dinucleotide phosphate (NADPH), L-arabinose, and formaldehyde solution (36.5% by weight) were obtained from Sigma. N^5,N^{10}-methylene-5,6,7,8-tetrahydrofolate (CH_2H_4folate) and folinic acid were a gracious gift by Eprova Inc. (Schaffhausen, Switzerland). 5D-dUMP was synthesized according to the previously published procedure via cysteine-catalyzed H/D exchange on dUMP,[85] and purified by analytical HPLC. [5-^{3}H]-dUMP and [6-^{3}H]-dUMP were purchased from Moravek Biochemicals. Sodium dithionite powder was purchased from J.T. Baker, and tris(hydroxymethyl)aminomethane (Tris) was obtained from Research Products International Corp.

Thermatoga maritima FDTS (*Tm*FDTS, TM0449, GenBank accession number NP228259) was expressed with an N-terminal His tag in *E. coli* HK100, which has been transformed with SpeedET plasmid containing wild-type *thyX* gene. The protein expression was carried out in Luria-Broth media at 37^{o}C overnight and induced by addition of L-arabinose (1.5 g/L). Bacteria were lysed by passing the cell suspension through French press in Lysis Buffer [50 mM Tris, pH 8.0, 1 mM EDTA, 400 mM NaCl, 20 mM $MgCl_2$, 3 mg/mL lysozyme, 0.1 mg/mL DNAase I, EDTA-free protease inhibitor pellets (Roche)]. The cell debris was removed by centrifugation. Heat-sensitive proteins in the soluble fraction were then denatured by incubation at 65^{o}C for 30 min and pelleted by centrifugation. *Tm*FDTS in the supernatant was further purified via Ni-NTA (Qiagen) affinity column equilibrated in Wash Buffer (50 mM Tris, pH 8.0). The resin was washed with Wash Buffer and protein eluted with Wash Buffer containing 250 mM imidazole. The eluted fractions were dialyzed against Wash Buffer to remove imidazole.

Analytical methods

Separations were carried out on an Agilent series HPLC, with UV/vis diode array detector or flow-scintillation analyzer (for radioactive samples). An analytical reverse phase Supelco column (Discovery series 250 mm X 4.6 mm) was used for 5D-dUMP

purification with isocratic elution in 100 mM Tris buffer at pH 7.10. Elution of the pyrimidine was followed by UV absorbance (at 265 nm). The concentration of enzyme for rapid-quenching and stopped-flow experiments was determined by the 454 nm absorbance of bound FAD (ε = 11,300 $cm^{-1}M^{-1}$). Liquid chromatography-mass spectrometry (LC-MS) analysis was performed on Waters Acquity^{TM} Ultra Performance LC system, using an eluent gradient of water and acetonitrile containing 0.1% formic acid, followed by a Waters Q-TOF mass spectrometer.

Stopped-flow kinetics of FDTS reaction

A solution of oxidized FDTS (100 μM) was made anaerobic in a sealed tonometer by cycles of equilibration with argon and evacuation. The anaerobic enzyme was reduced stoichiometrically (following 454 nm absorbance) with a solution of dithionite. The reduced FDTS was then mixed with dUMP (30 μM) from a side-arm of the tonometer and loaded in the Applied Photophysics SX-20 Stopped-Flow Spectrophotometer, which has been previously scrubbed of oxygen with glucose (10 mM)/glucose oxidase solution (50 units/mL). An anaerobic 800 μM CH_2H_4folate solution was prepared containing 50 units/mL glucose oxidase, 10 mM glucose (to assure anaerobic conditions) and 30 mM formaldehyde (to stabilize CH_2H_4folate). The instrument zero reading was taken with CH_2H_4folate solution in the optical cell. FDTS reactions were then initiated by rapid mixing of the enzyme/dUMP and CH_2H_4folate solutions in the instrument at room temperature. The flavin absorbance was followed at 420 nm for 400 s (t_∞), and absorbance traces from several shots (3-5) were averaged.

Hydrogen isotope exchange on dUMP

For D_2O experiments, all reagents and buffers were exchanged into D_2O by two cycles of lyophilization and re-suspension in D_2O. Oxidized FDTS (78 μM) was made anaerobic in a sealed anaerobic cuvette by cycles of equilibration with an atmosphere of argon and evacuation. The anaerobic enzyme was reduced with either a solution of

dithionite or NADPH, and mixed with dUMP (70 μM) from the side-arm of the cuvette. The mixture was then incubated at room temperature for 1-3 hours, after which a portion of the solution was mixed with HCl to denature the protein, and the released enzyme-bound dUMP was analyzed by LCMS. To ensure anaerobicity in the experiments with NADPH reduction, glucose/glucose oxidase system was included. No D-dUMP was observed in experiments with free reduced FAD.

To confirm the C5 of dUMP as the location of hydrogen isotope exchange, reduced FDTS was anaerobically incubated for 1 hour at room temperature with either 5D-dUMP, [5-^{3}H]-dUMP, or [6-^{3}H]-dUMP in H_2O buffer, and the hydrogen label was tracked by LCMS (for deuterium) or HPLC with flow-scintillation analyzer (for tritium). The C5 hydrogen label was lost to the solvent during this incubation (Figures 3.8 and 3.9), while C6 label remained on dUMP, in accordance with hydrogen isotope exchange occurring at C5 of uracil (Figure 3.7). This hydrogen isotope exchange on the uracil has been observed with a myriad of nucleophiles in solution via attack on C6[85-88] and in fact was employed here to synthesize 5D-dUMP (see Materials above). In case of FDTS, the hydride of $FADH_2$ could serve as the nucleophile activating dUMP for the hydrogen isotope exchange.

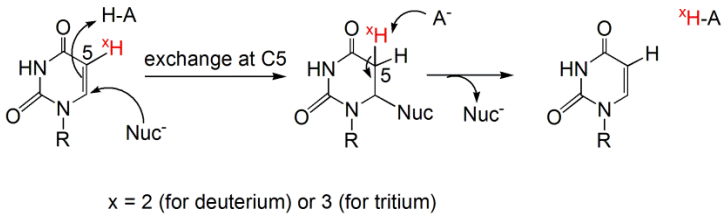

Figure 3.7 Mechanism of the hydrogen isotope exchange at C5 of dUMP

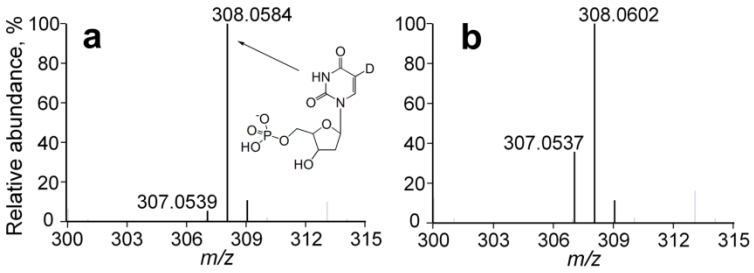

Figure 3.8 ESI-MS spectra of 5D-dUMP (*m/z* 308) incubated in H_2O with dithionite (a) and dithionite-reduced FDTS (b). Note the increase in *m/z* 307 in (b), corresponding to unlabeled dUMP.

Testing for reduced dUMP intermediate at the early stages of the reaction

In the newly proposed mechanism (Figure 3.6 in the main text of the chapter), we suggest a rapid (under 10 ms) reversible hydride transfer between FAD and dUMP (steps 1-3) that allows the methylene of CH_2H_4folate to be transferred to the uracil ring. We tested a stoichiometrically reduced enzyme ($FADH_2$) for such ability to reduce dUMP, following the flavin's UV/Vis absorbance spectrum. If significant fraction of reduced dUMP were to accumulate, some oxidized flavin could be detected. We also employed an unreactive analogue of CH_2H_4folate, folinic acid, in which N5 methylene is replaced with a formyl group (Figure 3.10), to better mimic the reactive complex in question. A solution of oxidized FDTS (54 μM) was made anaerobic by cycles of argon equilibration and vacuum. The anaerobic enzyme was stoichiometrically reduced with sodium dithionite (following 454-nm absorbance), mixed with dUMP (50 μM) and incubated for 5 min while following the UV/Vis absorbance. Then, folinic acid (54 or 400 μM) was added to this mixture from the side arm of the cuvette and incubated for 10 min while monitoring the UV/Vis absorbance.

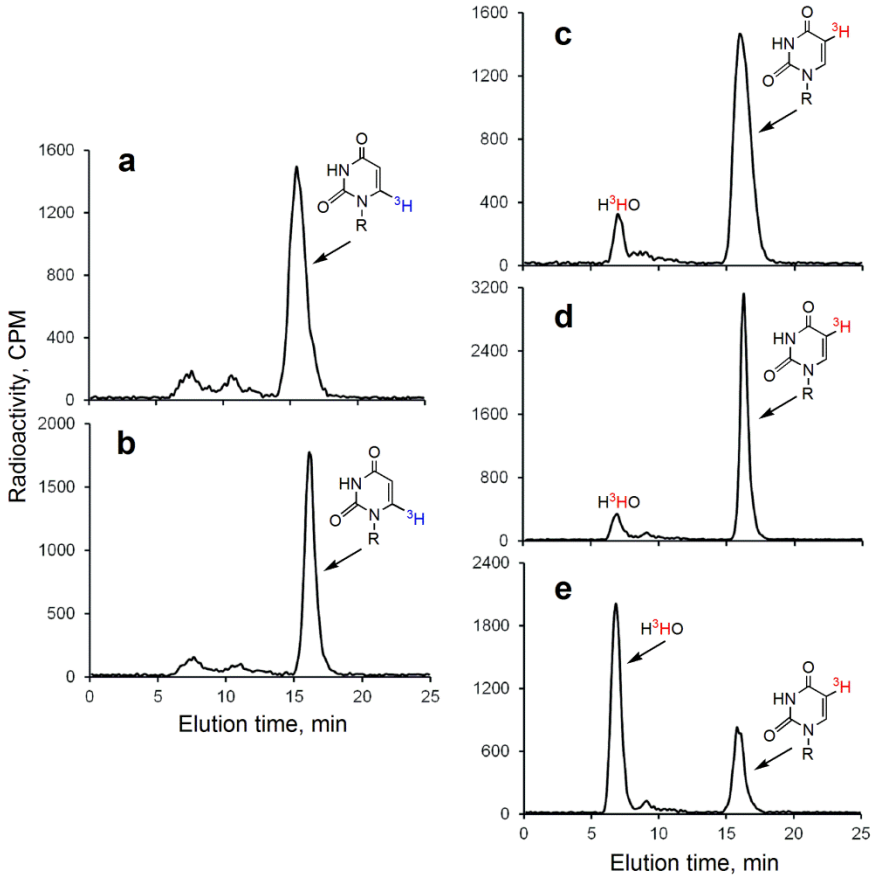

Figure 3.9 HPLC radiograms of [6-^{3}H]-dUMP (*left panel*) and [5-^{3}H]-dUMP (*right panel*). a) A commercial [6-^{3}H]-dUMP elutes at 16 min (contains small amounts of radioactive impurities eluting between 6 and 13 min). b) Incubation of this [6-^{3}H]-dUMP with reduced FDTS does not change its radiogram. c) Commercial [5-^{3}H]-dUMP contains ~10% tritiated water (7 min peak). d) That material remains unchanged following incubation with oxidized FDTS. e) The water peak increases significantly upon incubation with reduced FDTS, in accordance with H5 exchange with solvent.

As seen in Figure 3.10, no oxidized flavin could be detected. While oxidized flavin formation would have supported the new mechanism proposed in Figure 3.6, the current observation is not conclusive. Since the reduced dUMP proposed in Figure 3.6 is likely to form only in a catalytic amount, that amount could very well be below the spectroscopic detection limit. Alternatively, the reactive CH_2H_4folate is needed to push the equilibrium towards the reduced dUMP. In summary, the current observation is

consistent with either lack of sufficient accumulation of such reduced dUMP, or a critical need in CH_2H_4folate for its formation, or a mechanism that does not involve such early dUMP reduction (e.g., Figure 3.1b in the main text of the chapter).

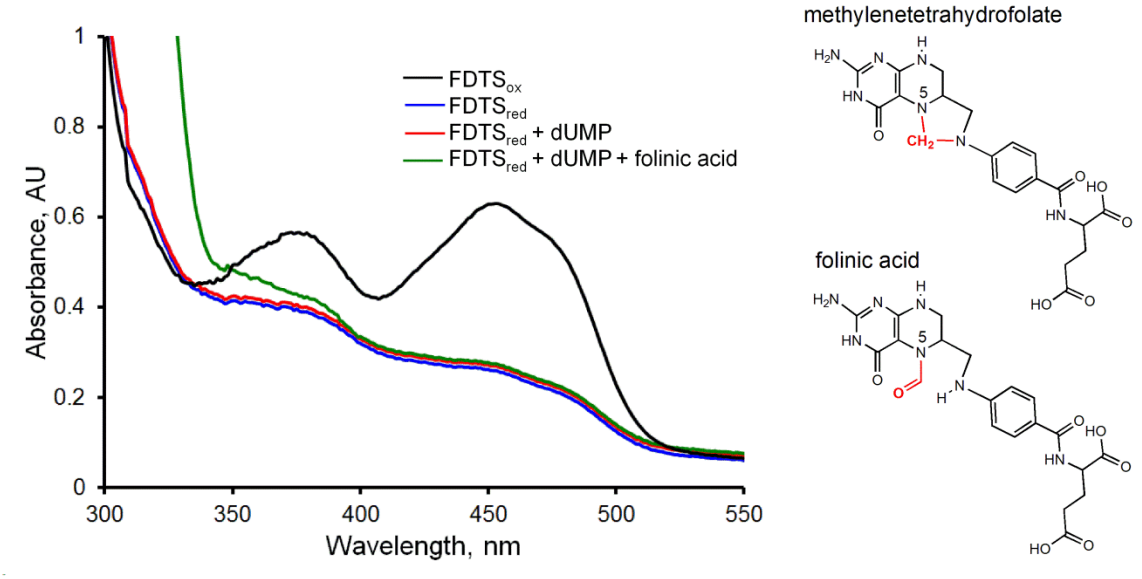

Figure 3.10 Absorbance spectra of FDTS-ligand complexes. Note that neither dUMP nor folate substrate analogue (folinic acid, shown on the right) oxidize the enzyme-bound flavin.

CHAPTER IV

SYNTHESIS AND APPLICATION OF ISOTOPICALLY LABELED FLAVIN NUCLEOTIDES[iv]

Abstract

Flavin nucleotides (FMN and FAD) are utilized as prosthetic groups and/or substrates by a myriad of proteins, ranging from metabolic enzymes to light receptors. Isotopically labeled flavins have served as invaluable tools in probing the structure and function of these flavoproteins. In this chapter, we present an enzymatic synthesis of several radio- and stable-isotope labeled flavin nucleotides from commercially available labeled riboflavin and ATP. The synthetic procedure employs a bifunctional enzyme, *Corynebacterium ammoniagenes* FAD synthetase, that sequentially converts riboflavin to FMN and then to FAD. The final flavin product (FMN or FAD) is controlled by the concentration of ATP in the reaction. Utility of the synthesized labeled FAD cofactors is demonstrated in flavin-dependent thymidylate synthase. The described synthetic approach can be easily applied to the production of flavin nucleotide analogues from riboflavin precursors.

Introduction

Flavins are incredibly versatile compounds capable of carrying out one- and two-electron redox, nucleophilic and electrophilic chemistry.[89, 90] This versatility makes flavins invaluable as electron-carriers, prosthetic groups of proteins and even precursors in the biosynthesis of other biologically important molecules.[91] Isotopically labeled flavins and flavin analogues have been used in the past to probe the structural dynamics

[iv] This chapter has been submitted by Tatiana V. Mishanina and Amnon Kohen for publication to *Analytical Biochemistry*.

of light receptors,[92, 93] elucidate flavin transport and metabolism in healthy and diseased cells,[94, 95] and gain insight into the mechanisms of flavoproteins, [96-98] among other applications. Due to their utility, efficient synthetic routes to the isotopically labeled flavins and analogues are of great interest.

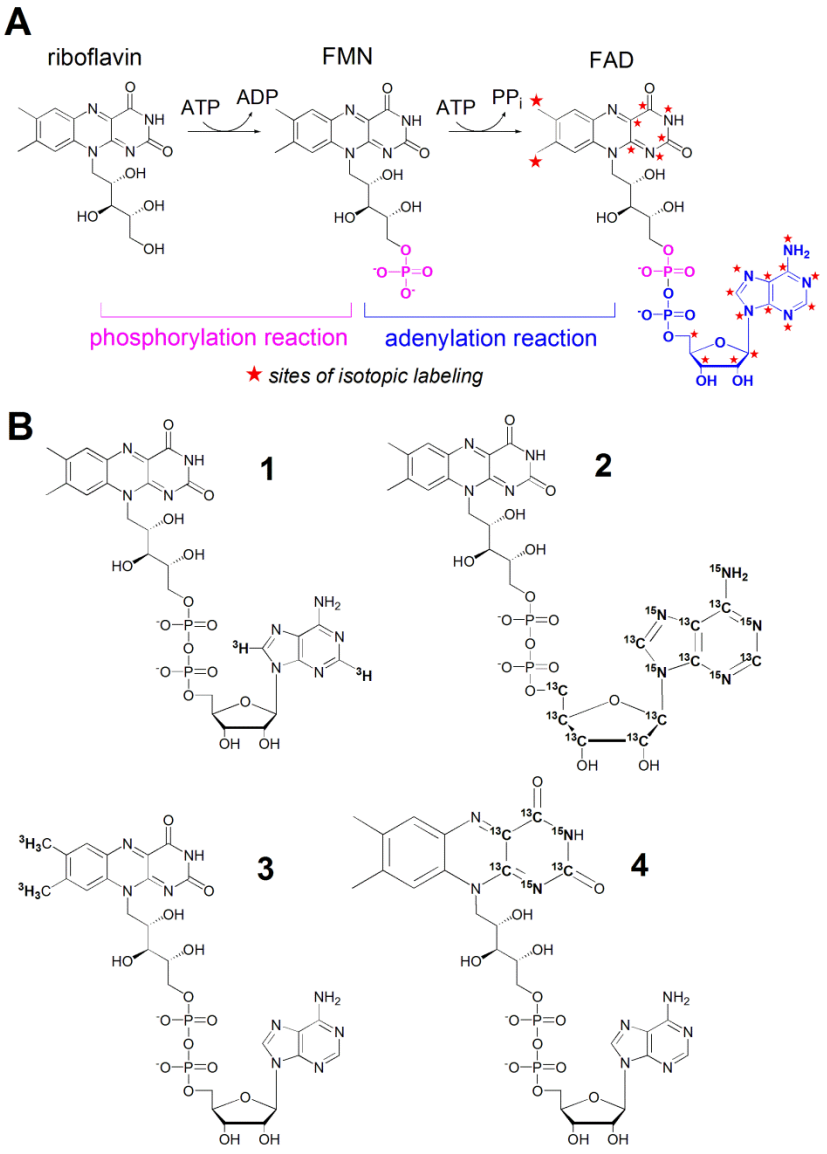

Figure 4.1 Synthesis of flavin nucleotides. A) *C. ammoniagenes* FAD synthetase-catalyzed synthesis of flavin nucleotides from riboflavin, employed in current chapter. B) Structures of the isotopically labeled FAD molecules synthesized in this chapter.

The most widely utilized flavins in nature are the "nucleotide" forms of the vitamin riboflavin: flavin mononucleotide (FMN) and flavin adenine dinucleotide (FAD). FMN is traditionally generated from riboflavin via chemical phosphorylation of 5′ hydroxyl.[99, 100] However, this route invariably generates isomeric monophosphates and bisphosphates, which could be challenging to remove.[101] In fact, commercially available FMN synthesized this way contains ~30% of phosphorylated impurities. Enzymatic phosphorylation by riboflavin kinase (also known as flavokinase, FMN synthetase, ATP:riboflavin 5′-phosphotransferase), on the other hand, yields pure FMN. A second enzyme, FAD synthetase (also known as FAD pyrophosphorylase, FMN adenylyl transferase, ATP:FMN adenylyltransferase), can subsequently be used to adenylylate FMN into FAD. This enzymatic FMN→FAD conversion is much more efficient than the chemical routes to FAD[102]; however, it does require preparation of an additional protein. The advantage of the synthetic approach described here lies in using a single enzyme, *Corynebacterium ammoniagenes* FAD synthetase, to selectively convert riboflavin to either FMN or FAD, by varying the reagent concentrations.

C. ammoniagenes FAD synthetase is a bifunctional enzyme that combines the activities of a riboflavin kinase and adenylyltransferase (Fig. 4.1A). The recombinant enzyme has been overexpressed in *E. coli* and purified in the past, and its steady-state kinetics has been characterized.[103] Here we use partially purified *C. ammoniagenes* FAD synthetase to produce FAD isotopically labeled at either the adenylyl tail or the isoalloxazine core (Fig. 4.1B) starting from commercially available isotopically labeled ATP or riboflavin, respectively. FMN labeled at isoalloxazine can also be obtained via this route, by using stoichiometric amounts of riboflavin and ATP in the synthetic mixture.

Following the description of the synthesis of FADs with four different labeling patterns (Fig. 4.1B), one application is presented for the use of these labeled flavins in the mechanistic studies of an enzyme flavin-dependent thymidylate synthase (FDTS). FDTS

employs FAD prosthetic group to reductively methylate 2′-deoxyuridine-5′-monophosphate (dUMP) to 2′-deoxythymidine-5′-monophosphate (dTMP), a DNA precursor, in many human pathogens[7, 9, 10, 37] (Fig. 4.2). FDTS presents an exciting new target for antibiotics with low toxicity, considering that its mechanism of action differs drastically from "classical" thymidylate synthase encoded by *thyA* gene in most organisms, including humans.[36, 73] The details of FDTS chemical mechanism are still under investigation, and our recent acid-trapping of an intermediate in FDTS-catalyzed reaction has provided some insight into the timing of chemical events in this enzyme.[74] Surprisingly, a different derivative of an intermediate(s) is trapped under basic conditions, which contains the pyrimidine substrate plus an unknown adduct (chapter V of this thesis). The currently reported isotopically labeled FAD molecules are employed in efforts to identify this mysterious adduct and add another piece to the mechanistic puzzle of FDTS.

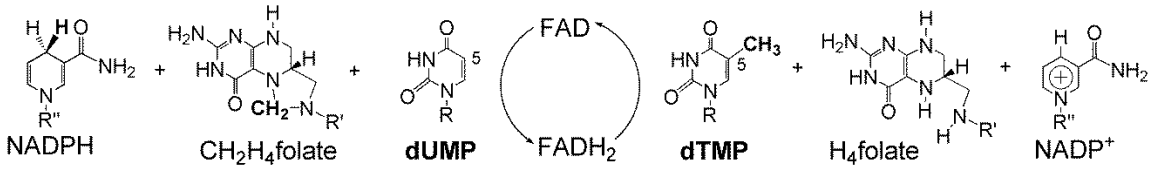

Figure 4.2 Reaction catalyzed by flavin-dependent thymidylate synthase. R=2′-deoxyribose-5′-phosphate; R′=(*p*-aminobenzoyl)-glutamate; R″=adenosine-5′-pyrophosphate-ribityl.

Results and Discussion

Synthesis of labeled flavin nucleotides

In our excursion into the synthesis of labeled flavins, we were mostly interested in labeled FAD, with purpose of employing it in mechanistic studies of flavin-dependent thymidylate synthase. Adenyl- and isoalloxazine-labeled FAD molecules were each

synthesized from the labeled ATP and riboflavin, respectively. The incorporation of the isotopic labels was confirmed by MS for ^{13}C,^{15}N-labeled flavins (Fig. 4.3) or scintillation counting for tritiated compounds. Inclusion of ADP→ATP recycling system (phosphocreatine/creatine phosphate kinase) significantly improved final FAD yields, reaching nearly100% with respect to riboflavin after 24-hour reactions (Fig. 4.4). Large excess of ATP over riboflavin (at least 20-fold) was key to complete conversion to FAD product. Amounts of ATP stoichiometric to riboflavin, on the other hand, halted reaction at FMN stage – conditions that may be used in the synthesis of labeled FMN. FADs with all four isotopic-labeling patterns illustrated in Fig. 4.1B were synthesized and HPLC purified, as described under Methods.

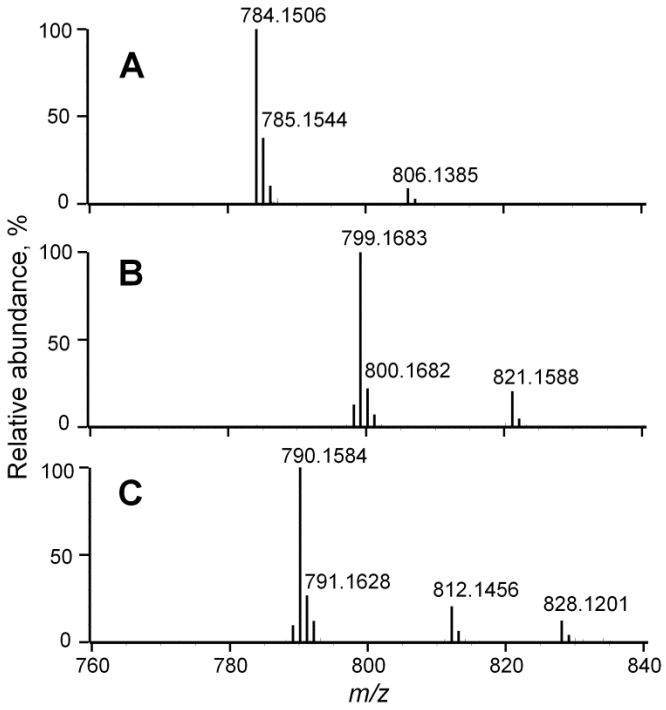

Figure 4.3 Negative-ion ESI-MS spectra of unlabeled FAD standard (A), purified **2** (B) and **4** (C). Note the expected mass shift of +15 for **2** and +6 for **4**. Ions in *m/z* 800 region are due to formation of sodium adducts.

Demonstration of the utility of labeled FAD cofactors in mechanistic studies of flavin-dependent thymidylate synthase

Our rapid acid-quench of FDTS reactions produced a trapped intermediate derivative, 5-hydroxymethyl-dUMP (chapter II of this thesis and ref 74). In a base-quenching experiment, on the other hand, a completely different species is trapped. To test whether the base-trapped intermediate contains any component of the enzyme-bound FAD, we reconstituted the enzyme with isotopically labeled FAD, using all four labeling patterns presented in Fig. 4.1B. No shift in mass of the trapped intermediate was observed with compounds **2** or **4**, and no radioactivity was found on the trapped intermediate when using compound **1**. However, FDTS reconstituted with **3** produced a tritiated trapped-intermediate species (Fig. 4.5). These findings indicate that the

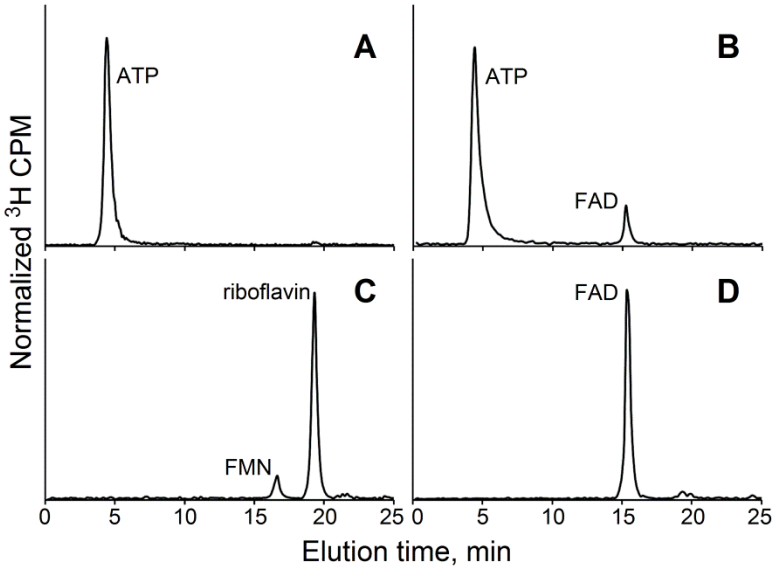

Figure 4.4 HPLC radiograms of reaction mixtures for the synthesis of ^{3}H-labeled FAD: **1** (*top panel*) and **3** (*bottom panel*). (A, C) Synthetic mixtures at t-zero. Note rapid formation of FMN intermediate in (C). (B, D) Reaction mixtures after 24-hour incubation.

dimethylbenzyl moiety of FAD cofactor, but not the rest of the isoalloxazine ring or the adenyl tail, is part of the base-trapped intermediate. This is highly unusual, since no covalent involvement of the flavin has ever been proposed for FDTS.[36, 74] The efforts to elucidate the full structure of this base-trapped intermediate are described in chapter V of this thesis.

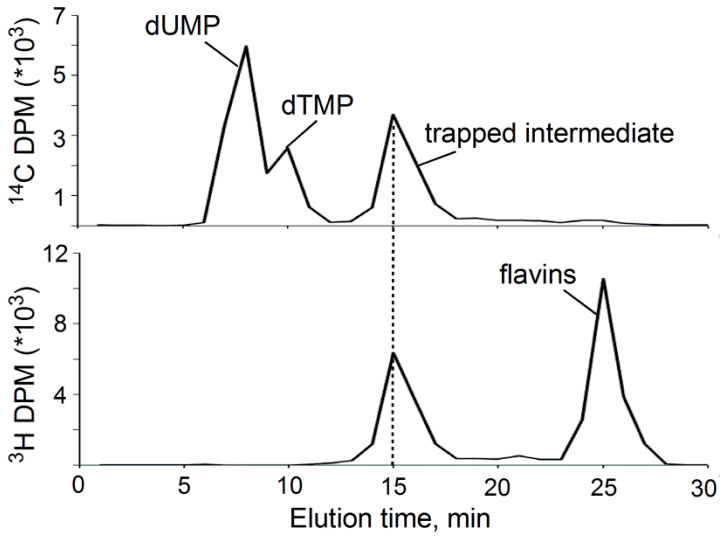

Figure 4.5 HPLC radiogram for the reaction of **3**-reconstituted FDTS with [2-^{14}C]-dUMP quenched at 1 s with 1M NaOH. Radioactive counts from ^{14}C (*top*) and ^{3}H (*bottom*) were determined by liquid-scintillation counting. The base-trapped intermediate clearly contains the ^{3}H-labeled isoalloxazine portion of FAD.

Methods

Materials

Chemicals were reagent grade and used as purchased unless specified otherwise. Unlabeled and [$^{13}C_4$,$^{15}N_2$-dioxopyrimidine]-riboflavin, unlabeled and $^{13}C_4$,$^{15}N_2$-ATP, phosphocreatine and creatine phosphokinase from rabbit muscle were obtained from Sigma-Aldrich. [2-^{14}C]-dUMP (53.2 mCi/mmol), [2,8-^{3}H]-ATP (32 Ci/mmol) and [7a,8a-^{3}H]-riboflavin (6.2 Ci/mmol) were purchased from Moravek Biochemicals. The

FDTS from *Thermatoga maritima* (TM0449, GenBank accession number NP228259) was expressed and purified as described in chapter III of this thesis. The *E. coli* expression system for *C. ammoniagenes* FAD synthetase was a gracious gift from Prof. Dale E. Edmonson (Emory University). Magnesium chloride was purchased from BDH Chemicals, ammonium acetate, ammonium sulfate and sodium chloride from Fisher Scientific, and tris(hydroxymethyl)aminomethane [Tris] base from Research Products International Corp.

Expression and partial purification of FAD synthetase

C. ammoniagenes FAD synthetase was produced by *E. coli* following a modified procedure of ref 103. Bacteria were grown overnight at 30^{o}C in 6 L LB medium containing 200 mg/L ampicillin. The cells (34 g paste) were harvested and lysed by passing the cell suspension through French press at 4^{o}C in Lysis Buffer [100 mL of 100 mM Tris, pH 7.45, 10 mM EDTA, 1 mM DTT, 400 mM NaCl, 20 mM $MgCl_2$, 3 mg/mL lysozyme, 0.1 mg/mL DNAase I, EDTA-free protease inhibitor pellets (Roche)]. The cell debris was removed by centrifugation, and the soluble fraction was treated with solid ammonium sulfate to 50% saturation. The precipitated proteins were pelleted by centrifugation, and ammonium sulfate was added to the supernatant to 80% saturation. After centrifugation, the pellet containing partially purified FAD synthetase was dissolved in 36 mL of 100 mM Tris, pH 7.45, 10 mM EDTA, 1 mM DTT, dialyzed against 1 L of water for 1 hour and then against 1 L of 50 mM Tris, pH 7.45 overnight at 4^{o}C. This crude protein preparation was used in the synthesis of flavins.

Synthesis of labeled flavins

Reactions for the synthesis of labeled FAD contained the following: 50 μM riboflavin, 8 mM $MgCl_2$, 1 mM ATP, 196 mM phosphocreatine, 800 units/mL of creatine phosphokinase in 50 mM Tris buffer, pH 7.6. The reactions were initiated by addition of 100 μL partially purified FAD synthetase (prepared as described above) per mL of

synthetic mixture and incubated at 25^{o}C until completion (typically 24 hours), as determined by analytical HPLC. Radiolabeled FAD synthesis was carried out in a final volume of 500 μL with 30-50 μCi of tritiated reactant (ATP or riboflavin for compounds **1** and **3**, respectively). ^{13}C,^{15}N-labeled FAD (compounds **2** and **4**) was synthesized in a final reaction volume of 10 mL.

Analytical methods

Separations were carried out on an Agilent series HPLC, with UV/vis diode array detector, flow-scintillation analyzer (FSA, for radioactive synthetic mixtures), or liquid scintillation counting (LSC, for base-quenched FDTS reactions containing ^{3}H-labeled FAD). An analytical reverse phase Supelco column (Discovery series 250 mm X 4.6 mm, 5 μm) was used at 0.8 mL/min for monitoring the progress of FAD synthetase reactions. The column was pre-equilibrated in 85:15 buffer:methanol mixture and the following method was employed for separation of flavins (5 mM ammonium acetate buffer, pH 6.5 as solvent A; methanol as solvent B): 0-5 min 15% B; 5-25 min 15-75% B; 25-26 min 100% B. Elution of the flavins was followed by UV absorbance (at 264 and 450 nm). The concentration of riboflavin for the reactions was determined by the absorbance at 445 nm (ε = 12,200 cm^{-1}M^{-1}) and that of final purified FAD at 450 nm (ε = 11,300 cm^{-1}M^{-1}). The concentration of FDTS for rapid-quenching experiments was determined by the 454 nm absorbance of bound FAD (ε = 11,300 cm^{-1}M^{-1}). Electrospray ionization mass spectrometry (ESI-MS) analysis was performed on a Waters Q-TOF mass spectrometer.

Purification of synthesized labeled flavins

The final synthesis mixture was passed through an Amicon® Ultra centrifugal filter (10,000 MWCO) to remove proteins and applied to an HPLC semi-preparative reverse phase Supelco column (Discovery series 250 mm X 10 mm, 5 μm) at a flow rate of 3.2 mL/min. Elution of the flavins was monitored by 450 nm absorbance. Eluent

containing FAD (~15 min) was collected, purged with argon to remove methanol, frozen and lyophilized to dryness. Care was taken to minimize exposure of the flavin to light.

ApoFDTS preparation and reconstitution with labeled FAD

Recombinant FDTS from *T. maritima* was prepared as described in chapter III of this thesis. The enzyme was purified with a tightly bound FAD. To remove this native FAD from the enzyme, sodium chloride solid was added to the solution of FDTS to a final concentration of 30% w/v. This enzyme solution was warmed to 40^{o}C and gently inverted to dissolve NaCl solid. The aggregated protein was pelleted by centrifugation at 13,000 rpm and 4^{o}C, and washed with 30% w/v NaCl solution until the pellet was visibly white, hence lacking bound FAD. This apoFDTS was re-suspended in 50 mM Tris buffer, pH 8.0, 1 mM EDTA and washed with Tris buffer by filtration to remove excess NaCl. ApoFDTS was then incubated with labeled FAD at 1:1 concentration ratio overnight. Binding of FAD to FDTS was corroborated by the shift of flavin λ_{max} from 450 nm (free FAD) to 454 nm (FDTS-bound FAD). This reconstituted FDTS was washed with Tris buffer to remove any unbound FAD, until the 280:454 nm absorbance ratio, indicative of protein and flavin content in the solution, was ~6. With radiolabeled FAD-FDTS, the amount of enzyme-bound ^{3}H-FAD was determined by liquid-scintillation counting. The ability of the reconstituted enzyme to convert dUMP to dTMP was always tested prior to quenching experiments, and no loss in this thymidylate synthase activity was ever observed upon reconstitution.

Base-quenching of labeled FAD-FDTS reactions

Rapid-quenching experiments with flavin-labeled FDTS were carried out according to the published procedure (chapter II of this thesis and ref 74), except with 1 M NaOH as the reaction quencher. Reaction time points containing maximal accumulation of the base-trapped intermediate were analyzed by HPLC-LSC (radioactive samples) or LCMS (stable-isotope labeled samples). In the experiments with ^{3}H-labeled

FAD, [2-^{14}C]-dUMP substrate was used to track the base-trapped intermediate in HPLC analysis.

Conclusions

We report the successful synthesis of four different isotopically-labeled FAD cofactors in high yields. Our synthetic route utilizes a bifunctional FAD synthetase, which offers control over the final flavin nucleotide product (FMN vs. FAD). The synthetic procedure described here can be easily modified to convert riboflavin analogues into their nucleotide forms.

To demonstrate their applicability to mechanistic problems, we incorporated labeled FADs into flavin-dependent thymidylate synthase and followed the integration of isotopes into the unidentified base-trapped intermediate in the FDTS-catalyzed reaction. The synthesized FAD cofactors provided critical information about the FDTS mechanism which otherwise would be challenging to obtain, i.e., that the dimethylbenzyl component of the isoalloxazine moiety is part of the base-trapped intermediate, while the pyrimidine and adenyl portions are not.

CHAPTER V

ISOLATION AND CHARACTERIZATION OF AN UNUSUAL FLAVIN-PYRIMIDINE COVALENT ADDUCT IN FAD-DEPENDENT BIOSYNTHESIS OF THYMIDYLATE

Abstract

FAD-dependent thymidylate synthase (FDTS) catalyzes the last crucial step in the *de novo* biosynthesis of thymidylate, a DNA building block. Because FDTS is absent in humans while present in several human pathogens, its inhibition is of interest from pharmaceutical stand point. The understanding of chemical mechanism of FDTS would greatly facilitate rational design of mechanism-based inhibitors. In this chapter, we present the discovery that the previously observed acid-trapped intermediate derivative (chapter II and ref 74) actually originates from at least two different reaction intermediates. By using base as the quencher in a quench-flow experiment, we found that the first intermediate yields a trapped compound different from the one trapped in acid. The second intermediate, on the other hand, forms dTMP product upon base quenching, which is surprising given that the flavin cofactor is still reduced at this stage (according to flavin's UV spectrum). We also describe the partial structural identification of the base-trapped intermediate. Although no covalent bond between the FAD and the substrate has been suggested by any proposed FDTS mechanism, the trapped intermediate contains such a covalent linkage between the flavin and thymidylate moiety. These mechanistic features will surely be important to the rational design of inhibitors as leads to novel antibiotic drugs.

Introduction

DNA synthetic machinery is one of the primary targets of chemotherapeutic and antibiotic agents. It comes as no surprise then that the enzymes that supply this machinery with required building blocks are of pharmaceutical interest. One class of

these enzymes, thymidylate synthases (TSases), catalyzes the last committed step in the *de novo* synthesis of a DNA nucleotide thymidylate (2′-deoxythymidine-5′-monophosphate, or dTMP), by reductively methylating 2′-deoxyuridine-5′-monophosphate (dUMP). Flavin-dependent thymidylate synthase (FDTS) carries out this function in many human pathogens, and the gene coding for this enzyme does not exist in humans.[7, 9] The mechanistic intricacies of FDTS-catalyzed reaction, necessary for rational design of mechanism-based inhibitors as antimicrobials leads, are still under investigation (e.g. see Figs. 3.1 and 3.6 of this thesis for currently postulated chemical mechanisms). One of the most persuasive pieces of evidence in favor of any specific mechanism is the identification of reaction intermediates. Our rapid-quenching experiments with *T. maritima* FDTS (*Tm*FDTS) revealed a significant accumulation of an acid-trapped intermediate in single-turnover reactions (ref 74 and chapter II of this thesis). This acid-trapped species was identified to be 5-hydroxymethyl-dUMP. Since reactive intermediates are likely to behave differently under various solution conditions, we were curious to test whether the same or different derivative(s) of intermediates is trapped in basic quencher. We found that the base-trapped intermediate accumulates in the same time phase as the acid-trapped one but disappears much faster, indicating that two different intermediates were trapped by the acid to afford 5-hydroxymethyl-dUMP. The second of these intermediates yields the dTMP product in base, even though the UV trace still suggests a reduced flavin at the time of quenching.

The base-trapped intermediate is partially comprised of the thymidylate moiety and the FAD cofactor-derived dimethylbenzene. This observation is unexpected for FDTS. Covalent catalysis by the flavin cofactor is not rare among other flavoenzymes. For example, covalent C4a-(hydro)peroxy flavin adduct is a common reaction intermediate in flavin-dependent oxidases and oxygenases.[104] The evidence is also available for the existence of covalent substrate-flavin intermediate complexes through the N5 of isoalloxazine nucleus, e.g. in UDP-galactopyranose mutase[39] and TrmFO t-

RNA methyltransferase,[105] among other systems. No such covalent involvement of the flavin, however, has ever been proposed for FDTS. Efforts toward the complete structural identification of the base-trapped intermediate and its mechanistic implications are discussed.

Results and Discussion

We carried out the quench-flow experiments according to the procedure published for acid quench,[74] except with a strong base as reaction quencher. Briefly, the enzyme-bound FAD was stoichiometrically reduced with sodium dithionite under anaerobic conditions. This pre-reduced enzyme solution was mixed with dUMP; the catalytic turnover was then initiated anaerobically by rapid addition of CH_2H_4fol, and quenched with aerobic 1 M NaOH at various time points. Below we present the findings of these base-quenching experiments.

Tracking intermediate formation using radiolabeled substrates

The initial analysis of the base-quenched FDTS reactions with the radiolabeled nucleotide, [2-^{14}C]-dUMP, confirmed the presence of a new radioactive species. Figure 5.1A shows the HPLC radiogram of a reaction quenched after 1 s, where ~50% of total radioactivity was found in this newly developed peak under the experimental conditions. Unlike the acid-trapped 5-hydroxymethyl-dUMP, which eluted between dUMP and dTMP on a reverse-phase column, the base-trapped nucleotide was much more hydrophobic than either the reactant or the product, indicating that a quite different intermediate derivative is being trapped by the base. Importantly, the fraction of radioactivity associated with the base-trapped species accumulated and decayed during the course of the reaction, as expected of enzymatic intermediates (Fig. 5.2).

The relationship between the kinetics of intermediate derivatives trapped by the base (this chapter) and acid[74] suggests that at least two different intermediates are being

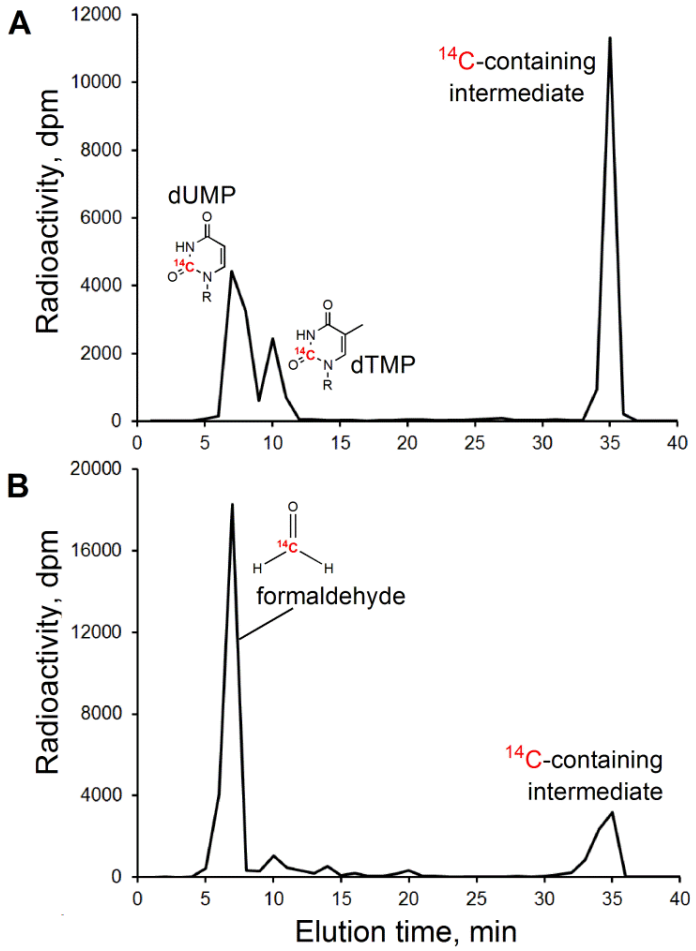

Figure 5.1 Intermediate trapping with ^{14}C-labeled substrates. Shown are the HPLC radiograms of FDTS reactions with [2-^{14}C]-dUMP (A) and [11-^{14}C]-CH_2H_4fol (B) quenched at 1 s with 1 M NaOH. The same chemical species is trapped in both experiments, as corroborated by the identical elution times (~35 min). This species contains both the pyrimidine moiety of dUMP and the methylene of CH_2H_4fol cofactor.

trapped by the acid as 5-hydroxymethyl-dUMP (Fig. 5.2, bottom panel). The earlier intermediate (I_1) is trapped in different chemical forms in acidic vs. basic media. The later intermediate (I_2) is trapped as 5-hydroxymethyl-dUMP in acid, but converted to dTMP in base *prior* to flavin oxidation (Fig. 5.2, green trace). This astonishing observation could suggest that I_2 already contains the reducing equivalents from the flavin, and the stopped-flow absorbance trace at 420 nm reports on a chromophore other

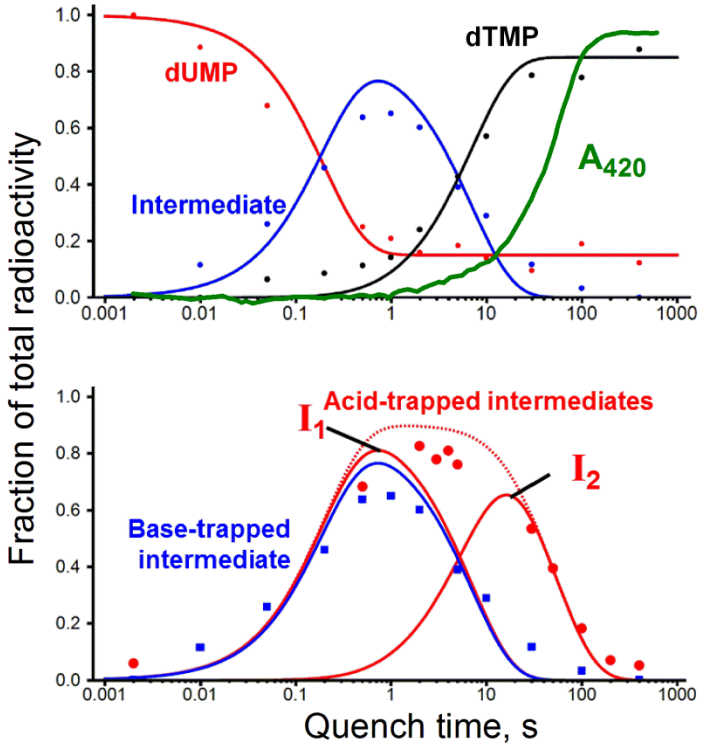

Figure 5.2 (*Top panel*) Single-turnover FDTS reaction kinetics from rapid base-quench, overlaid with stopped-flow flavin absorbance trace (green, from chapter III of this thesis). Each time point was obtained from a radiogram like the one shown in Fig. 5.1A. Note the significant lag in flavin oxidation relative to dTMP formation. (*Bottom panel*) Base-trapped intermediate kinetics (blue curve) overlaid with acid-trapped intermediate data (red dots) globally fitted to a two-intermediate model (red curves). The earlier intermediate (I_1) is assumed to be the same species as trapped by the base. The combined total between the two intermediates is shown as dashed red curve.

than the reduced flavin (i.e., the flavin has already been oxidized but does not absorb at this wavelength due to complex effects). Such scenario would also require I_2 to be re-oxidized in acid to yield 5-hydroxymethyl-dUMP, as was proposed in one of the acid-trapping mechanisms in ref 74. Alternatively, the base quench might catalyze the hydride transfer from $FADH_2$ to I_2, although this scenario seems less likely since the enzyme should quickly fall apart during the quenching. This option could be more viable if the

second intermediate included a covalent bond between the reduced flavin and the nucleotide.

Characterization of the base-trapped intermediate

To determine whether this new compound contains the methylene of the folate cofactor, we reacted FDTS with [11-^{14}C]-CH_2H_4fol under the same conditions as above. We observed a radioactive peak with the same retention time as when starting with [2-^{14}C]-dUMP (Fig. 5.1B). This indicates that the methylene has already been transferred to the nucleotide intermediate prior to it being trapped by the base.

With the HPLC elution profile and the time course of the base-trapped intermediate in hand (Fig. 5.2, blue curve), we quenched FDTS reactions with non-radioactive substrates at 1 s, which produced the largest amount of the trapped derivative, and purified the trapped compound by HPLC (see Methods section). The purified molecule was analyzed by high-resolution ESI-LC-MS and MSMS (Fig. 5.3), and its mass was found to be $[M-H]^-$ 570.1380, or $[M+H]^+$ 572.1523. The MSMS of the base-trapped intermediate contained all of the fragments associated with dTMP moiety, as confirmed by MSMS analysis of a dTMP standard (Fig. 5.6), which is in agreement with findings of the radiolabeling experiments discussed above. The mass difference between the trapped species (~571 Da) and dTMP (~322 Da) is 249 Da, which belongs to some adduct bound to the trapped nucleotide. None of the remaining ion fragments in the MSMS fit this exact mass difference or could be assigned to either folate or buffer components of the quenched reaction mixture.

Efforts towards identification of the adduct bound to the base-trapped nucleotide intermediate

Perhaps the most logical (and mechanistically desirable) candidate for the nucleotide-bound adduct is the pterin moiety of CH_2H_4fol. The positive identification of adduct as a pterin would have been the first experimental evidence for the postulated

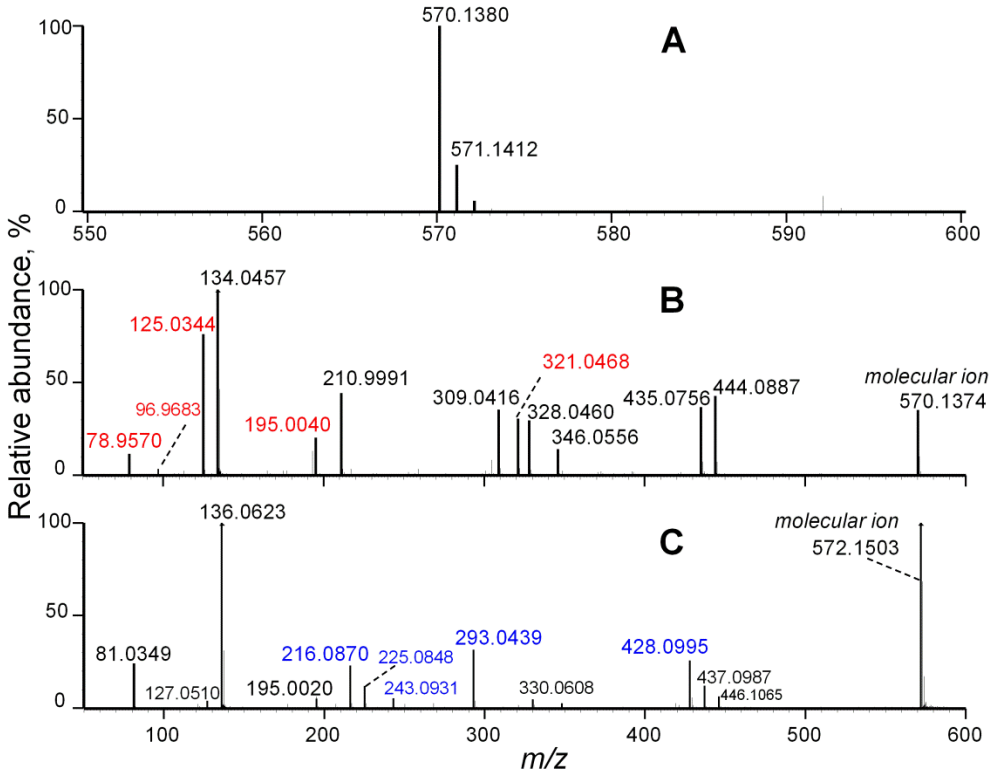

Figure 5.3 ESI-MS analysis of the base-trapped intermediate. (A) Negative-ion mode high-resolution (HR) ESI-MS. (B) Negative-ion mode HR-ESI-MSMS. The fragments observed in dTMP standard are highlighted in red. See Supporting Information for dTMP fragmentation spectrum. (C) Positive-ion mode HR-ESI-MSMS. The fragments unique to the positive-ion mode detection are highlighted in blue.

direct methylene transfer from CH_2H_4fol to dUMP. The UV-vis spectrum of the base-trapped intermediate revealed absorbance peaks at 265 and 340 nm (Fig. 5.4), and various folates are indeed known to absorb in 340-nm region. Although no folate fragments could be identified in the MSMS spectrum of the trapped intermediate, it is possible that the folate adduct has been chemically modified in basic medium. To test for the pterin adduct, we conducted base-quenching experiment with [2-^{14}C]-dUMP (as a tracer) and [6-^{3}H]-CH_2H_4fol, where the tritium label was on the pterin ring of the folate. Since the hydrogen at C6 position of the folate cofactor does not participate in the FDTS

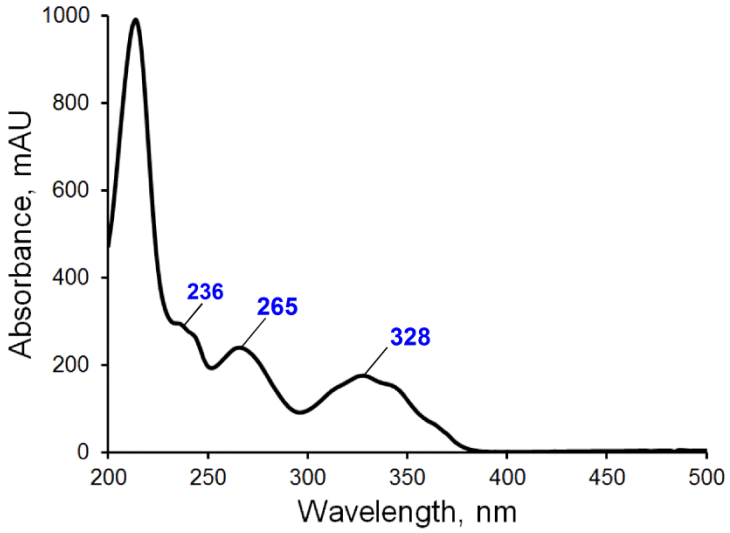

Figure 5.4 UV-visible absorbance spectrum of the purified base-trapped intermediate in Tris buffer

reaction, and was still identified in the H_4fol product,[27] it could have been part of the intermediate. Thus if that moiety of the pterin were a part of the base-trapped species, then the trapped derivative would contain the ^{3}H label. As seen in Fig. 5.8A, no tritium was found on the trapped intermediate. The 6*R* position on the pterin, however, is prone to oxidation. To conclusively exclude pterin as an adduct candidate, we repeated the quenching experiment with [3',5',7,9-^{3}H]-CH_2H_4fol, where the labeled hydrogens are resistant to oxidation. The HPLC radiogram of the reaction quenched at 1 s (Fig. 5.8B) shows that none of the ^{3}H-labeled constituents of [3',5',7,9-^{3}H]-CH_2H_4fol (pterin and *p*-aminobenzoate) are part of the base-trapped intermediate.

Upon closer examination of the MSMS spectrum of the trapped compound, we noticed that the mass of the major unidentified fragment ion (*m/z* 134.0457 in negative or 136.0623 in positive-ion mode) corresponded to that of an adenine, as confirmed by the HR-MS and elemental composition report of an adenine standard. The sole source of adenine in FDTS reaction mixtures is the adenine of FAD prosthetic group. Although all

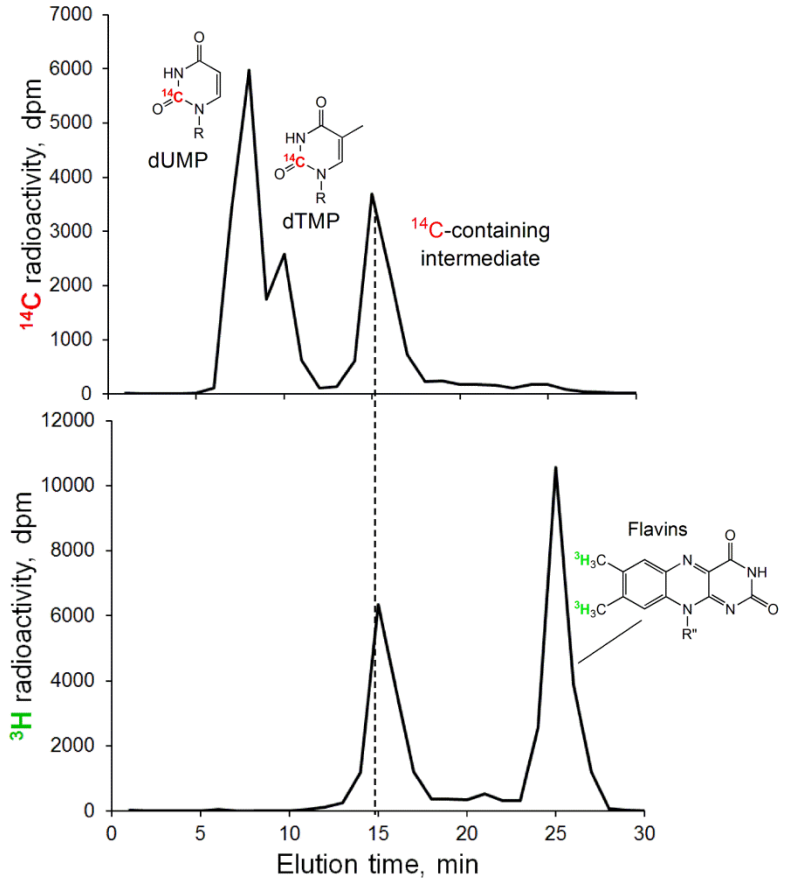

Figure 5.5 HPLC radiogram of [7a,8a-^{3}H]-FAD-FDTS reaction with [2-^{14}C]-dUMP quenched at 1 s with 1 M NaOH. The radioactivity counts were determined by liquid scintillation counting. The trapped intermediate derivative eluting at ~15 min clearly contains the labeled dimethylbenzene portion of FAD.

crystal structures of FDTSs place the FAD's adenine very far from dUMP, the above observation warranted an examination of that option. To do so, we removed the native flavin from purified FDTS and reconstituted the resulting apoenzyme with FAD labeled with either ^{3}H or ^{13}C and ^{15}N at the adenyl tail (see chapter IV of this thesis for reconstitution details and Fig. 5.9 for FAD structure and nomenclature). This reconstituted FDTS was then reacted with [2-^{14}C]-dUMP and CH_2H_4fol and quenched at 1 s with 1 M NaOH. None of the labeled adenyl atoms were incorporated into the base-

trapped intermediate, as evident from Figs. 5.10 and 5.11B, suggesting that the observed MSMS fragment is not due the adenine of enzyme-bound FAD.

The remaining constituent of the quenched FDTS reactions that could potentially be the source of adduct is the isoalloxazine core of FAD. To explore this possibility, we carried out the quench-flow experiments with FDTS which has been reconstituted with FAD isotopically labeled at various isoalloxazine positions. To our surprise, the reaction of [7a,8a-^{3}H]-FAD-FDTS produced a tritiated trapped intermediate upon quenching with base (Fig. 5.5; see Fig. 5.9 for atomic numbering of the flavin), indicating that the labeled dimethylbenzene portion of isoalloxazine is in fact a part of the trapped species. This finding was unexpected because neither of the mechanisms proposed for FDTS so far invoke covalent involvement of the flavin (see Figs. 3.1 and 3.6 of this thesis for proposed FDTS mechanisms). Traditionally, covalent flavin adducts form through the N5 or C4a positions on the isoalloxazine nucleus.[89] The 5-carba-5-deaza-FAD-FDTS, where the N5 of the flavin has been replaced with a carbon, has been previously shown to be active.[36] Thus if the base-trapped nucleotide were to be bound to isoalloxazine at N5, it would likely represent a side product of the quenching process and not a mechanistically relevant snapshot (since C5 would no longer be nucleophilic/electrophilic[96] and be incapable of forming a covalent bond with substrate/intermediates).

Finally, the mass of the trapped intermediate isolated in a quench-flow experiment with [Dioxopyrimidine-^{13}C,^{15}N]-FAD-FDTS was identical to that with unlabeled enzyme (Fig. 5.11C), which implies that the entire "C" ring of isoalloxazine including the C4a position (Fig. 5.9) is missing from the trapped compound. Examples of isoalloxazine core cleavage, either enzyme-catalyzed[91] or chemically induced,[106-109] exist in literature. For instance, the "flavin destructase" BluB cannibalizes the isoalloxazine ring system of its FMN cofactor to form 5,6-dimethylbenzimidazole (DMB), the lower ligand of vitamin B_{12}.[91] In this process, all of the ring "C" atoms and most of the ribityl tail of FMN are lost. Such chemistry was also shown to occur non-enzymatically, although under highly

basic conditions and 100^{o}C.[107] With these examples in mind, it is conceivable that the combination of the basic quenching conditions and the reactive intermediate(s) existing in the active site of FDTS at the time of quench could cause the fragmentation of the isoalloxazine nucleus of FAD.

In summary, we have determined that the entire dTMP moiety and the FAD-derived dimethylbenzene are included in the base-trapped FDTS reaction intermediate. These two constituents alone, however, do not make up for the mass of the trapped compound (combined mass ~425 Da vs. needed 571 Da). The locus of the covalent link between them is yet to be identified.

Mechanistic implications

The C4a and N5 positions on FAD are unlikely to be the sites of the covalent linkage to the base-trapped nucleotide intermediate, as discussed above (at least not in a mechanistically relevant context). The remaining atom that could bind a reactive intermediate is the C6 of isoalloxazine (Fig. 5.9). The precedent for C6 covalent flavin adducts exists in cholesterol oxidase,[110] general acyl-CoA dehydrogenase,[111] and D-lactate dehydrogenase[112]; although in all of these cases, the adduct formation was promoted by the highly reactive suicide substrates and resulted in inactivation of the enzymes. If C6 of flavin turns out to be the locus of covalent bond in FDTS, a few implications could be envisaged: (i) C6 is electrophilic in the oxidized flavin state.[110, 112] Thus if the nucleotide intermediate trapped by the base was in its reduced, electron-rich form prior to quenching (implying that the flavin was oxidized at this point), this would allow the intermediate to nucleophilically attack flavin's electrophilic C6. (ii) The reducing equivalents were still on the flavin prior to the base quench, i.e. as $FADH_2$. The C6 of $FADH_2$ could have potentially acted as a nucleophile which, for instance, initially activated dUMP for the methylene transfer. This scenario would be very interesting mechanistically because it would suggest a dual role for the reduced flavin in FDTS, i.e.

as a Michael nucleophile (C6) and the source of the reducing hydride (N5-H). (iii) The reduced $FADH_2$ could nucleophilically attack the proposed exocyclic methylene intermediate, although it is not clear how this could be mechanistically productive.

Methods

Materials

Chemicals were reagent grade and used as purchased without further purification, unless stated otherwise. 2′-deoxyuridine 5′-monophosphate (dUMP), glucose oxidase powder, D-glucose, D_2O, and formaldehyde solution (36.5% by weight) and reduced nicotinamide adenine dinucleotide phosphate (NADPH) were obtained from Sigma-Aldrich. Non-radiolabeled *(6R)*-N^5,N^{10}-methylene-5,6,7,8-tetrahydrofolate and 5,6,7,8-tetrahydrofolate were provided by Eprova Inc. (Schaffhausen, Switzerland). Radiolabeled [2-^{14}C]-dUMP, ^{14}C-formaldehyde, and [3',5',7,9-^{3}H]-folic acid were purchased from Moravek Biochemicals. [6-^{3}H]-CH_2H_4fol was synthesized following published chemo-enzymatic protocol.[69] Sodium dithionite powder was purchased from J.T. Baker. Tris(hydroxymethyl)aminomethane was obtained from Research Products International Corp. Radio- and stable-isotope labeled FAD cofactors were synthesized as previously described (chapter IV of this thesis).The FDTS from *Thermatoga maritima* (TM0449, GenBank accession number NP228259) was expressed and purified following procedure outlined in chapter III of this thesis. The FDTS was reconstituted with isotopically labeled flavins as detailed elsewhere (chapter IV of this thesis). *E. coli* dihydrofolate reductase for the synthesis of labeled folates was expressed and purified in house as described in ref 113.

Synthesis of radiolabeled N^5,N^{10}-methylenetetrahydrofolate (CH_2H_4fol)

[11-^{14}C]-CH_2H_4fol was produced by chemically trapping non-radioactive H_4fol with ^{14}C-labeled formaldehyde. Specifically, 50 μCi of radioactive formaldehyde solution was added to 2 mg of H_4fol powder with a gastight syringe, in a sealed vial purged with argon. To this, 200 μL of ice-cold anaerobic buffer containing 10 mM ascorbate and 8.5 mM citrate, known to stabilize folates, was added. The vial was vigorously vortexed and incubated on ice for 20 min, under argon. The resulting [11-^{14}C]-CH_2H_4fol was purified by semipreparative HPLC.

[3',5',7,9-^{3}H]-CH_2H_4fol was synthesized chemo-enzymatically following a modified published procedure.[69] Briefly, [3',5',7,9-^{3}H]-dihydrofolate (H_2fol) was prepared by sodium dithionite reduction of commercial [3',5',7,9-^{3}H]-folic acid (Moravek), as described in ref 114. [3',5',7,9-^{3}H]-H_2fol was then converted to [3',5',7,9-^{3}H]-tetrahydrofolate (H_4fol) in the reaction with NADPH catalyzed by *E. coli* dihydrofolate reductase, and H_4fol was trapped with formaldehyde to yield the final CH_2H_4fol product.

Analytical methods

Separations were carried out on an Agilent 1100 series HPLC, with UV-vis diode array detector and 500TR series Packard flow scintillation analyzer. An analytical reverse phase Supelco column (C18, Discovery series 250 mm X 4.6 mm) was used for all analyses. To assess formation of CH_2H_4fol in radioactive syntheses, the folates (H_2fol, H_4fol and CH_2H_4fol) were separated in 4 mM KH_2PO_4 at pH 7.5 with a gradient of methanol. The concentration of enzyme for rapid-quenching experiments was determined by the 454 nm absorbance of bound FAD (ε = 11,300 $cm^{-1}M^{-1}$). The mobile phase for analysis of quenched FDTS reactions consisted of 100 mM Tris buffer at pH 7.8 and a methanol gradient appropriate for separating the base-trapped intermediate from other

labeled components of the reaction mixture. In separations of the base-quenched FDTS reactions with [2-^{14}C]-dUMP and tritiated folate or flavin cofactors, the eluent was collected in 1-mL fractions, mixed with liquid scintillation cocktail, and counted by liquid scintillation counter. Liquid chromatography-mass spectrometry (LC-MS) analysis of purified trapped intermediate was performed on Waters LC system, using an eluent gradient of water and methanol, followed by a Q-TOF mass spectrometer.

Purification methods

The radiolabeled CH_2H_4fol was purified from the synthesis mixtures by HPLC using a semipreparative (Discovery series 250 mm X 10 mm) reverse-phase Supelco column, with a UV-vis diode array detector. Mobile phase used for separation was a gradient of 100 mM Tris buffer at pH 7.8 and methanol. Elution of CH_2H_4fol was followed by observing real-time absorbance spectra. CH_2H_4fol eluted with ~10% methanol. Eluent containing the pure CH_2H_4fol was collected, purged with argon for 20 min on ice and lyophilized to dryness. The chemical and radioactive purity of CH_2H_4fol was confirmed by HPLC analysis of the purified material, prior to its use in rapid-quenching experiments (Fig. 5.7). Base-trapped intermediate was isolated from the crude quenched reactions via analytical HPLC, in 100 mM Tris buffer, pH 7.8, containing 20% methanol. The elution of the trapped species was followed by the absorbance at 258 and 340 nm (trapped derivative absorbs at both wavelengths). The solution of the purified trapped compound was purged with argon to remove the methanol and freeze dried for future analysis.

Data fitting for FDTS-catalyzed reaction kinetics

The base-quench data were globally fitted to a kinetic model with one intermediate using Mathematica (Fig. 5.2, top panel):

$$\text{dUMP} \xrightarrow{k_1} I_1 \xrightarrow{k_2} \text{dTMP}$$

The following set of rate equations was used in the fitting:

$$\frac{d}{dt}[dUMP] = -k_1 \bullet [dUMP]$$

$$\frac{d}{dt}[I_1] = k_1 \bullet [dUMP] - k_2 \bullet [I_1]$$

$$\frac{d}{dt}[dTMP] = k_2 \bullet [I_1]$$

The acid-quench data from ref 74 were globally fitted to a two-intermediate model (Fig. 5.2, bottom panel):

$$dUMP \xrightarrow{k_1} I_1 \xrightarrow{k_2} I_2 \xrightarrow{k_3} dTMP$$

where the intermediate I_1 was assumed to be the one trapped by the base and hence the k_1 and k_2 rate constants (obtained from the one-intermediate fitting above) were held constant. The set of rate equations below was used in the fitting:

$$\frac{d}{dt}[dUMP] = -k_1 \bullet [dUMP]$$

$$\frac{d}{dt}[I_1] = k_1 \bullet [dUMP] - k_2 \bullet [I_1]$$

$$\frac{d}{dt}[I_2] = k_2 \bullet [I_1] - k_3 \bullet [I_2]$$

$$\frac{d}{dt}[dTMP] = k_3 \bullet [I_2]$$

Conclusions

Rapid base-quenching experiments with *Tm*FDTS led to chemical trapping of an intermediate derivative different from the one isolated in acid. The trapped ^{14}C-methylene containing species was present in reactions quenched at as short times as 10 ms, suggesting that the condensation between CH_2H_4fol and dUMP occurs very early in FDTS mechanism. This is curious considering that out of the hundreds of seconds required for a complete *Tm*FDTS turnover the enzyme spends only a small fraction of time on one of the most challenging tasks – carbon-carbon bond formation. Partial composition of the base-trapped compound was determined and found to include dTMP moiety and flavin-derived dimethylbenzene. Such unique species containing a covalent

link between the pyrimidine base and part of the flavin has never been observed or suggested for FDTS. The efforts are underway to reveal the complete structure of this molecule by NMR. Regardless of the exact chemical form the intermediate is trapped in by the base, it adds a new piece to the kinetic model for FDTS. By relating the base- and acid-trapped intermediate kinetics, it appears that at least two intermediates accumulate over the course of FDTS turnover: both are trapped as 5-hydroxymethyl-dUMP in acid, while the first is trapped as a flavin-nucleotide adduct and the second is converted to dTMP product in base. Earlier acid-quench data points (2 ms – 0.5 s), missing from the time course at present, will help validate the two-intermediate model fit in the future. While the base-trapped derivative might turn out to be an artifact of the quenching process, its kinetics is valuable and its structure will still teach us about the active-site architecture of the enzyme in action, i.e. the orientation of the reactive intermediate(s) relative to the isoalloxazine of FAD.

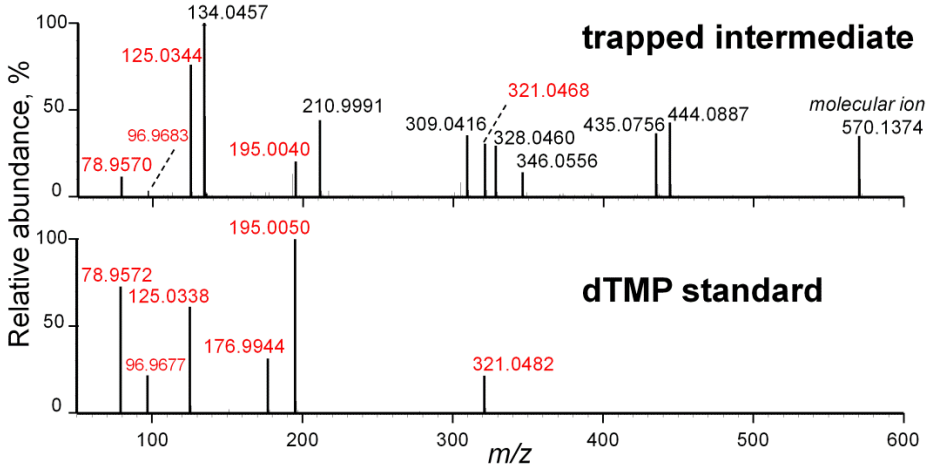

Figure 5.6 HR-ESI-MSMS of the base-trapped intermediate and dTMP standard. The common ion fragments are highlighted in red. The spectra were collected in the negative-ion mode.

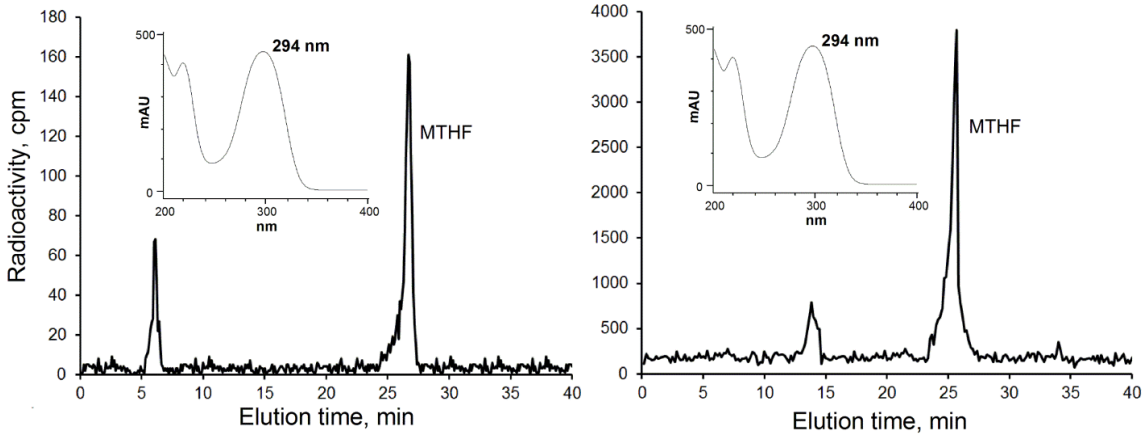

Figure 5.7 (*Left*) HPLC radiogram of purified [11-^{14}C]-CH_2H_4fol. The 6-min peak is due to the free ^{14}C-formaldehyde in solution. (*Right*) Radiogram of purified [3',5',7,9-^{3}H]-CH_2H_4fol. The 14-min peak is due to the free tritiated (*p*-aminobenzoyl)-glutamate tail of CH_2H_4fol, a common decomposition product of such folates. The inserts illustrate UV-vis absorbance spectra of CH_2H_4fol peak.

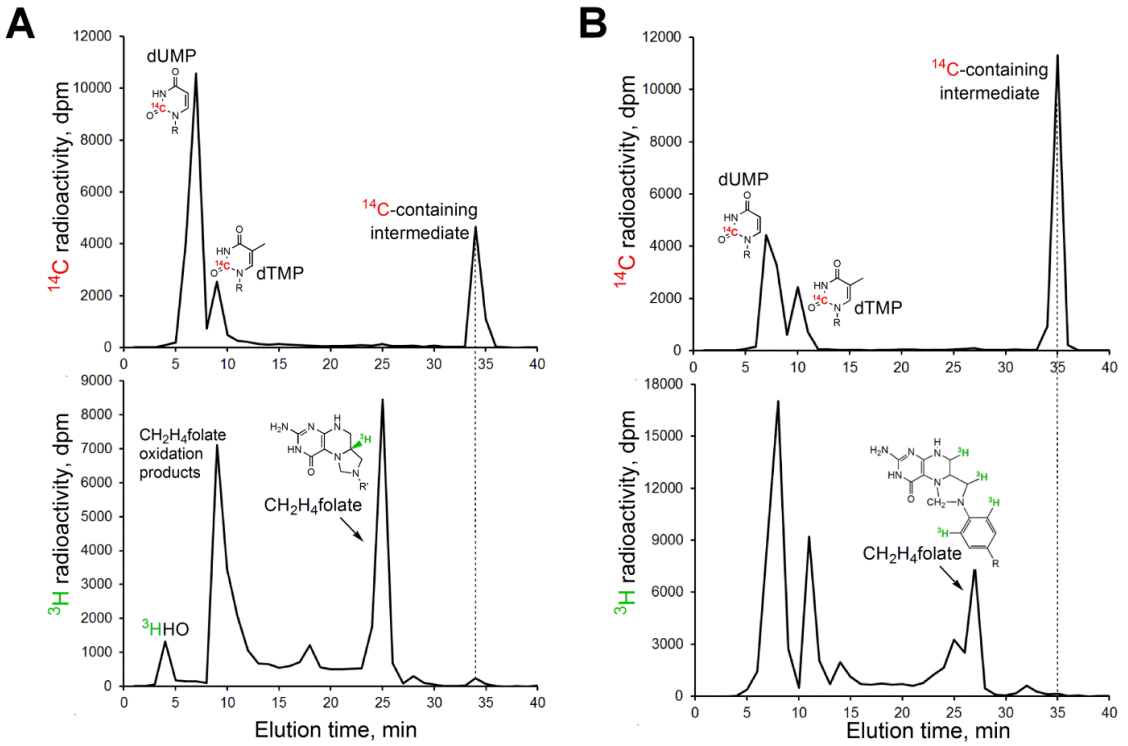

Figure 5.8 Radiograms of FDTS reactions with [2-^{14}C]-dUMP and either [6-^{3}H]-CH_2H_4fol (A) or [3',5',7,9-^{3}H]-CH_2H_4fol (B), quenched with 1 M NaOH. Radioactive counts were determined by liquid scintillation counting. In both cases, the base-trapped intermediate carries no tritium, indicating that no portion of the folate is a part of the trapped species.

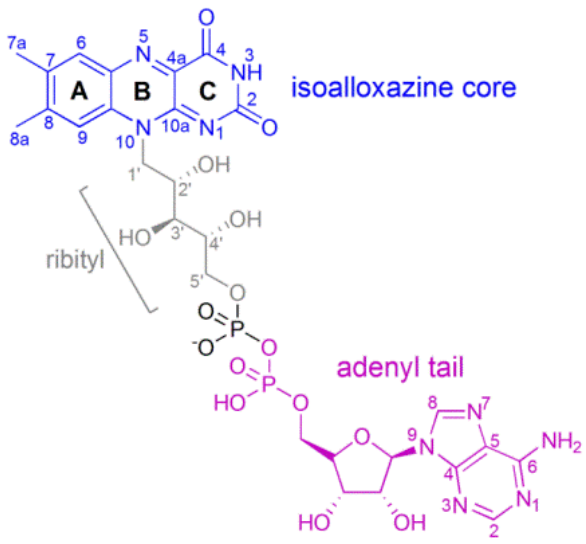

Figure 5.9 Atomic numbering and nomenclature of flavin adenine dinucleotide (FAD) used in the main text. The adenyl tail labeling is denoted as "Ad" followed by the location of the isotope label. Ring C of the isoalloxazine is referred to as "dioxopyrimidine."

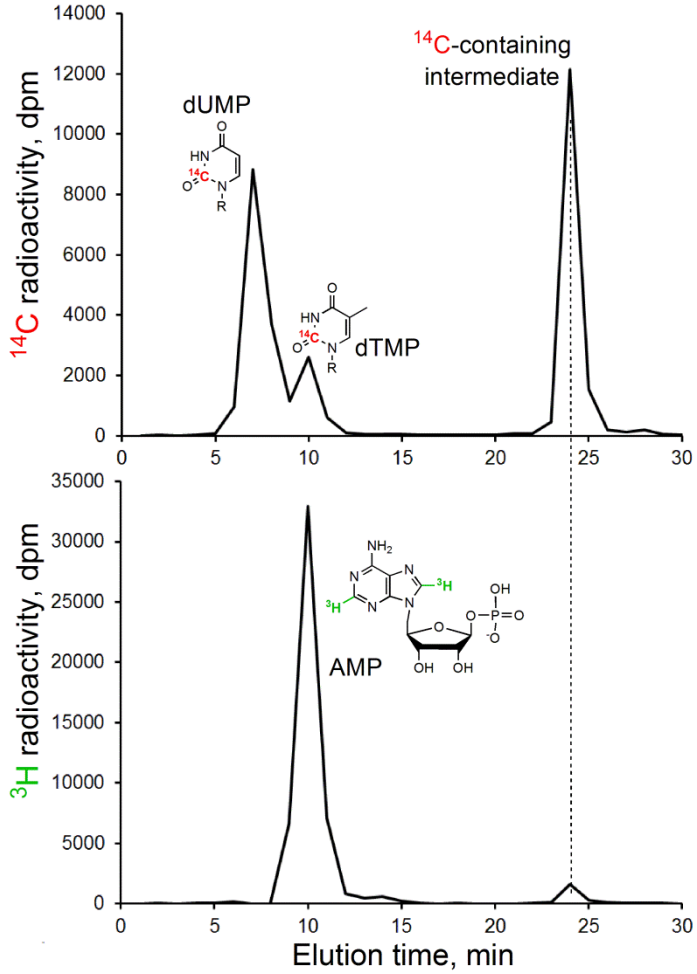

Figure 5.10 HPLC radiogram of [Ad-2,8-^{3}H]-FAD-FDTS reaction with [2-^{14}C]-dUMP, quenched with 1 M NaOH. Note that FAD has mostly been hydrolyzed under quenching conditions. The small tritiated peak at ~24 min is due to remaining FAD and not the trapped intermediate (as this peak is present in control reactions). Radioactive counts were determined by liquid scintillation counting. The base-trapped intermediate carries no tritium, indicating that the adenine portion of enzyme-bound FAD is not a part of the trapped species.

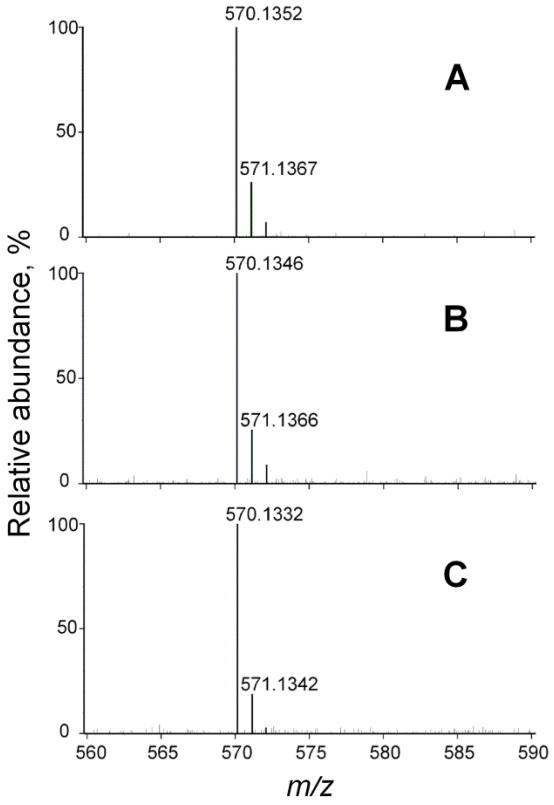

Figure 5.11 HR-ESI-MS of the base-trapped intermediate isolated in the reactions with (A) unlabeled FAD-FDTS, (B) [Ad-^{13}C,^{15}N]-FAD-FDTS, and (C) [Dioxopyrimidine-^{13}C,^{15}N]-FAD-FDTS. No isotopic enrichment of the trapped molecule was observed. All spectra were collected in the negative-ion mode.

CHAPTER VI

CONCLUSIONS AND FUTURE DIRECTIONS

We have examined the mechanism of flavin-dependent thymidylate synthase through chemical trapping of reaction intermediates, substrate isotope exchange, and spectroscopic features of the bound flavin. The studies presented here emphasize the uniqueness of FDTS's approach to pyrimidine methylation. While all known pyrimidine-methylating enzymes covalently anchor their intermediates during catalysis, FDTS realizes its chemistry through non-covalent protein interactions. The acid-trapping of a derivative of such non-covalent intermediate(s), described in chapter II, supports this aspect of FDTS. The fact that this trapped species has never been isolated in other uracil-methylating proteins further highlights the difference between classical enzymes and FDTS. FDTS still has to activate the substrate for the reaction; however, the nature of the nucleophile (if any) carrying out this function is quite different in FDTS, as discussed in chapter III. Our findings show that one of the two key chemical transformations – methylene transfer – happens very quickly in FDTS (within first tens of milliseconds). What does the enzyme spend the rest of hundreds of seconds doing? This remains a mystery. The observation of a covalent flavin-pyrimidine adduct presented in chapter V challenges the mechanisms proposed so far, and invokes the possibility of covalent involvement of the flavin in catalysis (although not through its commonly reactive centers N5 or C4a). This unexpected finding raises the question of what other surprises FDTS has in store for researchers. Although the unified understanding of FDTS catalysis is still missing, the stark differences between FDTS and classical uracil-methylating enzymes lend confidence to the selective targeting of pathogenic thymidylate biosynthesis in the future.

An important direction that springs from the described studies will be characterization of the chemically unmodified reaction intermediates. The methodology

developed in chapter II and the resulting time course for FDTS reaction will be crucial in pursuing this direction. For instance, chemically inert quenchers (e.g. organic solvents) or alternative means of stopping the enzymatic reaction (e.g. time-resolved mass spectrometry) may be employed to detect the intermediates shown to accumulate between 50 ms and 100 s. These studies may also reveal whether the covalent flavin-pyrimidine species isolated in base-quenched reactions is mechanistically relevant or an artifact of the quenching process.

Another aspect that should be investigated in the future is the remarkable difference in reactivity of the second accumulating intermediate in acidic vs. basic solution. Namely, this intermediate is trapped as 5-hydroxymethyl-dUMP in acid (chapter II), but converted to dTMP product in base (chapter V) while the flavin appears to still be reduced (according to its UV signature). Several scenarios could be envisioned that would explain this observation: the intermediate may already contain the reducing equivalents from the flavin and is isomerized into dTMP in base, and not in acid (challenging the interpretation of the flavin's UV spectrum and emphasizing the need of the acid-quench for re-oxidation of this second intermediate). Another conceivable explanation could be that the base quench catalyzes the hydride transfer from $FADH_2$ to the intermediate, which seems less likely since the enzyme presumably falls apart quickly upon quenching. Quenchers with reactivity different from the tested acid and base (e.g. reducing/oxidizing agents) may resolve the question of where the reducing equivalents are at various times in the reaction. These quenchers could result into additional trapped derivatives, which might reflect different redox state of the intermediates.

Altogether, our work constitutes a significant step forward towards understanding the molecular machinery of FDTS. The tools developed here for *T. maritima* model system will be critical in testing whether mechanistic features are conserved in all FDTSs, including those from pathogens. The intermediate identification experiments

with these enzymes will greatly facilitate the efforts to design intermediate- and/or transition state-based inhibitors as leads for novel antibiotics.

BIBLIOGRAPHY

1. J. S. Finer-Moore; D. V. Santi; R. M. Stroud, *Biochemistry* **2003,** 42, 248-256.

2. H. Myllykallio; S. Skouloubris; H. Grosjean; U. Liebl, *DNA and RNA modification enzymes: structure, mechanism, function and evolution*. Landes Bioscience: 2009.

3. G. R. Bjork, *Prog. Nucleic Acid Res. Mol. Biol.* **1995,** 50, 263-338.

4. S. Agarwalla; J. T. Kealey; D. V. Santi; R. M. Stroud, *J. Biol. Chem.* **2002,** 277, 8835-8840.

5. C. Persaud; Y. Lu; A. Vila-Sanjurjo; J. L. Campbell; J. Finley; M. O'Connor, *Biochem. Biophys. Res. Comm.* **2010,** 392, 223-227.

6. C. T. Madsen; J. Mengel-Jorgensen; F. Kirpekar; S. Douthwaite, *Nucleic Acids Res.* **2003,** 31, 4738-4746.

7. H. Myllykallio; G. Lipowski; D. Leduc; J. Filee; P. Forterre; U. Liebl, *Science* **2002,** 297, 105-107.

8. Centers for Disease Control and Prevention http://www.cdc.gov

9. D. Leduc; S. Graziani; L. Meslet-Cladiere; A. Sodolescu; U. Liebl; H. Myllykallio, *Biochem. Soc. Trans.* **2004,** 32, 231-235.

10. H. Myllykallio; D. Leduc; J. Filee; U. Liebl, *Trends Microbiol.* **2003,** 11, 220-223.

11. E. M. Koehn; A. Kohen, *Arch. Biochem. Biophys.* **2010,** 493, 96-102.

12. B. C. Persson; C. Grustafsson; D. E. Berg; G. R. Bjork, *Proc. Natl Acad. Sci USA* **1992,** 89, 3995-3998.

13. C. W. Carreras; D. V. Santi, *Annu. Rev. Biochem.* **1995,** 64, 721-762.

14. D. A. Matthews; J. E. Villafranca; C. A. Janson; W. W. Smith; K. Welsh; S. Freer, *J. Mol. Biol.* **1990,** 214, 937-948.

15. M. A. Moore; F. Ahmed; R. B. Dunlap, *Biochemistry* **1986,** 25, 3311-3317.

16. W. Huang; D. V. Santi, *J. Biol. Chem.* **1994,** 269, 31327-31329.

17. J. E. Barrett; D. A. Maltby; D. V. Santi; P. G. Schultz, *J. Am. Chem. Soc.* **1998,** 120, 449.

18. Z. Wang; A. Kohen, *J. Am. Chem. Soc.* **2010,** 132, 9820-9825.

19. N. Touroutoglou; R. Pazdur, *Clin. Cancer Res.* **1996,** 2, 227-243.

20. T. I. Kalman; D. Goldman, *Biochem. Biophys. Res. Comm.* **1981,** 102, 682-689.

21. S. Gabbara; D. Sheluho; A. S. Bhagwat, *Biochemistry* **1995,** 34, 8914-8923.

22. N. Kanaan; S. Ferrer; S. Marti; M. Garcia-Viloca; A. Kohen; V. Moliner, *J. Am. Chem. Soc.* **2011,** 133, 6692-6702.

23. S. A. Lesley; P. Kuhn; A. Godzik; A. M. Deacon; I. I. Mathews; A. T. Kreusch; G. Spraggon; H. E. Klock; D. McMullan; T. Shin; J. Vincent; A. Robb; L. S. Brinen; M. D. Miller; T. M. McPhillips; M. A. Miller; D. Scheibe; J. M. Canaves; C. Guda; L. Jaroszewski; T. L. Selby; M. A. Elslinger; J. Wooley; S. S. Taylor; K. O. Hodgson; I. A. Wilson; P. G. Schultz; R. C. Stevens, *Proc. Natl. Acad. Sci. U. S. A.* **2002,** 99, 11664-11669.

24. A. G. Murzin, *Science* **2002,** 297, 61-62.

25. K. M. Ivanetich; D. V. Santi, *FASEB* **1990,** 4, 1591-1597.

26. R. Cella; B. Parisi, *Physiol. Plant.* **1993,** 88, 509-521.

27. N. Agrawal; S. A. Lesley; P. Kuhn; A. Kohen, *Biochemistry* **2004,** 43, 10295-10301.

28. B. Hong; F. Maley; A. Kohen, *Biochemistry* **2007,** 46, 14188-14197.

29. P. Kuhn; S. A. Lesley; I. I. Mathews; J. M. Canaves; L. S. Brinen; X. Dai; A. M. Deacon; M. A. Elslinger; S. Eshaghi; R. Floyd; A. Godzik; C. Grittini; S. K. Grzechnik; C. Guda; K. O. Hodgson; L. Jaroszewski; C. Karlak; H. E. Klock; E. Koesema; J. M. Kovarik; A. T. Kreusch; D. McMullan; T. M. McPhillips; M. A. Miller; M. Miller; A. Morse; K. Moy; J. Ouyang; A. Robb; K. Rodrigues; T. L. Selby; G. Spraggon; R. C. Stevens; S. S. Taylor; H. van den Bedem; J. Velasquez; J. Vincent; X. Wang; B. West; G. Wolf; J. Wooley; I. A. Wilson, *Proteins: Struct. Funct. Genet.* **2002,** 49, 142-145.

30. P. Sampathkumar; S. Turley; J. E. Ulmer; H. G. Rhie; C. H. Sibley; W. G. J. Hol, *J. Mol. Biol.* **2005,** 352, 1091-1104.

31. S. B. Graziani; J. Bernauer; S. Skouloubris; M. Graille; C. Z. Zhou; C. Marchand; P. Decottignies; H. Tilbeurgh; H. Myllykallio; U. Liebl, *J. Biol. Chem.* **2006,** 281, 24048-24057.

32. K. Wang; Q. Wang; J. Chen; L. Chen; H. Jiang; X. Shen, *Prot. Sci* **2011,** doi: 10.1002/pro.668.

33. P. Sampathkumar; S. Turley; C. Sibley; W. G. J. Hol, *J. Mol. Biol.* **2006,** 360, 1-6.

34. J. E. Ulmer; Y. Boum; C. D. Thouvenel; H. Myllykallio; C. H. Sibley, *J. Bacteriol.* **2008,** 190, 2056-2064.

35. D. Leduc; S. Graziani; G. Lipowski; C. Marchand; P. Le Marechal; U. Liebl; H. Myllykallio, *Proc. Natl. Acad. Sci. U. S. A.* **2004,** 101, 7252-7257.

36. E. M. Koehn; T. Fleischmann; J. A. Conrad; B. A. Palfey; S. A. Lesley; I. I. Mathews; A. Kohen, *Nature* **2009,** 458, 919-924.

37. I. I. Mathews; A. M. Deacon; J. M. Canaves; D. McMullan; S. A. Lesley; S. Agarwalla; P. Kuhn, *Structure (Camb.)* **2003,** 11, 677-690.

38. Y. Wataya; D. V. Santi, *Biochem. Biophys. Res. Comm.* **1975,** 67, 818-823.

39. M. Soltero-Higgin; E. E. Carlson; T. D. Gruber; L. L. Kiessling, *Nat. Struc. Mol. Biol.* **2004,** 11, 539-543.

40. Z. Wang; A. Chernyshev; E. M. Koehn; T. D. Manuel; S. A. Lesley; A. Kohen, *FEBS Journal* **2009,** 276, 2801-2810.

41. S. B. Graziani; Y. Xia; J. R. Gurnon; J. L. Van Etten; D. Leduc; S. P. Skouloubris; H. Myllykallio; U. Liebl, *J. Biol. Chem.* **2004,** 279, 54340-54347.

42. A. Chernyshev; T. Fleischmann; A. Kohen, *Appl. Microbiol. Biotechnol.* **2007,** 74, 282-289.

43. F. Esra Önen; Y. Boum; C. Jacquement; M. V. Spanedda; N. Jaber; D. Scherman; H. Myllykallio; J. Herscovici, *Bioorg. Med. Chem. Lett.* **2008,** 18, 3628-3631.

44. M. Kogler; B. Vanderhoydonck; S. De Jonghe; J. Rozenski; K. Van Belle; J. Herman; T. Louat; A. Parchina; C. Sibley; E. Lescrinier; P. Herdewijn, *J. Med. Chem.* **2011,** 54, 4847-4862.

45. J. Griffin; C. Roshick; E. Iliffe-Lee; G. McClarty, *J. Biol. Chem.* **2005,** 280, 5456-5467.

46. J. T. Kealey; X. Gu; D. V. Santi, *Biochimie* **1994,** 76, 1133-1142.

47. A. Alian; T. T. Lee; S. L. Griner; R. M. Stroud; J. Finer-Moore, *Proc. Natl Acad. Sci USA* **2008,** 105, 6876-6881.

48. A. S. Delk; D. P. Nagle, Jr.; J. C. Rabinowitz, *J. Biol. Chem.* **1980,** 255, 4387-4390.

49. J. Urbonavicius; S. Skouloubris; H. Myllykallio; H. Grosjean, *Nucleic Acids Res.* **2005,** 33, 3955-3964.

50. J. Urbonavicius; C. Brochier-Armanet; S. Skouloubris; H. Myllykallio; H. Grosjean, *Methods Enzymol.* **2007,** 425, 103-119.

51. H. Nishimasu; R. Ishitani; K. Yamashita; C. Iwashita; A. Hirata; H. Hori; O. Nureki, *Proc. Natl Acad. Sci USA* **2009,** 106, 8180-8185.

52. D. Hamdane; M. Argentini; D. Cornu; H. Myllykallio; S. Skouloubris; G. Hui-Bon-Hoa; B. Golinelli-Pipaneau, *J. Biol. Chem.* **2011,** 286, 36268-36280.

53. C. W. Carreras; D. V. Santi, *Annu. Rev. Biochem.* **1995,** 64, 721-762.

54. J. S. Finer-Moore; D. V. Santi; R. M. Stroud, *Biochemistry* **2003,** 42, 248-256.

55. H. Myllykallio; G. Lipowski; D. Leduc; J. Filee; P. Forterre; U. Liebl, *Science* **2002,** 297, (5578), 105-107.

56. E. M. Koehn; T. Fleischmann; J. A. Conrad; B. A. Palfey; S. A. Lesley; I. I. Mathews; A. Kohen, *Nature* **2009,** 458, (7240), 919-923.

57. J. A. Conrad; M. Ortiz-Maldonado; S. W. Hoppe; B. A. Palfey, **2011**, unpublished results.

58. R. R. Sotelo-Mundo; J. Ciesla; J. M. Dzik; W. Rode; F. Maley; G. F. Maley; L. W. Hardy; W. R. Montfort, *Biochemistry* **1999,** 38, (3), 1087-94.

59. Y. Takemura; A. L. Jackman, *Anticancer Drugs* **1997,** 8, (1), 3-16.

60. J. E. Barrett; D. A. Maltby; D. V. Santi; P. G. Schultz, *J. Am. Chem. Soc.* **1998,** 120, 449.

61. M. Kogler; B. Vanderhoydonck; S. De Jonghe; J. Rozenski; K. Van Belle; J. Herman; T. Louat; A. Parchina; C. Sibley; E. Lescrinier; P. Herdewijn, *J. Med. Chem.* **2011,** 54, (13), 4847-4862.

62. E. M. Koehn; A. Kohen, *Arch. Biochem. Biophys.* **2010,** 493, (1), 96-102.

63. N. Agrawal; S. A. Lesley; P. Kuhn; A. Kohen, *Biochemistry* **2004,** 43, 10295-10301.

64. A. Chernyshev; T. Fleischmann; A. Kohen, *Appl. Microbiol. Biotechnol.* **2007,** 74, 282-289.

65. S. Graziani, *J. Biol. Chem.* **2006,** 281, 24048-24057.

66. J. Griffin; C. Roshick; E. Iliffe-Lee; G. McClarty, *J. Biol. Chem.* **2005,** 280, (7), 5456-5467.

67. A. Chernyshev, Fleischmann, T., Koehn, E. M., Lesley, S. A., Kohen, A., *Chem. Commun.* **2007**, (27), 2861-2863.

68. Z. Wang; A. Chernyshev; E. M. Koehn; T. D. Manuel; S. A. Lesley; A. Kohen, *FEBS Journal* **2009,** 276, (10), 2801-2810.

69. N. Agrawal; C. Mihai; A. Kohen, *Anal. Biochem.* **2004,** 328, 44-50.

70. S. Hazra; S. Ort; M. Konrad; A. Lavie, *Biochemistry* **2010,** 49, 6784-6790.

71. D. Leduc, *Proc. Natl. Acad. Sci. USA* **2004,** 101, 7252-7257.

72. S. G. Gattis; B. A. Palfey, *J. Am. Chem. Soc.* **2005,** 127, 832-833.

73. T. V. Mishanina; E. M. Koehn; A. Kohen, *Bioorg. Chem.* **2012,** 43, 37-43.

74. T. V. Mishanina; E. M. Koehn; J. A. Conrad; B. A. Palfey; S. A. Lesley; A. Kohen, *J. Am. Chem. Soc.* **2012,** 134, 4442-4448.

75. B. J. Brown; Z. Deng; P. A. Karplus; V. Massey, *J. Biol. Chem.* **1998,** 273, (49), 32753-32762.

76. R. L. Fagan; M. N. Nelson; P. M. Pagano; B. A. Palfey, *Biochemistry* **2006,** 45, (50), 14926-14932.

77. C. W. Carreras; S. C. Climie; D. V. Santi, *Biochemistry* **1992,** 31, (26), 6038-6044.

78. L. Burlamacchi; G. Guarini; E. Tiezzi, *Trans. Faraday Soc.* **1969,** 65, 496-502.

79. L. W. Rider; M. B. Ottosen; S. G. Gattis; B. A. Palfey, *J. Biol. Chem.* **2009,** 284, (16), 10324-10333.

80. F. Yu; Y. Tanaka; K. Yamashita; T. Suzuki; A. Nakamura; N. Hirano; T. Suzuki; M. Yao; I. Tanaka, *Proc. Natl. Acad. Sci. U. S. A.* **2011,** 108, (49), 19593-19598.

81. B. Lohkamp; N. Voevodskaya; Y. Lindqvist; D. Dobritzsch, *Biochim. Biophys. Acta* **2010,** 1804, 2198-2206.

82. E. M. Koehn; L. L. Perissinotti; S. Moghram; A. Prabhakar; S. A. Lesley; I. I. Mathews; A. Kohen, *Proc. Natl. Acad. Sci. U. S. A.* **2012,** 109, (39), 15722-15727.

83. Z. Wang; S. Ferrer; V. Moliner; A. Kohen, *Biochemistry* **2013,** 52, (13), 2348-2358.

84. A. S. Fivian-Hughes; J. Houghton; E. O. Davis, *Microbiology* **2012,** 158, (2), 308-318.

85. Y. Wataya; H. Hayatsu; Y. Kawazoe, *J. Am. Chem. Soc.* **1972,** 94, (25), 8927-8928.

86. D. V. Santi; C. F. Brewer, *J. Am. Chem. Soc.* **1968,** 90, 6236-6238.

87. H. Hayatsu; Y. Wataya; K. Kai; S. Iida, *Biochemistry* **1970,** 9, (14), 2858-2865.

88. D. V. Santi; C. F. Brewer, *Biochemistry* **1973,** 12, 2416-2424.

89. V. Massey, *Biochem. Soc. Trans.* **2000,** 28, 283-296.

90. R. Teufel; A. Miyanaga; Q. Michaudel; F. Stull; G. Louie; J. P. Noel; P. S. Baran; B. Palfey; B. S. Moore, *Nature* **2013,** 503, 552-556.

91. M. E. Taga; N. A. Larsen; A. R. Howard-Jones; C. T. Walsh; G. C. Walker, *Nature* **2007,** 446, 449-453.

92. A. Haigney; A. Lukacs; R.-K. Zhao; A. L. Stelling; R. Brust; R.-R. Kim; M. Kondo; I. Clark; M. Towrie; G. M. Greetham; B. Illarionov; A. Bacher; W. RoÌˆmisch-Margl; M. Fischer; S. R. Meech; P. J. Tonge, *Biochemistry* **2011,** 50, (8), 1321-1328.

93. J. Mehlhorn; H. Steinocher; S. Beck; J. T. M. Kennis; P. Hegemann; T. Mathes, *PLoS ONE* **2013,** 8, (11), e79006.

94. W. Rhead; V. Roettger; T. Marshali; B. Amendt, *Pediatr. Res.* **1993,** 33, 129-135.

95. M. Barile; T. A. Giancaspero; C. Brizio; C. Panebianco; C. Indiveri; M. Galluccio; L. Vergani; I. Eberini; E. Gianazza, *Curr. Pharm. Des.* **2013,** 19, (14), 2649-2675.

96. S. Ghisla; V. Massey, *Biochem. J.* **1986,** 239, (1), 1-12.

97. D. P. Ballou; V. Massey, *Biochemistry* **1997,** 36, (50), 15713-15723.

98. P. Chaiyen; J. Sucharitakul; J. Svasti; B. Entsch; V. Massey; D. P. Ballou, *Biochemistry* **2004,** 43, (13), 3933-3943.

99. L. A. Flexner; W. G. Farkas, *Chem. Abstr.* **1953,** 47, 8781a.

100. G. Scola-Nagelschneider; P. Hemmerich, *Eur. J. Biochem.* **1976,** 66, (3), 567-577.

101. P. Nielsen; P. Rauschenbach; A. Bacher, *Methods Enzymol.* **1986,** 122, 209.

102. S. M. H. Christie; G. W. Kenner; A. R. Todd, *J. Chem. Soc.* **1954,** 46, (0), 46-52.

103. I. Efimov; V. Kuusk; X. Zhang; W. S. McIntire, *Biochemistry* **1998,** 37, (27), 9716-9723.

104. W. J. van Berkel; N. M. Kamerbeek; M. W. Fraaije, *J. Biotechnol.* **2006,** 124, (4), 670-89.

105. D. Hamdane; M. Argentini; D. Cornu; B. Golinelli-Pimpaneau; M. Fontecave, *J. Am. Chem. Soc.* **2012,** 134, (48), 19739-19745.

106. L. A. Maggio-Hall; P. C. Dorrestein; J. C. Escalante-Semerena; T. P. Begley, *Org. Lett.* **2003,** 5, (13), 2211-2213.

107. P. Renz; R. Wurm; J. Horig, *Z Naturforsch C.* **1977,** 32, 523-527.

108. A. Schonbrunn; R. H. Abeles; C. T. Walsh; S. Ghisla; H. Ogata; V. Massey, *Biochemistry* **1976,** 15, (9), 1798-1807.

109. A. Wessiak; G. E. Trout; P. Hemmerich, *Tet. Lett.* **1980,** 21, (8), 739-742.

110. N. S. Sampson, *Antioxid Redox Signal.* **2001** 3, (5), 839-846.

111. H.-D. Zeller; S. Ghisla in: *Inactivation of general acyl-CoA dehydrogenase from pig kidney by the suicide substrate methylenecyclopropylacetyl-CoA. Structure of one of the covalent flavin-inhibitor adducts.*, International Symposium on Flavins and Flavoproteins, Atlanta, Georgia, USA, 1987; D. E. Edmondson; D. B. McCormick, (Eds.) De Gruyter, Walter, Inc.: Atlanta, Georgia, USA, 1987; pp 161–164.

112. S. Ghisla; S. T. Olson; V. Massey; J.-M. Lhoste, *Biochemistry* **1979,** 18, (21), 4733-4742.

113. G. P. Miller; S. J. Benkovic, *Biochemistry* **1998,** 37, 6327-6335.

114. R. L. Blakley, *Nature* **1960,** 188, 231-232.